AD NUMBER

AD093442

NEW LIMITATION CHANGE

TO

Approved for public release, distribution unlimited

FROM

Distribution authorized to U.S. Gov't. agencies and their contractors; Administrative/Operational Use; MAR 1956. Other requests shall be referred to Office of Naval Research, One Liberty Center, 875 North Randolph Street, Arlington, VA 22203-1995.

AUTHORITY

ONR ltr dtd 9 Nov 1977

Office of Naval Research

Contract N50RI-76 • Task Order No.1 • NR-372-012

THE HALL EFFECT IN FERROMAGNETIC METALS AND SEMICONDUCTORS

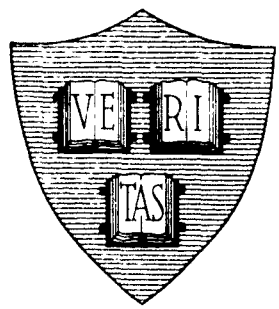

By

Jerome M. Lavine

March 10, 1956

Technical Report No. 225

Cruft Laboratory
Harvard University
Cambridge, Massachusetts

Office of Naval Research

Contract N5ori-76

Task Order No. 1

NR-372-012

Technical Report

on

The Hall Effect in Ferromagnetic Metals and Semiconductors

by

Jerome M. Lavine

March 10, 1956

The research reported in this document was made possible through support extended Cruft Laboratory, Harvard University, jointly by the Navy Department (Office of Naval Research), the Signal Corps of the U. S. Army and the U. S. Air Force, under ONR Contract N5ori-76, T.O.1.

Technical Report No. 225

Cruft Laboratory

Harvard University

Cambridge, Massachusetts

Table of Contents

Abstract

Hall measurements on Ni were made between room temperature and 568°C using an a-c measurement technique. The ordinary Hall coefficient of Ni is roughly constant between room temperature and 300°C. The data suggest that the extraordinary Hall effect persists into the paramagnetic region. The strong temperature dependence of the observed effect does not exhibit a temperature dependence similar to the susceptibility and hence there is ambiguity in the determination of the ordinary Hall coefficient above the Curie temperature. Hall measurements on a 70 Ni - 30 Cu alloy also suggest the presence of the extraordinary Hall effect above the Curie temperature, but in this alloy, the observed effect possesses a $1/T-\theta$ temperature dependence. The ordinary Hall coefficient of the 70 Ni - 30 Cu alloy is smaller in absolute value above the Curie temperature than at liquid air temperature. These data are discussed using Pugh's two-band and four-band models.

Hall measurements at room temperature were made on a synthetic crystal of Fe_3O_4 and on a synthetic single crystal of $(NiO)_{.75}(FeO)_{.25}(Fe_2O_3)$. The ordinary Hall measurement on Fe_3O_4 suggests that the number of conduction electrons at room temperature is large, in rough agreement with Verwey's hypothesis. The ordinary Hall coefficient of $(NiO)_{.75}(FeO)_{.25}(Fe_2O_3)$ also suggests a large carrier concentration. The conductivities of $(NiO)_{.75}(FeO)_{.25}(Fe_2O_3)$ and of a synthetic single crystal of $(NiO)_{.56}(ZnO)_{.14}(FeO)_{.30}(Fe_2O_3)$ are compared with the conductivity of Fe_3O_4 employing a simple model for the mobility and associating the activation energy obtained from resistivity data with the number of conduction electrons. The observed data are in good agreement with the simple model.

Extraordinary Hall measurements were made on Grade A Ni (99.4 Ni), 499 Alloy (99.9 Ni), and R-63 Alloy (95 Ni, 4 Mn, 1 Si) between liquid air temperature and their Curie temperatures, and on the 80 per cent Ni-Fe alloys, Supermalloy, Mumetal, and Carpenter Hymu 80 between liquid air temperature and room temperature. The extraordinary Hall coefficients of these materials do not generally exhibit the resistivity dependence predicted by Karplus-Luttinger theory, but they do suggest that the essential features of the theory are probably correct. The extraordinary Hall coefficients of

Fe_3O_4 and $(NiO)_{.75}(FeO)_{.25}(Fe_2O_3)$ between -100°C and their Curie temperatures indicate no resistivity dependence, and their magnitude, temperature dependence, and sign reversal have not been explained.

Auxiliary measurements of resistivity as a function of temperature, for all samples, and the thermoelectric power of Fe_3O_4 against Cu are also reported.

TR225

THE HALL EFFECT IN FERROMAGNETIC METALS AND SEMICONDUCTORS

by

Jerome M. Lavine

Division of Engineering and Applied Physics

Harvard University, Cambridge, Massachusetts

I. INTRODUCTION

1.1 The Hall Effect in Ferromagnetics

The Hall effect in the ferromagnetic metals Fe, Co, and Ni was first investigated by E. H. Hall [1] in 1881. In 1885 measurements in the temperature region near room temperature were made by Hall [2,3] and over a wider range of temperature by Clough and Hall [4] in 1892. In 1893 Kundt [5] performed measurements on Fe, Co, and Ni which indicated that the Hall effect in ferromagnetics was proportional to the intensity of magnetization (M) rather than to the induction (B). In 1910, A. W. Smith [6] made Hall measurements on Fe, Co, and Ni over a wide range of temperature and with relatively high fields, and correlated the temperature dependence of the saturation effect in the Hall voltage with the temperature dependence of the magnetization. In 1929, Smith and Sears [7] found it possible to separate the Hall voltage in Permalloy into two components, one of which they attributed to the intensity of magnetization, and the other to the H-field in the material. In 1930 Pugh [8] and in 1932 Pugh and Lippert [9] showed conclusively that the Hall voltage was a linear single-valued function of the intensity of magnetization at low fields, in K. S. magnet steel, in hardened high-carbon steel, in electrolytic Fe, in a 50Fe-50Co alloy, and in a 70Fe-30Ni alloy. Following the suggestion of Smith and Sears [7], Pugh [8] proposed that the Hall voltage for ferromagnetics, normalized with respect to geometry and current, be written

$$e_H = R_o H + R_1 M, \qquad (1.1)$$

where e_H is the normalized Hall voltage,
M is the intensity of magnetization,
H is the field in the material,
R_o, R_1 are constants.

In 1950, Pugh, Rostoker, and Schindler [10] made careful high-field measurements on Ni near room temperature which suggested that R_o had the magnitude of the ordinary Hall coefficient of a metal. Their analysis of Smith's [6] data on Ni indicated that R_o was relatively temperature-independent, supporting their suggestion that R_o was the ordinary Hall coefficient. They called the coefficient of M the extraordinary Hall coefficient and further suggested that Eq. (1.1) be written

$$e_H = R_o(H + 4\pi a M), \qquad (1.2)$$

where $a = \frac{R_1}{4\pi R_o}$. They characterized $h = H + 4\pi a M$ as the effective uniform field acting on the conduction electrons.

The speculation of an effective field acting on the conduction electrons required a value of $a \cong 10$ at room temperature to account for the extraordinary Hall effect in Ni. Analysis of Smith's [6] data by Pugh, Rostoker, and Schindler [10] indicated that a in Ni increased from a value near 2 at liquid air temperature to a value near 60 at the Curie temperature. The temperature dependence of a in Ni was confirmed by Jan [11] who also showed that a in Fe increased from a value near 1/2 at liquid air temperature to a value near 500 at 800°K. Thus, the effective field formulation indicated that at room temperature a field 10 times larger than the B-field in Ni and 25 times larger than the B-field in Fe was present at the location of the conduction electrons, and, further, that this field increased with increasing temperature. On the basis of known magnetic interactions, neither the magnitude nor the temperature dependence of a could be explained.

On the other hand, the recognition that R_o could be derived from precise high-field measurements seemed to afford an opportunity to examine the 3d and 4s band electrons of the fourth period transition elements. From saturation magnetization measurements and from considerations that the 3d

electrons provide the major contribution to the saturation magnetization, it had been previously concluded that there are approximately 0.6 holes/atom in the 3d band of Ni, and an equal number of electrons/atom in the 4s band. Since specific heat data indicate that the 0.6 3d holes/atom have a relatively large effective mass, one would expect a negligibly small contribution to the conductivity, and hence to the Hall coefficient, from these carriers. The value of R_o deduced by Pugh [10] required that the 3d holes contribute about one third of the conductivity of Ni. This large contribution from the 3d holes was not in accord with the expected result and cast some doubt on the information derived from the ordinary Hall measurements.

In 1954, Karplus and Luttinger [13] presented a theory which explained the unusually large magnitude and strong temperature dependence of the extraordinary Hall coefficient, R_1, as the effect of the spin-orbit interaction of polarized conduction electrons. They showed that the interband matrix elements of the applied electric potential energy combined with the spin-orbit perturbation to give a current perpendicular to both the applied electric field and the magnetization. This current, J_y, is related to the magnetization M_z, and the applied electric field E_x in the following way:

$$J_y = rM_z E_x, \tag{1.3}$$

where r should depend only weakly upon temperature and impurity content. The strong temperature dependence of the experimentally observed effect comes about as a consequence of the manner in which the effect is measured. Since

$$\rho J_y = E_y, \tag{1.4}$$

provided that we make the measurement with a high-impedance device, then,

$$E_y = \rho r M_z E_x = \rho^2 r M_z J_x. \tag{1.5}$$

Therefore, the observed voltage is proportional to the square of the resistivity simply as a consequence of the measurement of a current-dependent field instead of a field-dependent current.

We must still take into account the fact that the conduction electrons see a field which is larger than the H-field in the material. Wannier [14]

has shown that this field is of the form

$$H_{effective} = H + 2\pi(1+p)M, \qquad (1.6)$$

where p is the probability of coincidence of a conduction electron with the magnetic dipoles contributing to the magnetization. Wannier has estimated that $p \ll 1$ for most electrons in a metal. Equation (1.1) now becomes

$$e_H = R_o[H + 2\pi(1+p)M] + R_1' M, \qquad (1.7)$$

where $R_1' = \rho^2 r$

and $$R_1 = 2\pi(1+p)R_o + R_1' \qquad (1.8)$$

Analysis of Jan's [11] data, ignoring the $2\pi(1+p)R_o$ term which is significant only at low temperatures, indicated that the Karplus-Luttinger theory did indeed account for the order of magnitude of R_1 in both Fe and Ni, and did provide a mechanism for the observed temperature dependence. R_1 in Fe was proportional to $\rho^{1.94}$, in good agreement with Eq. (1.8). However, R_1 in Ni was proportional to $\rho^{1.40}$.

1.2 The Ferrites

Over 2500 years ago the ancient Greeks observed the properties of specimens of magnetite found in Magnesia, a district in Thessaly. Available in the form of natural single crystals, Fe_3O_4 has played an important part in the experimental investigations of the phenomenon of ferromagnetism. In 1909, Hilpert [15] showed that a series of ferromagnetic ferrites could be obtained by replacing the FeO in $FeO\,Fe_2O_3$ with other bivalent metal oxides.

The ferrites crystallize in the spinel structure ($MgOAl_2O_3$). The unit cell of the structure contains 32 oxygen ions in an almost cubic close-packed arrangement, plus 24 metallic ions, 8 bivalent and 16 trivalent, distributed on two types of sites. In the normal spinel structure (nonmagnetic) the 8 bivalent ions occupy 8 tetrahedral sites and the 16 trivalent ions occupy 16 octahedral sites. In the inverse spinel structure (magnetic) the 8 bivalent ions plus 8 of the 16 trivalent ions are distributed at random over the 16 occupied octahedral sites. The remaining 8 trivalent ions occupy 8 tetrahedral sites.

The value of the saturation magnetization of Fe_3O_4 corresponds to four Bohr magnetons per Fe_3O_4 group. If all of the iron ions contribute to the magnetization, we would expect 14 Bohr magnetons, 4 from the bivalent (ferrous) and 5 each from the trivalent (ferric) ions. This phenomenon has been explained by Néel [16] on the basis of a negative exchange coupling between the ions in the octahedral and in the tetrahedral sites. This exchange coupling results in an antiparallel alignment of the spins, and has been confirmed by neutron diffraction studies [17]. Thus, only the bivalent ions contribute to the net magnetization. This type of behavior, observed in all the inverted spinels, has been called ferrimagnetic by Néel.

The ferrites possess a negative temperature coefficient of resistivity, and hence they are classified as semiconductors. Fe_3O_4 has the lowest room temperature resistivity (10^{-2} ohm-cm), and a behavior not characteristic of the other ferrites. In particular, at -153.8°C, Fe_3O_4 goes through a transition causing marked changes in its physical characteristics [18]. In the case of stoichiometric Fe_3O_4, the conductivity increases by a factor of 100 in passing through the transition. Verwey [19] has proposed that the high conductivity of Fe_3O_4 above the transition is due to the free exchange of electrons between equivalent ions with different valence in the octahedral sites. The inverted spinel structure of Fe_3O_4 has one Fe^{2+} and one Fe^{3+} ion per Fe_3O_4 group located in octahedral sites. This may be alternatively described as two Fe^{3+} ions plus one electron. Since all occupied octahedral sites are equivalent in the absence of any order, Verwey has proposed that these extra electrons are distributed at random on the Fe^{3+} ions in the octahedral sites. This random distribution is then connected with a continuous interchange of the extra electrons of the Fe^{2+} ions.

Verwey [20] has further proposed that the low temperature transition in Fe_3O_4 is due to the ordering of ferrous and ferric ions in the octahedral sites resulting in a reduction of the free exchange of electrons and hence in a reduced conductivity. Verwey has also postulated that the effect of ordering would be to change the crystal symmetry and produce an anisotropy in the conductivity. This has been observed by Calhoun [18].

Because of their unusual electric and magnetic behavior, the ferrites in general and magnetite in particular have been the subject of many physical investigations through the years. More recently, the usefulness of the ferrites in electronic technology has initiated extensive studies of their properties [21,22,23].

1.3 The Purpose of the Experiment

At the time this research was undertaken, it seemed desirable to test the effective field formulation in a class of materials (ferrites) in which the density of conduction electrons, and hence R_o, varied strongly with temperature. With the presentation of the Karplus-Luttinger theory, it became even more desirable to test the basic hypothesis of a ρ^2 dependence of R_1 in these materials, especially in Fe_3O_4, which displayed a 100-fold change of resistivity at the transition temperature.

The mechanism proposed by Verwey to explain the room temperature conductivity of Fe_3O_4 suggests that approximately one electron per Fe_3O_4 group contributes to the current. This then implies that the number of conduction electrons in Fe_3O_4 is very nearly equal to the number of electrons in a metal, while the conductivity is three orders of magnitude smaller. An ordinary (R_o) Hall measurement, verifying the high carrier concentration, could then attribute the low conductivity to a low electron mobility. Furthermore, measurements made on ferrites in which other bivalent metal ions were substituted for some of the Fe^{2+} ions in octahedral sites might yield additional information about the Verwey model and the conductivity of the ferrites. For example, if one expects that electrons will exchange only between octahedral ions belonging to Fe_3O_4 molecules, then in a material such as $(NiO)_{.75}(FeO)_{.25}(Fe_2O_3)$ one would expect approximately one quarter the carrier concentration. Thus, it seemed desirable to make ordinary Hall measurements on this material as well.

The ordinary Hall measurement on Ni near room temperature made by Pugh [10] and his extrapolations from the old temperature data of Smith pointed out the desirability of repeating the room temperature R_o data on Ni and extending the observation over a range of temperature. These measurements were carried out to temperatures above the Curie temperature and led

to an investigation of R_o both above and below the Curie temperature in the 70 Ni - 30 Cu alloy.

The deviation of R_1 from a ρ^2-dependence in Ni indicated that the mechanism provided by the Karplus-Luttinger theory did not accurately describe the effect in Ni. Since Jan's was the only temperature data taken with a simultaneous measurement of resistivity, it seemed worth while to repeat the R_1 measurement on Ni. The results of the measurement on Grade A Ni differed somewhat from those of Jan[11] and led to an investigation of the extraordinary Hall effect in Ni with varying impurity concentrations and in some Ni-Fe alloys.

II.

THE MEASUREMENT PROBLEM

2.1 The Experimental Arrangement

If we denote by I, the total current in the x direction flowing through the sample (Figure 2-1) of thickness t, and H, the magnetic field in the z direction, normal to the plane of the current and the Hall leads, then the Hall voltage for a non-magnetic metal observed in the y direction is given by

$$V_H = R_o H \frac{I}{t} \qquad (2.1)$$

where V_H is in units of practical volts, H is in oersteds, I is in amperes, and t is in cm.

In the case of ferromagnetics, the Hall voltage is composed of two parts; one part is due to $R_1 M$, which we call the extraordinary Hall voltage, and superposed on this is a much smaller voltage due to $R_o H$ which we call the ordinary Hall voltage. We propose to measure this smaller voltage in the region of H where M is a constant, as suggested by Pugh [10]. Thus for ferromagnetics,

$$V_H = (R_o H + R_1 M) \frac{I}{t} \qquad (2.2)$$

and if we differentiate this expression with respect to H, above technical saturation where M is constant we obtain

$$\Delta V_H = R_o \, \Delta H \frac{I}{t} \qquad (2.3)$$

where ΔV_H is the increment of Hall voltage due to the change of field, ΔH.

Technical saturation is obtained at a value of applied field determined by both the magnetization of the material and the demagnetizing factor of the shape of the sample. Technical saturation is achieved in thin strips of Ni at an applied field of the order of 6500 oersteds, and in the cylindrical sample of Fe_3O_4 at an applied field of the order of 3000 oersteds. Therefore, in the case of ferromagnetics we must work at relatively high fields.

We are then concerned with the magnitude of the voltage measured for

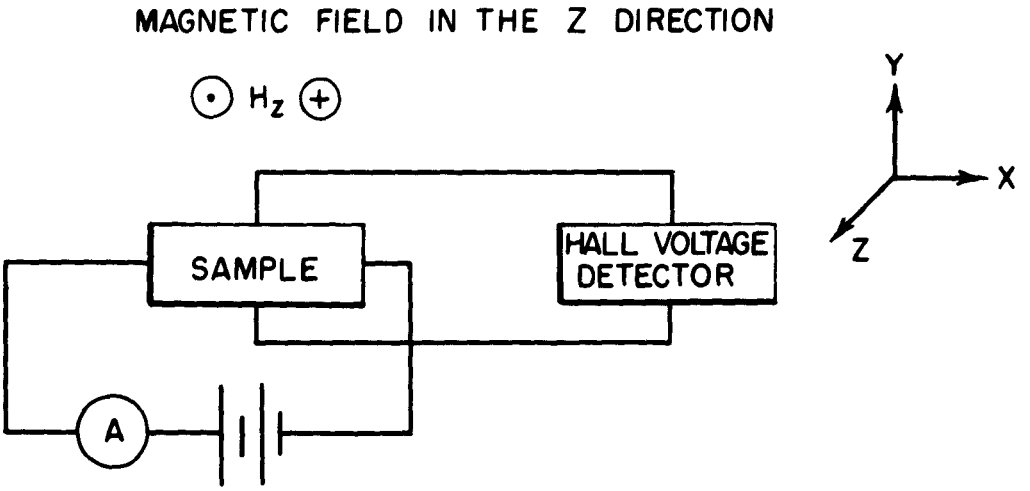

FIG. 2-1 A BLOCK DIAGRAM OF THE EXPERIMENTAL HALL CIRCUIT

fields readily obtained in the laboratory. We compare the voltage observed in Ni with that observed in Fe_3O_4 for values of $\Delta H = 5000$ oersteds above technical saturation. In the case of Ni, $R_o \simeq -6 \times 10^{-13} \frac{\text{volt-cm}}{\text{amp -oersted}}$, $I = 1$ amp., and $t \simeq 1.2 \times 10^{-2}$ cm , we obtain

$$\Delta V_H \simeq \frac{(6 \times 10^{-13})(5 \times 10^{3})(1)}{1.2 \times 10^{-2}} \simeq 2.5 \times 10^{-7} \text{ volts} \qquad (2.4)$$

In the case of Fe_3O_4, $t \simeq 0.5$ cm , with a current limited to 300 ma for reasons explained below, and $R_o \simeq -1.8 \times 10^{-11} \frac{\text{volt-cm}}{\text{amp.-oersted}}$, we obtain

$$\Delta V_H \simeq \frac{(1.8 \times 10^{-11})(5 \times 10^{3})(3 \times 10^{-1})}{5 \times 10^{-1}} \simeq 5 \times 10^{-8} \text{ volts} \qquad (2.5)$$

Thus, we note that the determination of the ordinary Hall coefficient in these materials requires the measurement of relatively small voltages. Moreover, these small voltages must be measured in the presence of large voltages. We have already pointed out the existence of the large extraordinary Hall voltage. In addition, due to the unavoidable asymmetry in the positioning of the probes, we have a voltage present even in the absence of a magnetic field and even with the sample in a demagnetized state. This voltage is due to the positioning of the Hall probes on different equipotential lines, and can be many times larger than the ordinary Hall voltage. Voltages also occur across the Hall probes due to unavoidable thermal gradients in the sample. These voltages are field-and temperature-dependent and impose certain requirements upon the system used to make the ordinary Hall measurement. In the following sections we discuss these effects in greater detail, and describe the methods of eliminating or overcoming the difficulties they present.

2.2 The Interfering Effects

(A) The Other Transverse Effects

Sommerfeld and Frank [24] have given an explanation of the galvanomagnetic and thermomagnetic effects in metals. Using the Boltzmann equation and the free electron theory of metals, they have discussed two types of effects; (1) isothermal effects subject to the condition that the

the temperature in the y direction (perpendicular to the primary current and magnetic field) is constant, i.e., $\frac{\partial T}{\partial y} = 0$, and (2) adiabatic effects in which no heat is allowed to flow in the y direction, i.e., $w_y = 0$, where w_y is the y-directed thermal current. The equations describing the electrical and thermal current densities, due to Sommerfeld and Frank, have recently been altered by Johnson and Shipley [25] to include the lattice contribution to the thermal conductivity. The equations below describe the electrical and thermal current densities.

$$j_x = L_{11}E_x + L_{12}H_zE_y + L_{13}\frac{\partial T}{\partial x} + L_{14}H_z\frac{\partial T}{\partial y} \tag{2.6}$$

$$j_y = -L_{12}H_zE_x + L_{11}E_y - L_{14}H_z\frac{\partial T}{\partial x} + L_{13}\frac{\partial T}{\partial y} \tag{2.7}$$

$$w_x = L_{31}E_x + L_{32}H_zE_y - (L_{33} + K_L)\frac{\partial T}{\partial x} + L_{34}H_z\frac{\partial T}{\partial y} \tag{2.8}$$

$$w_y = -L_{32}H_zE_x + L_{31}E_y - L_{34}H_z\frac{\partial T}{\partial x} - (L_{33} + K_L)\frac{\partial T}{\partial y} \tag{2.9}$$

where j_x, j_y are electric current densities

w_x, w_y are thermal current densities

$\frac{\partial T}{\partial x}$, $\frac{\partial T}{\partial y}$ are temperature gradients

E_x, E_y are electric fields

H_z is the magnetic field

K_L is the lattice contribution to the total thermal conductivity and the L_{ij} are integrals (involving products of the electron velocity, mean free path, electron distribution function, and derivatives over the volume of momentum space and) which need not be known exactly for the purpose of the following argument. They are, in general, different from zero.

The four common transverse effects may now be defined by means of Eqs. (2.6) to (2.9) plus the appropriate conditions.

Isothermal effects:

(1) The Hall effect is defined as

$$E_y = R_o j_x H_z \tag{2.10}$$

subject to the conditions $j_y = \frac{\partial T}{\partial x} = \frac{\partial T}{\partial y} = 0$.

(2) The Nernst effect is defined as

$$E_y = Q H_z w_x \tag{2.11}$$

subject to the conditions $j_x = j_y = \frac{\partial T}{\partial y} = 0$.

Adiabatic effects:

(3) The Ettingshausen effect is defined as

$$\frac{\partial T}{\partial y} = P H_z j_x \tag{2.12}$$

subject to the condition $w_y = j_y = \frac{\partial T}{\partial x} = 0$.

(4) The Righi-Leduc effect is defined as

$$\frac{\partial T}{\partial y} = S H_z w_x \tag{2.13}$$

subject to the condition $j_x = j_y = w_y = 0$.

Since we are primarily concerned with the measurement of the isothermal Hall effect, and since introduction of the adiabatic Hall and Nernst effects does not amplify the following argument, they are not considered here. If we insert the conditions for the Hall effect, i.e., $\frac{\partial T}{\partial x} = \frac{\partial T}{\partial y} = j_y = 0$ into Eqs. (2.6) and (2.7) we obtain

$$j_x = L_{11} E_x + L_{12} H_z E_y \tag{2.14}$$

$$0 = - L_{12} H_z E_x + L_{11} E_y \tag{2.15}$$

whence to the first order in H_z

$$E_y = \frac{\begin{vmatrix} L_{11} & j_x \\ -L_{12} H_z & 0 \end{vmatrix}}{\begin{vmatrix} L_{11} & L_{12} H_z \\ -L_{12} H_z & L_{11} \end{vmatrix}} = \frac{L_{12} H_z j_x}{L_{11}^2} = R_o j_x H_z \tag{2.16}$$

In the case of metal measurements, the conditions $\frac{\partial T}{\partial x} = \frac{\partial T}{\partial y} = 0$ may be fulfilled by immersing the sample in a temperature bath. Thus, contributions to $\frac{\partial T}{\partial x}$ and $\frac{\partial T}{\partial y}$ from contact resistances and Peltier heat can be excluded by virtue of the high thermal conductivity of metals and the thermal capacity of the bath. However, where the sample cannot be immersed in a temperature bath, and especially in the case of semiconductors where large $\frac{\partial T}{\partial x}$ can be generated due to unequal resistances at the current contacts and to large Peltier heat, the isothermal conditions of the Hall measurement are not fulfilled.

In such cases Eqs. (2.6) and (2.7) must be solved subject only to the condition $j_y = 0$, and $\frac{\partial T}{\partial x}$, $\frac{\partial T}{\partial y}$ must be known. An examination of the solution of the above set of equations subject to these conditions shows that:

(1) $E_y \neq R_o j_x H_z$ and the effects superposed are not directly relatable to the transverse effects defined above, as is usually stated in the literature.

(2) The Hall field can be separated out in such cases by suitable combinations of electric (E_x) and magnetic field reversals provided that $\frac{\partial T}{\partial x}$ and $\frac{\partial T}{\partial y}$ remain constant during the field reversal. The Peltier and Thomson effects [26] usually exclude this possibility .

(3) If the electric field E_x is made to alternate with frequency f_o, while H_z is kept fixed, then even with the conditions $\frac{\partial T}{\partial x} \neq 0$, $\frac{\partial T}{\partial y} \neq 0$ the Hall field may be separated out by a suitable filtering device which is tuned to the frequency f_o. While the effects due to $\frac{\partial T}{\partial x}$ and $\frac{\partial T}{\partial y}$ will still be present, they occur at zero frequency.

(4) If the magnetic field H_z is made to alternate with frequency f_1, while E_x is kept fixed, then $E_y \neq R_o j_x H_z$ as may be seen by examination of Eqs. (2.6) and (2.7).

In order to estimate the magnitude of the deviation of the field E_y from the Hall field in the case where $\frac{\partial T}{\partial x} \neq 0$, $\frac{\partial T}{\partial y} \neq 0$, the L_{ij} must be known. In principle, they cannot be obtained by measurement of the transverse effects, nor can they be calculated exactly. We may speculate upon the order of magnitude of the deviation by supposing that we do have superposed on the Hall field, fields due to the other transverse effects. In the case of ferromagnetic metals, even this approximation is denied, since no high-field measurements of these effects have been made. In the ferrites investigated in this research, the Hall voltage was of the same order of magnitude as in metals, and nothing was known of the other transverse effects. However, with a thermo-electric power of the order of 40 microvolts/^oC, a transverse temperature gradient of $10^{-3}{}^oC$ would be sufficient to totally obscure the Hall voltage in the Fe_3O_4 sample. Therefore, it is necessary to insure that $\frac{\partial T}{\partial x} = \frac{\partial T}{\partial y} = 0$, or to use an alternating E_x to make the Hall measurement in this material.

(B) The Magneto-resistance Effect

The second-order change of resistance with magnetic field is usually

small in most metals and semiconductors. However, in ferromagnetics, it is a complicated function of M and H and can be several tenths of a per cent per kilogauss in the region above technical saturation. Due to the unavoidable asymmetry in the position of the Hall probes, a magneto-resistance voltage equal to or greater than the Hall voltage can be generated in ferromagnetics.

For example, in a Ni sample with thickness t = 0.005", width w = 0.750", $\rho \simeq 10^{-5}$ ohm-cm., the uncertainty in the alignment of the soldered Hall probes can be as large as 0.010". The IR drop between probes is given by

$$IR = I\rho \frac{\Delta \ell}{w \cdot t} \qquad (2.17)$$

where $\Delta \ell$ is the uncertainty in the probe alignment. For a current of 1 ampere,

$$IR \simeq \frac{(1)(10^{-5})(10^{-2})}{(.75)(5 \times 10^{-3})(2.54)} \simeq 10^{-5} \text{ volts} \qquad (2.18)$$

For a field of 5,000 oersteds above saturation Bozorth [12, p. 749) indicates that the change of resistance with magnetic field is

$$\frac{\Delta \rho}{\rho} \simeq 10^{-2} \qquad (2.19)$$

Therefore,

$$\frac{I \Delta R}{IR} = \frac{\Delta \rho}{\rho} \simeq 10^{-2} \qquad (2.20)$$

where ΔR is the increase of R due to H, and

$$I \Delta R \simeq 10^{-7} \text{ volts.} \qquad (2.21)$$

The ordinary Hall voltage for this sample is estimated in Eq. (2.4) to be $\Delta V_H \simeq 2.5 \times 10^{-7}$ volts. Therefore,

$$\frac{\Delta V_H}{I \Delta R} \simeq \frac{2.5 \times 10^{-7}}{10^{-7}} \simeq 2.5 \qquad (2.22)$$

In the case of Fe_3O_4, the measurement was made on a cylindrical sample, d = 0.250". Since $\rho \simeq 10^{-2}$ ohm-cm., care was taken in the probe alignment to minimize the IR drop. Nevertheless, $\Delta \ell$ was probably not much less than 0.005". Therefore, the IR drop between the probes for a current of 300 ma. is

$$IR = \frac{I\rho\Delta\ell}{\pi r^2} \simeq \frac{(3 \times 10^{-1})(10^{-2})(5 \times 10^{-3})}{\pi(.125)^2(254)} \simeq 10^{-4} \text{ volts.} \qquad (2.23)$$

The order of magnitude of the magneto-resistance effect in Fe_3O_4 is approximately the same as in Ni. Masumoto and Shirakawa [27] have reported on magneto-resistance measurements on a natural single crystal of Fe_3O_4 at 0^oC. Their measurements and observed results both indicate that $\frac{\Delta\rho}{\rho} \simeq 5 \times 10^{-3}$ for 5000 oersteds above technical saturation. Therefore, the magneto-resistance voltage developed across the Hall probes is

$$I\Delta R \simeq IR \times 5 \times 10^{-3} \simeq 5 \times 10^{-7} \text{ volts.} \qquad (2.24)$$

The ordinary Hall voltage for this sample has been estimated in Eq. (2.5) to be $\Delta V_H \simeq 5 \times 10^{-8}$ volts. Thus,

$$\frac{\Delta V_H}{I\Delta R} \simeq \frac{5 \times 10^{-8}}{5 \times 10^{-7}} \simeq 10^{-1} \qquad (2.25)$$

(C) The Extraordinary Effect

The ordinary Hall voltage is superposed on the extraordinary voltage as given by the expression for the normalized Hall voltage in Eq. (1.1)

$$e_H = R_o H + R_1 M \qquad (2.26)$$

The ratio of the ordinary Hall effect to the extraordinary Hall effect in Ni is given by

$$\frac{R_o \Delta H}{R_1 M_s} \simeq 6 \times 10^{-2} \qquad (2.27)$$

for $\Delta H = 5000$ oersteds, at room temperature.

In the case of Fe_3O_4,

$$\frac{R_o \Delta H}{R_1 M_s} \simeq 6 \times 10^{-3} \qquad (2.28)$$

for $\Delta H = 5000$ oersteds, at room temperature. Therefore, if the ordinary effect in Fe_3O_4 is to be measured with an accuracy of 1 per cent, the two effects must be separated by a system with a resolution of at least 6 parts in 10^5.

(D) The Change in Magnetization above Technical Saturation

Having proposed that the Hall voltage in ferromagnetics be written

$$e_H = R_o H + R_1 M \tag{2.29}$$

Pugh, Rostoker, and Schindler [10] then suggested that R_o be obtained from the slope above technical saturation where M is constant

$$\frac{\Delta e_H}{\Delta H} = R_o \tag{2.30}$$

where Δe_H, ΔH denote increments in e_H and H.

If M is not exactly constant over the region in which R_o is measured, we must write Eq. (2.30) as

$$\frac{\Delta e_H}{\Delta H} = R_o + R_1 \frac{\Delta M}{\Delta H} = R_o\left(1 + \frac{R_1}{R_o} \frac{\Delta M}{\Delta H}\right) \tag{2.31}$$

Then, in the case of Ni where $\frac{R_1}{R_o} \simeq 2 \times 10^2$, a change in M of the order of 1/4 gauss in 5000 oersteds results in a 1 per cent error in R_o. In the case of Fe_3O_4, where $\frac{R_1}{R_o} \simeq 2 \times 10^3$, a similar change in M produces a 10 per cent error.

Although M displays a saturation effect, the approach to saturation is given by [ref. 12, p. 486].

$$M = M_s\left(1 - \frac{a}{H} - \frac{b}{H^2} \cdots\right) + K_o H, \tag{2.32}$$

where H is the field inside the material. The term in $\frac{a}{H}$ has been explained by Néel [28] as due to nonmagnetic cavities or inclusions in the material. The term in $\frac{b}{H^2}$ depends upon the magnetic anisotropy and the elastic state of the crystal. In the case of single crystals, the term in $\frac{b}{H^2}$ is strongly dependent upon orientation of the crystal axes with respect to the magnetic field. In the case of polycrystalline material, the term in $\frac{b}{H^2}$ has been obtained by Akulov [29] and Gans [30] by averaging over all crystal orientations. The K_o term which may be crudely described as the field alignment of temperature-disoriented spins has been calculated by Holstein and Primakoff [31] in good agreement with the values observed for Fe and Ni.

In the case of polycrystalline Ni, typical values of the coefficients are $\underline{a} \simeq 1/3$, and $\underline{b} = \frac{8K^2}{105M_s^2}$ provided that the sample is not severely strained,

where K is the first-order anisotropy constant and $K \simeq -59{,}000\ \text{ergs/cm}^3$ at room temperature. Thus, fields of the order of 1000 oersteds are required to eliminate any appreciable changes in M over the region in which R_o is measured. This means that in the case of Ni sheet, where the demagnetizing factor is very nearly 4π, applied fields greater than 7000 oersteds must be used to measure R_o. In the case of Ni, we still have a small change in M due to K_o, which is estimated to be about 0.5 gauss for a field of 5000 oersteds.

In the case of Fe_3O_4 these effects caused considerable difficulty and they are treated more fully in Appendix B.

(E) Temperature Stability

Temperature variation of the resistivity ρ, and hence of the IR drop between the Hall probes can cause error in the determination of R_o since the IR drop must be subtracted from the total voltage present in order to measure R_o.

As pointed out in Eq. (2.18), the IR drop in Ni is of the order of 10^{-5} volts.

$$\frac{1}{\rho}\frac{\partial \rho}{\partial T} \simeq 5 \times 10^{-3}/^{\circ}C \tag{2.33}$$

in Ni at room temperature [32].

$$\frac{1}{IR}\frac{\partial}{\partial T}(IR) \simeq 5 \times 10^{-3}/^{\circ}C \tag{2.34}$$

and

$$\frac{\partial}{\partial T}(IR) \simeq (5 \times 10^{-3})(10^{-5}) \simeq 5 \times 10^{-8}\ \text{volts}/^{\circ}C \tag{2.35}$$

The ordinary Hall voltage for Ni is estimated in Eq. (2.4) to be $\Delta V_H \simeq 2.5 \times 10^{-7}$ volts and

$$\frac{\frac{\partial}{\partial T}(IR)}{\Delta V_H} \simeq \frac{5 \times 10^{-8}}{2.5 \times 10^{-7}} \simeq 2 \times 10^{-1}/^{\circ}C. \tag{2.36}$$

Therefore, temperature stability of the order of $0.05^{\circ}C$ is required in a room temperature measurement of R_o in Ni.

The IR drop in Fe_3O_4, as pointed out in Eq. (2.23), is of the order of 10^{-4} volts.

$$\frac{1}{\rho}\frac{\partial \rho}{\partial T} \simeq 5 \times 10^{-3}/^{\circ}C \qquad (2.37)$$

at room temperature, and

$$\frac{\partial}{\partial T}(IR) \simeq (10^{-4})(5 \times 10^{-3}) \simeq 5 \times 10^{-7} \text{ volts}/^{\circ}C \qquad (2.38)$$

Since the ordinary Hall voltage estimated in Eq. 2.5 is $\Delta V_H \simeq 5 \times 10^{-8}$ volts,

$$\frac{\frac{\partial}{\partial T}(IR)}{\Delta V_H} \simeq \frac{5 \times 10^{-7}}{5 \times 10^{-8}} \simeq 10/^{\circ}C \qquad (2.39)$$

Therefore, temperature stability of the order of $10^{-3}{}^{\circ}C$ is needed to keep the uncertainty in R_o less than 1 per cent.

The temperature stability problem in Ni at room temperature is negligible. In the case of Fe_3O_4, thermal instability arises mainly from the large amount of heat generated at the current contacts and the poor thermal conductivity of the material. Although electrical contact is made at large area, Cu-plated, spring-loaded contacts, nevertheless, the resistance across the contacts is 5 to 100 times the body resistance in F_3O_4 and in the other ferrite sample. Therefore, in order to minimize heat generation and to assure temperature stability, the sample current must be limited to low values.

(F) Noise

The measurement of voltages below 0.1 microvolt is fundamentally concerned with noise in both the detection system and in the system under investigation. Techniques are available for noise minimization in both ac and dc detection systems [33,34]. Provided that the amplifier noise has been minimized, the noise problems occur in the sample.

Certain classes of semiconductors evidence noise power greater than that found in a metal resistor. The mean square voltage of this excess noise is roughly proportional to the current squared and inversely proportional to the frequency, down to very low frequencies. Rollin and Templeton [35,36] report that the I^2 and $\frac{1}{f}$ dependence occurs down to 2.5×10^{-4} cps in carbon resistors and Ge. While the noise in ferrites has not been examined in detail, the samples investigated in this research evidenced noise power which

appeared to possess the above characteristics.

The mean square noise voltage present in a metallic resistance R, at the absolute temperature T, in the bandwidth Δf is given by

$$\overline{e^2} = 4\,k\,TR\,\Delta f \tag{2.40}$$

where k is the Boltzmann constant. To take account of the excess noise in semiconductors, an effective noise temperature T' is defined such that the mean-square noise voltage in a semiconductor of resistance R over the bandwidth Δf is given by

$$\overline{e^2} = 4\,kT'R\,\Delta f \tag{2.41}$$

Then,

$$t = \frac{T'}{T} \tag{2.42}$$

where T is the absolute temperature of the semiconductor, and $t > 1$ for a semiconductor.

If we substitute the value of the resistance between the point contacts in the Fe_3O_4 sample ($\sim$10 ohms) and assume $\Delta f = 4$ cps then for $t = 1$ (no excess noise) we obtain

$$\overline{e^2} = (4)(1.38) \times 10^{-23}(300)(10)(4) = 66.2 \times 10^{-20}\text{volts}^2 \tag{2.43}$$

$$(\overline{e^2})^{1/2} \simeq 8 \times 10^{-10}\text{volts} \tag{2.44}$$

Therefore, in the case of metal samples in which no excess noise exists, sample noise poses no problem. In the case of semiconductors in which values of t at low frequencies of the order of 10^4 have been reported [37] sample noise can cause serious difficulty in a low-level Hall measurement.

Since the mean square excess noise voltage is proportional to I^2 in semiconductors, then

$$(\overline{e^2})^{1/2} \sim I \tag{2.45}$$

and no increase in signal-to-noise ratio can be obtained by increasing the current, because the Hall voltage is also linear in I.

Furthermore, if we assume that the excess noise power is due to conductivity modulation, then the excess noise power, which varies as $\frac{1}{f}$

about the current frequency has its maximum value at the current frequency. This means that if we reduce Δf in Eq. (2.41), we increase T' in such a manner that $\overline{e^2}$ remains practically constant. This can be shown in the following manner.

$$\overline{e^2} = K' I^2 \frac{df}{f} = K \frac{df}{f} \tag{2.46}$$

Suppose we reduce the bandwidth over which we examine the noise from 4 cps to 1 cps. In the case of a metallic resistance, Eq. (2.40) shows that we decrease the mean-square noise voltage by a factor of 4. In the case of a semiconductor from Eq. (2.46) we obtain the following:

$$\overline{e_1^2} = K \int_{\epsilon}^{4} \frac{df}{f} \tag{2.47}$$

is the excess noise present in a bandwidth of 4 cps where ϵ is a very small positive number.

$$\overline{e_2^2} = K \int_{\epsilon}^{1} \frac{df}{f} \tag{2.48}$$

is the excess noise present in a bandwidth of 1 cps. The ratio of the two mean-square excess noise voltages is then

$$\frac{\overline{e_2^2}}{\overline{e_1^2}} = \frac{K \int_{\epsilon}^{1} \frac{df}{f}}{K \int_{\epsilon}^{4} \frac{df}{f}} = \frac{\int_{\epsilon}^{1} \frac{df}{f}}{\int_{\epsilon}^{1} \frac{df}{f} + \int_{1}^{4} \frac{df}{f}} \tag{2.49}$$

$$\frac{\overline{e_2^2}}{\overline{e_1^2}} = \frac{1}{1 + \dfrac{\int_{1}^{4} \frac{df}{f}}{\int_{\epsilon}^{1} \frac{df}{f}}} = \frac{1}{1 + \dfrac{\ell n 4}{\ell n \frac{1}{\epsilon}}} \tag{2.50}$$

In the limit as $\epsilon \longrightarrow 0$

$$\lim_{\epsilon \to 0} \frac{\ell n\, 4}{\ell n\, 1/\epsilon} = 0 \qquad (2.51)$$

and

$$\frac{\overline{e_2^2}}{\overline{e_1^2}} = 1 \qquad (2.52)$$

Although this calculation has been carried out about zero frequency, the same conclusions obtain in the case of a semiconductor excited at the frequency f_o. In this case, the noise power is concentrated at the frequency f_o and varies as $\frac{1}{|f_o - f|}$. Thus, no reduction in excess noise power is achieved until the bandwidth is reduced almost to zero, since most of the excess noise power is concentrated in a very narrow bandwidth.

Fortunately, the Fe_3O_4 sample possessed a very low effective noise temperature, with a value of t of the order of 200 for the current used, and hence the measurement could be made with a 4 cps bandwidth.*

2.3 The Choice of an AC or DC System

One of the more important decisions made in the course of this research was the changeover from a dc to an ac system. In retrospect, the advantages of the ac system far outweigh the dc system. However, since the literature abounds in misstatements concerning the efficacy of both, the choice of the type of system to be used in the measurements is worthy of consideration under the topic of measurement problems.

An ac system is one in which either the electric field E_x, or the magnetic field H_z, or both are made to alternate. The discussion of section 2-2A shows that the alternation of the magnetic field only, does not insure complete separation of the Hall voltage from the other transverse effects. We therefore restrict our discussion to the cases where only E_x, or both E_x and H_z are made to alternate.

- - - - - -

*Recently, Van Vliet, Van Leeuwen, Blok, and Ris [38] have reported that the noise in high resistivity ferrites is down by a factor of 10^3 over the value in a carbon resistor, and that there are in some cases deviations from an f^{-1} spectrum ($f^{-1.1}$). Furthermore, they report an $I^{1.2}$ current dependence of excess noise. However, their measurements were made at very low current values.

As early as 1900, Des Coudres [39] made a Hall measurement on bismuth by passing the same alternating current through the sample and the magnet. The output was then read with a dc galvanometer. Such a system offers little advantage since the measurement is still subject to the difficulties which inhere in a low-level dc measurement. Furthermore, unless $\frac{\partial T}{\partial x} = \frac{\partial T}{\partial y} = 0$, the measurement is susceptible to uncertainty in the measured field, as can be seen by examination of Eqs. (2.6) and (2.7). A superior technique is to use a frequency f_o for the electric field E_x, and a frequency f_1 for the magnetic field H_z. Then, at the Hall probes of a nonmagnetic material, there exist the following voltages:

$$(V_y)_{total} = I_x R + I_x \Delta R(H_z^2) + V_H(I_x, H_z) + V_1(H_z, \frac{\partial T}{\partial x}) + V_2(H_z, \frac{\partial T}{\partial y}) + V_{dc} \quad (2.53)$$

where $I_x R$ is the voltage drop due to the misalignment of the probes, $I_x \Delta R(H_z^2)$ is the voltage due to the magnetoresistance effect, which is an even-valued function of the field. $V_H(I_x, H_z)$ is the Hall voltage. $V_1(H_z, \frac{\partial T}{\partial x})$ and $V_2(H_z, \frac{\partial T}{\partial y})$ are voltages which arise from the terms in $H_z \frac{\partial T}{\partial x}$, $H_z \frac{\partial T}{\partial y}$ in Eqs. (2.6) and (2.7). V_{dc} includes all terms in Eqs. (2.6) and (2.7) which do not vary at the frequency f_o, f_1 or combinations of these frequencies in addition to the usual contact potential, and thermoelectric potentials which occur in any low-level dc system. If we assume $E_x = E_o \cos \omega_o t$ and hence $I_x = I_o \cos \omega_o t$ and $H_z = H_o \cos \omega_1 t$, then provided that $\frac{\partial T}{\partial x}$ and $\frac{\partial T}{\partial y}$ do not vary at the frequency f_o, a condition which can be obtained by making f_o sufficiently large, we may write

$$(V_y)_{total} = I_o R \cos \omega_o t + I_o \Delta R \cos \omega_o t \cos^2 \omega_1 t + V_H \cos \omega_o t \cos \omega_1 t \quad (2.54)$$
$$+ V_1 \cos \omega_1 t + V_2 \cos \omega_1 t + V_{dc}$$

By trigonometric substitution,

$$(V_y)_{total} = I_o R \cos \omega_o t + \frac{I_o \Delta R}{2} \left\{ \cos \omega_o t + \frac{1}{2} \cos(\omega_o + 2\omega_1) t + \frac{1}{2} \cos(\omega_o - 2\omega_1) t \right\} \quad (2.55)$$

$$+ \frac{V_H}{2} \left\{ \cos(\omega_o + \omega_1) t + \cos(\omega_o - \omega_1) t \right\} + V_1 \cos \omega_1 t + V_2 \cos \omega_1 t + V_{dc}$$

Thus, if the detector is tuned to $\omega_o + \omega_1$ or $\omega_o - \omega_1$, only $\frac{V_H}{2}$ is observed. In Des Coudres' experiment, since $\omega_o = \omega_1$, a measurement at $2\omega_o$ would have excluded the unwanted effects.

An additional advantage to the above scheme accrues in semiconductor measurements where the maximum excess noise power occurs at the frequency f_o. Measurements made at $f_o \pm f_1$ encounter a noise power reduced by a factor of $\frac{1}{|f_o - f_1|}$.

Such techniques have been used recently. Russell and Wahlig [40] have used a 70 cps current, a 60 cps magnetic field, and a detector tuned at 10 cps. Pell and Sproull [41], have used a 24 cps current and a magnetic field which reverses every six seconds ($f_1 = \frac{1}{12}$ cps). Because $\omega_o \pm \omega_1 \simeq \omega_o$, the IR drop must be cancelled out by other means, and the advantage of reduction in noise power is lost. However, since much larger magnetic fields are available with this technique, the signal-to-noise ratio need not be decreased.

In the case of ferromagnetics, an additional term proportional to $R_1 M(H_z) I_x$ must be added to Eq. (2.53). In order to resolve the $R_o H_z I_x$ term from the $R_1 M(H_z) I_x$ term advantage must be taken of the saturation effect of M, and hence the alternating magnetic field must be superimposed upon a static field H_o, such that

$$H_z = H_o + H_1 \cos \omega_1 t \qquad (2.56)$$

where $H_o - H_1$ is sufficient to saturate the material. Since it is very difficult to obtain large alternating fields (Russell and Wahlig reported a field of 2000 oersteds), the additional requirement of a large static field precluded the use of such a technique in this research.

The important advantages of an ac system are the elimination of spurious contact potentials, thermoelectric potentials and their drifts with time and temperature, the exclusion of other transverse effects, and the ease with which signals may be amplified.

On the other hand, classical techniques using dc potentiometers and galvanometers are very adequate in making Hall measurements on low impedance samples where adequate precautions may be taken to exclude

the transverse effects, provided that voltages of the order of 50 microvolts or larger are to be measured. In this range, contact and thermoelectric potentials and their drifts do not pose too serious a problem. Furthermore, standard cells provide an absolute voltage reference, stable and accurate to one part in 10^5. Current and voltage stabilization may be readily accomplished by the use of dry or storage batteries, or by systems employing them as reference standards. Laboratory voltmeters and ammeters are readily available with an accuracy of 1/4 of 1 per cent. In addition, voltages greater than 10 millivolts can be read to one part in 10^4 and voltages up to 10 millivolts can be read to one microvolt.

While dc techniques can be employed in the submicrovolt range by calibrating the deflection of a galvanometer or by using a chopper-type dc amplifier, in addition to serious contact and thermoelectric potential problems, there are problems of galvanometer vibration and 60 cps pickup in dc amplifiers. Furthermore, although dc chopper-type amplifiers can achieve a sensitivity of 10^{-18} watts, this sensitivity may be obtained only with ideal experimental conditions. On the other hand, ac amplifiers can readily achieve a sensitivity of 10^{-19} watts under any normal experimental conditions. In comparison with the dc amplifier, a high sensitivity galvanometer matched to a low impedance sample, can have a sensitivity of the order 10^{-17} watts.

There are also very definite disadvantages to an ac measurement. One of the more serious difficulties is the effect of vibrations set up by the alternating current in the magnetic field. This induces a spurious voltage in the Hall loop which is not an even-valued function of the magnetic field and which can be large compared to the Hall voltage. In addition, absolute calibration of an ac system is difficult. Thermal meters provide about 1 per cent accuracy at impedance levels which are not usually optimum for the measurement. Nevertheless, these problems are much less severe than those encountered with a low level dc system.

2.4 Statement of the Problem

As evidenced in the previous sections, the measurement of the Hall voltage in Fe_3O_4 is a more difficult problem than the measurement in Ni.

Therefore, the equipment design must be predicated upon the Fe_3O_4 measurement. The detector must be capable of detecting a Hall voltage of the order of 5×10^{-8} volts in the presence of $\frac{1}{f}$ type noise While increase of sample current I results in an increase of the Hall voltage, there is no gain in signal-to-noise ratio since the mean square noise voltage is proportional to I^2, as previously noted. Furthermore, the attendant thermal instability with increase of current makes the IR subtraction more difficult. In order to eliminate the magneto-resistance effect, a field-reversal technique must be used since the required alternating magnetic field cannot be obtained. Equation (2.53) then shows that the IR drop estimated in Eq. (2.23) to be of the order of 10^{-4} volts, must be subtracted from the total voltage present at the Hall probes. Since the ratio of the IR drop to the Hall voltage estimated in Eqs. (2.23) and (2.5) is

$$\frac{IR}{\Delta V_H} \simeq \frac{10^{-4}}{5 \times 10^{-8}} \simeq 2 \times 10^3 \qquad (2.57)$$

both the current, I, and the voltage used to buck out the IR drop must be stable to at least 2 parts in 10^5 if the two effects are to be separated with an accuracy of 1 per cent. The transverse effects must be eliminated, or suitable provision must be made to insure that their effects are small. The $R_o \Delta H$ term must be separated from the $R_1 M_s$ term. Since the ratio of these two effects estimated in Eq. (2.28) is $\frac{R_o \Delta H}{R_1 M_s} \simeq 6 \times 10^{-3}$, the system must possess a voltage resolution of at least 6 parts in 10^5, if the Hall voltage is to be determined to 1 per cent.

These were the design criteria for the equipment used in this research

2.5 The Solution

An ac system using a 1000 cps current and a dc magnetic field was employed. The use of 1000 cps effectively eliminated the transverse effects the spurious dc potentials, and simplified the amplification problem. A high-gain amplifier (160 db) tuned at 1000 cps was fed into a narrow-band (4 cps) detector providing an adequate noise level (3×10^{-9} volts). With currents of approximately 300 ma, through the Fe_3O_4 sample, the noise level increased only by a factor of 3-4. Amplification problems are simple at 1000 cps;

60 cps pickup poses no problem. The field reversal technique and the method of resolving the ordinary Hall voltage from the extraordinary effect are outlined below. Sample current and bucking voltage were maintained stable by means of voltage and frequency regulation and large amounts of feedback.

Figure 2-2 Shows a block diagram of the equipment
Figure 2-3 Shows a typical curve of the Hall voltage in ferromagnetic.
Figure 2-4 Shows the field-reversal technique of making the ordinary Hall measurement.

The ≠1 bucking voltage was used to buck out all pick-up voltages, the IR drop due to misalignment of Hall contacts, and both the Hall and magneto-resistance voltages for one direction of the field at a point above saturation called H_1 down on the diagram. The field was then reversed, and the ≠2 unit switched into the circuit. The output voltage $2V_{H_1}$ for the value of the field H_1 was then stored in the ≠2 bucking voltage unit with its phase reversed. With the ≠2 bucking unit switched out, and the field at the point H_2 down, the ≠1 bucking unit was used to buck out the voltages added to those already present, namely, the ordinary Hall voltage and the magneto-resistance for the increment of field $H_2 - H_1 = \Delta H$. With the field reversed, i.e., point H_2 up on the diagram, the voltage stored in the ≠2 unit was inserted, performing the operation $2V_{H_2} - 2V_{H_1} = 2\Delta V_H$, where ΔV_H is the ordinary Hall voltage for the increment of field ΔH.

A vector diagram of the measurement technique with no attempt to retain the relative scale of the vectors since they may be of the order of 10^4:1 is shown in Fig. 2-5.

Since the signal-to-noise ratio at the output of the amplifier was low, the sign of ΔV_H and hence R_o was obtained in the following indirect manner: the sign of the extraordinary effect V_{H_1} was compared with the known sign of the extraordinary effect in Ni on the phase comparator oscilloscope. The sign of ΔV_H determined by the slope of the curve above saturation was then given by $V_{H_2}/V_{H_1} \gtrless 1$, or alternatively stated, whether $2V_{H_2}$ was greater than or less than the voltage stored in the ≠2 unit. This was most readily determined by increasing or decreasing the magnitude of the ≠2 bucking voltage and observing the output of the narrow-band detector.

The system possessed an important means of checking for the presence of spurious signals of the same order of magnitude as ΔV_H, which were H-dependent and not in phase with the current. As may be readily ascertained from the vector diagram, the addition of an H dependent voltage not in phase with the current results in $2V_{H_2}$ being of a different phase from $2V_{H_1}$, the voltage stored in the ≠2 bucking unit. Even if the spurious voltage is linear in H, this result obtains because the voltage V_{H_1} is proportional to R_1M and the voltage V_{H_2} is proportional to R_1M plus $R_o \Delta H$ and hence not linear in H. Thus, a voltage larger than the true Hall voltage would be observed on the output meter. Its presence could be determined by minimizing the output voltage with a phase adjustment of the ≠2 unit. This technique was used to assure that all effects of vibration were removed from the system.

In order to determine the extraordinary Hall coefficient, R_1, a field-reversal measurement was made at H_1 and the output voltage $2V_{H_1}$ was read directly. At the value of applied field H_1, it was assumed that the sample was saturated and that the field H inside the material was small. Hence Eq. (2.2) was approximated by

$$V_{H_1} \simeq R_1 M_s \frac{I}{t} \qquad (2.58)$$

Therefore, with a value of M_s appropriate to the temperature and the material, R_1 may be determined.

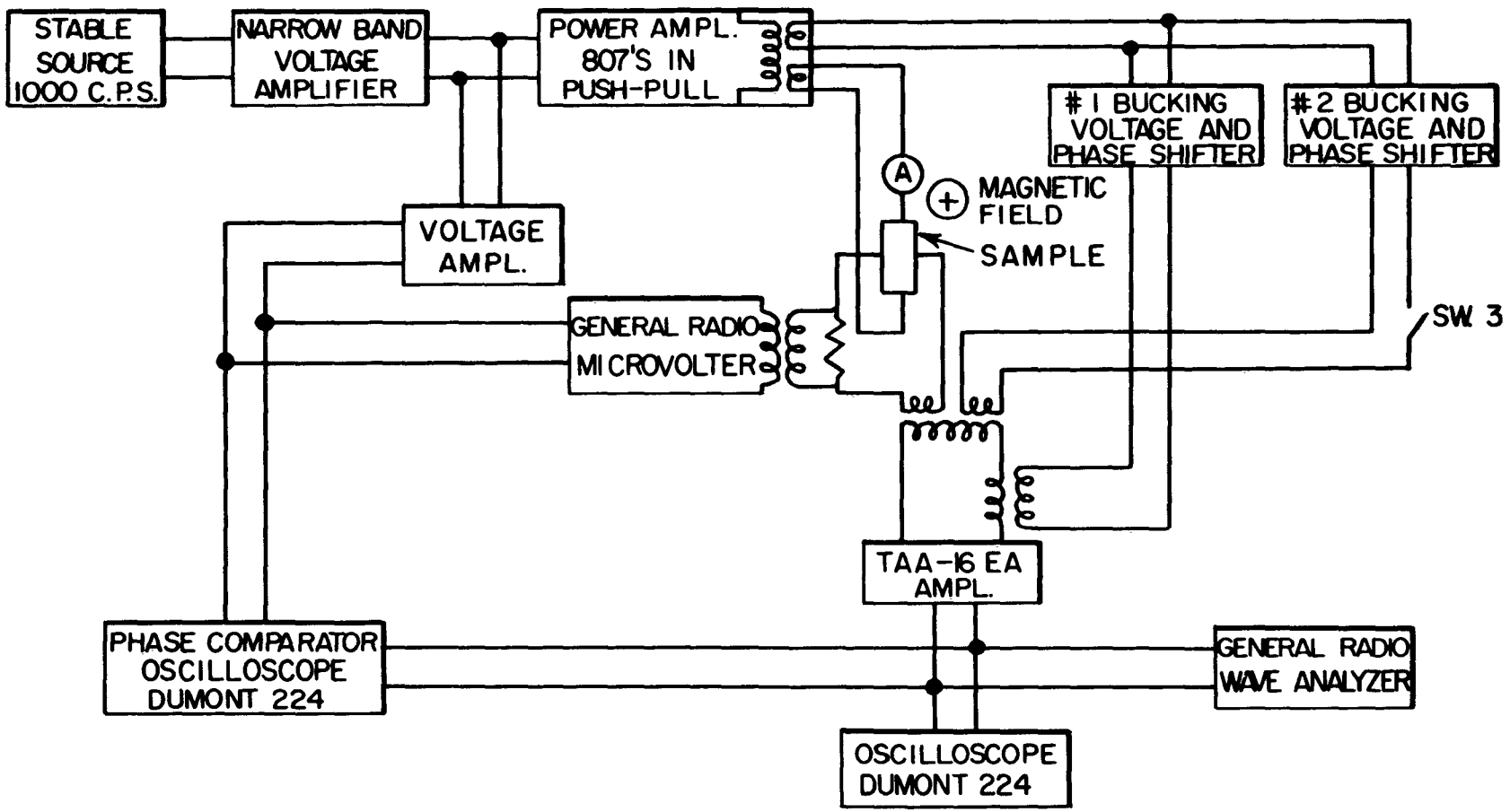

FIG. 2-2 BLOCK DIAGRAM OF EQUIPMENT

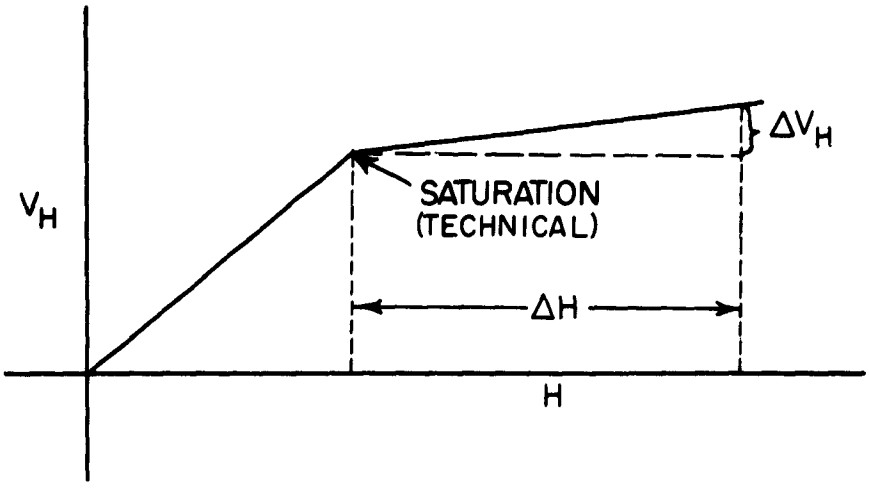

FIG. 2–3 A TYPICAL CURVE OF THE HALL VOLTAGE AS A FUNCTION OF THE APPLIED MAGNETIC FIELD IN A FERROMAGNETIC MATERIAL

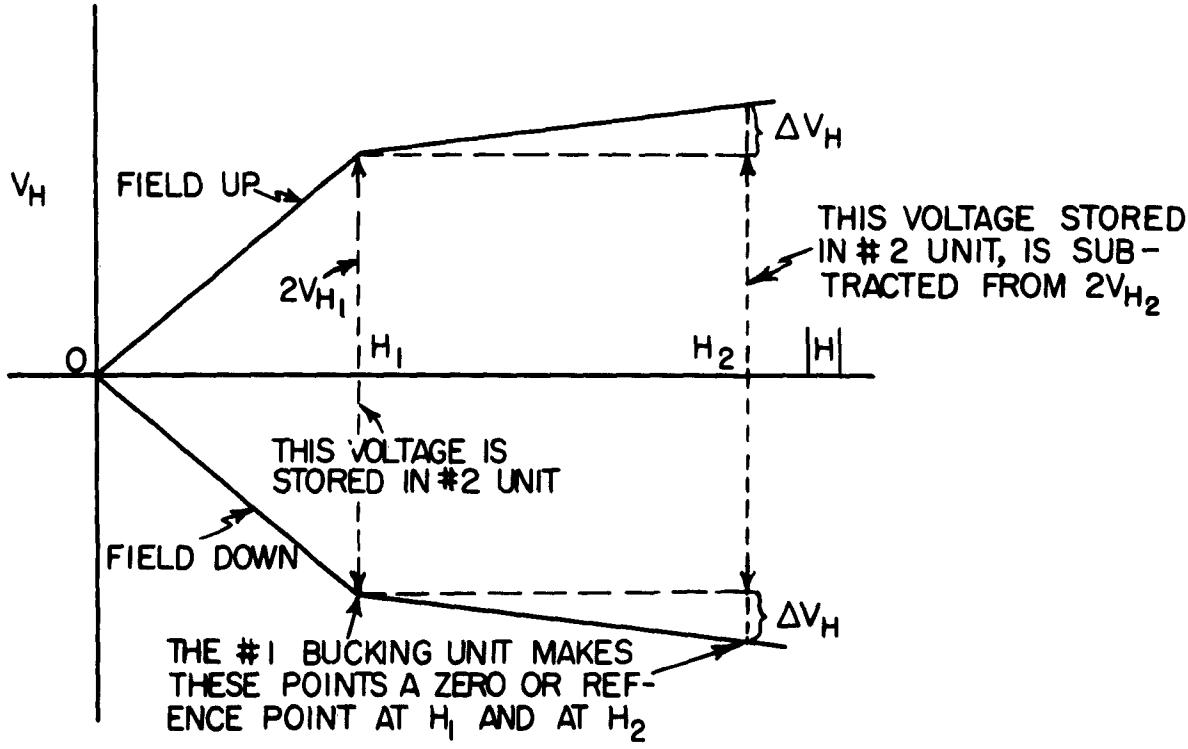

FIG. 2–4 THE FIELD REVERSAL TECHNIQUE OF MAKING THE ORDINARY HALL MEASUREMENT

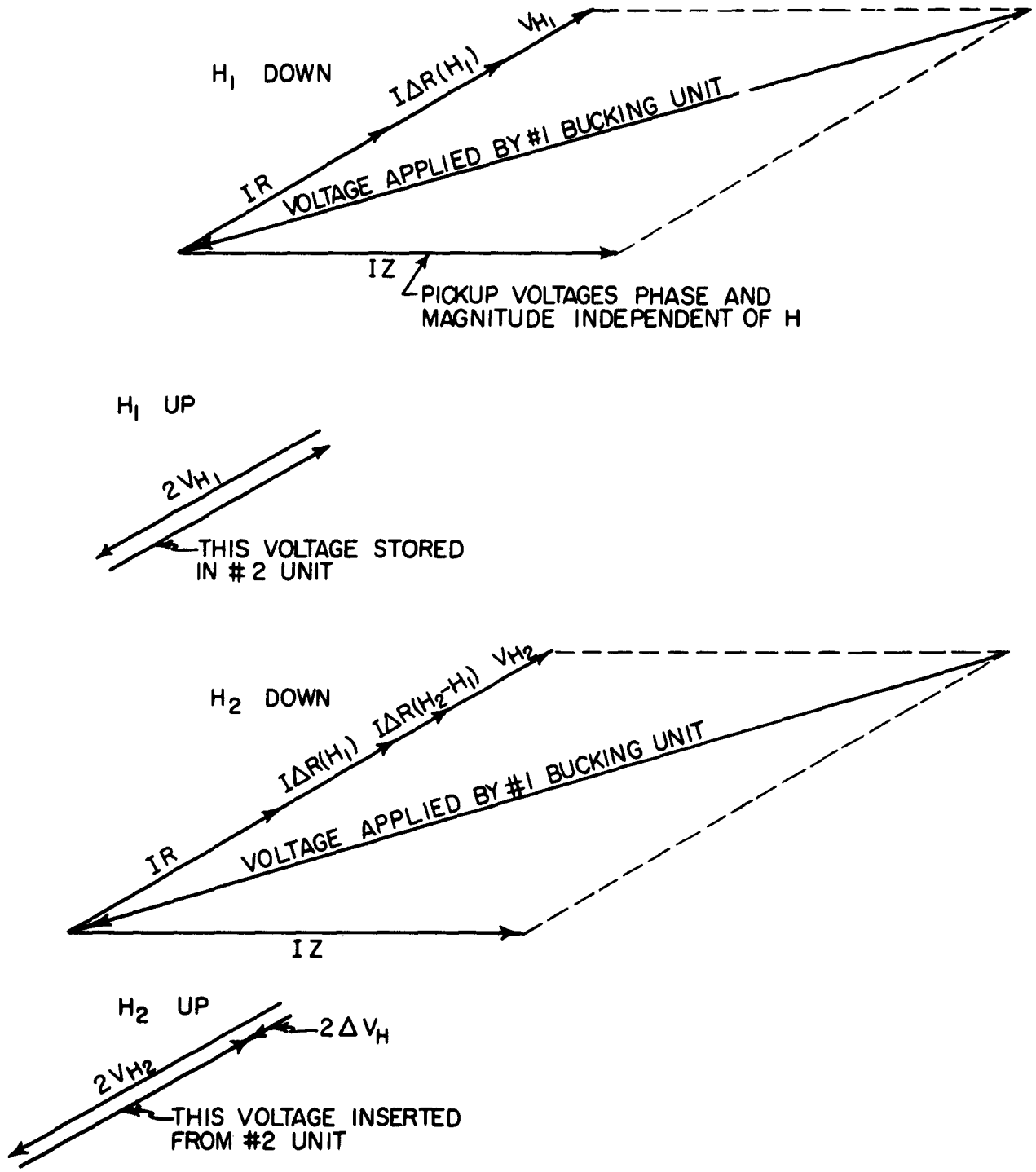

FIG. 2-5 A VECTOR DIAGRAM OF THE MEASUREMENT TECHNIQUE

III.

THE EXPERIMENTAL APPARATUS AND TECHNIQUES

3.1 The Measuring Equipment

(A) The 1000 cps Source

In order to subtract out the IR drop in Fe_3O_4, it was necessary that the sample current and bucking voltage remain stable to 2 parts in 10^5. The bucking system employed R-C phase shifters in order to obtain the necessary resolution in phase angle. Since the phase angle θ is proportional to $\frac{2}{\omega}$, the frequency stability requirement was of the order of one part in 10^5.

The 1000 cps source was obtained from a 100 kc oscillator maintained by the Wave Propagation Group at Harvard [42] and reduced by a 5-2-5-2 division. The oscillator with temperature controlled crystal, compensated for aging, was stable to at least one part in 10^9.

The output of the divider stages was passed through a low-pass filter, a high-Q stage of amplification and transmitted 350 feet over RG 58/U coaxial cable to the location of the experiment.

(B) The Power Amplifier Chassis

The 1000 cps signal was fed into the power amplifier chassis, Fig. 3-1, where the remaining high-frequency components of the source and 60 cycle pickup were removed by appropriate low-pass filters and twin-tees. The 0.5 volt delivered at the input was amplified in 6 single-ended stages and one push-pull stage to drive a pair of 807's in push-pull. The output transformer (U.T.C. LS6L4) was capable of handling 55 watts. Negative feedback was provided in the loop from the output transformer to the cathode of the fifth stage. The power amplifier was a standard 20-watt design with the exception of a bias control potentiometer for the 807's, to insure equal and opposite direct currents in the two halves of the split primary of the output transformer. The low-impedance secondary winding of the output transformer provided the sample current; the high-impedance (500 ohms) winding provided the voltage for bucking purposes. This scheme had the advantage of permitting

both the sample current and the bucking voltage to change by a small amount without upsetting the IR subtraction. The plate voltages of all stages of voltage and power amplification were regulated with standard supplies designed for the system. While capable of delivering 5 amperes into low-impedance samples (1. ohm), 1 ampere was standardized upon for all metal measurements. This provided adequate signal and optimum stability. The harmonic content of the sample current was of the order of 1 per cent, concentrated in the second and third harmonics.

One half of a 6 SL7, in a transformer-coupled stage, was used to drive a General Radio Microvolter for calibration purposes, and to provide a reference signal for phase comparisons.

The sample current was read by a 0-1 ampere, panel mounted meter calibrated with a laboratory standard. Provision was made for inserting an external meter into the circuit to read larger or smaller currents.

(C) The Detector

The detector consisted of two standard laboratory devices. The TAA-16EA Twin-Tee Amplifier designed at the M.I.T. Radiation Laboratory [43] and built by the Electronic Corporation of America provided a gain of 160 db. With the transformer input to the amplifier shown in Fig. 3-2 (impedance ~50 ohms) the noise level of the amplifier was of the order of 0.1 microvolt. The bandwidth of the detector system was further reduced by feeding the output of the amplifier into a General Radio-Wave Analyzer with a 4-cycle bandwidth. This provided the system with a noise level of 3×10^{-9} volts. The system linearity is shown in Fig. 3-3.

It was quite important in using a high gain amplifier in a system with large ground currents, that no closed ground loops exist between output and input of the amplifier.

(D) The Bucking, Adding, and Calibrating Circuits

The bucking units provided voltages of the proper amplitude and phase to cancel out specified signals. The units comprised only passive elements such as General Radio wire-wound potentiometers and U.T.C. LS X-type transformers, in order to take advantage of the effective stability provided by

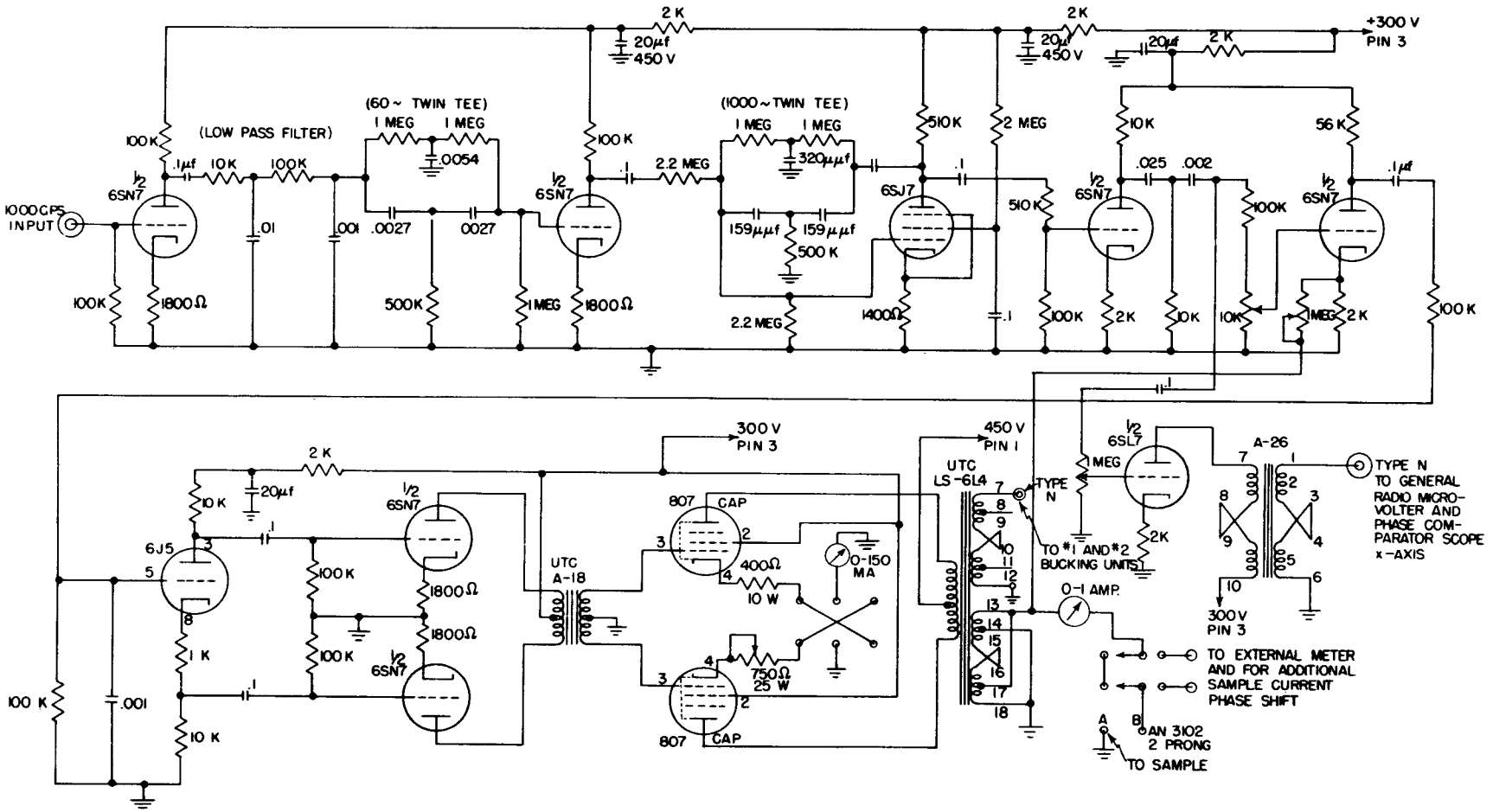

FIG. 3-1 NARROW BAND VOLTAGE AMPLIFIER AND POWER AMPLIFIER CIRCUITS

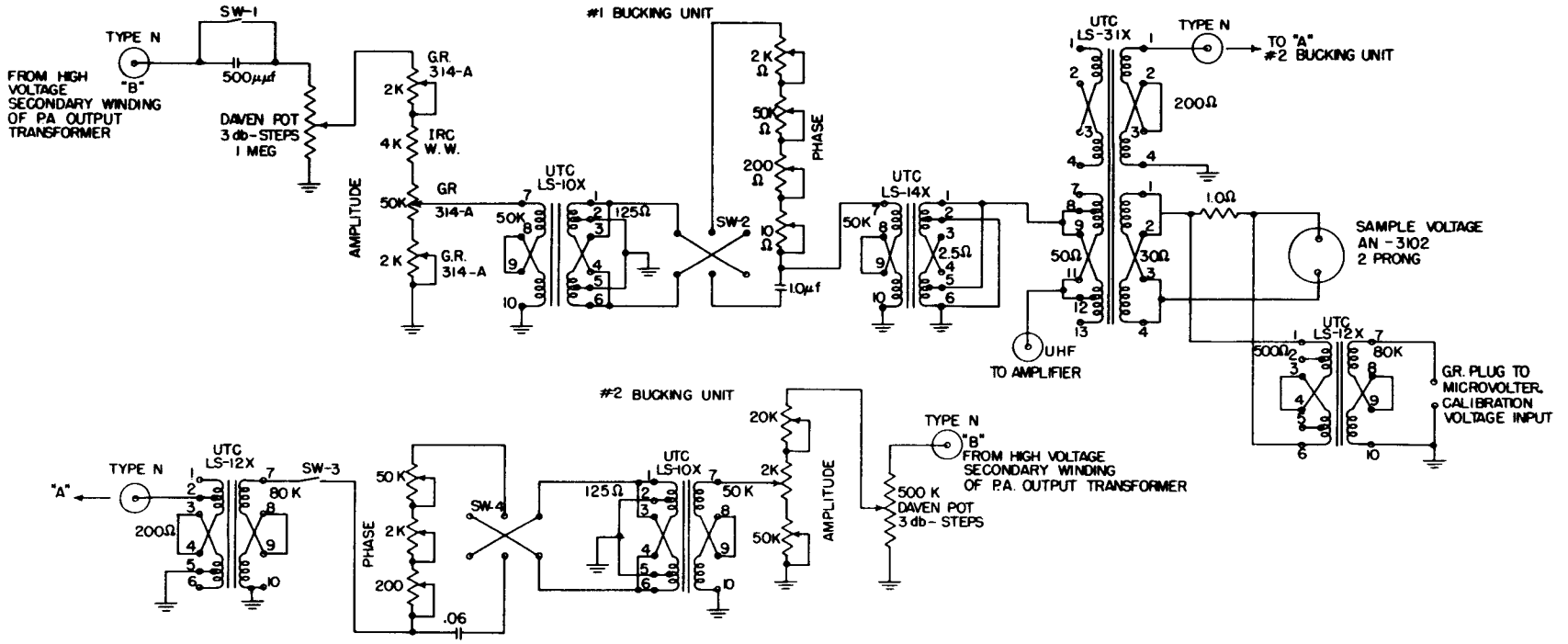

FIG. 3-2 THE BUCKING, ADDING AND CALIBRATING CIRCUITS

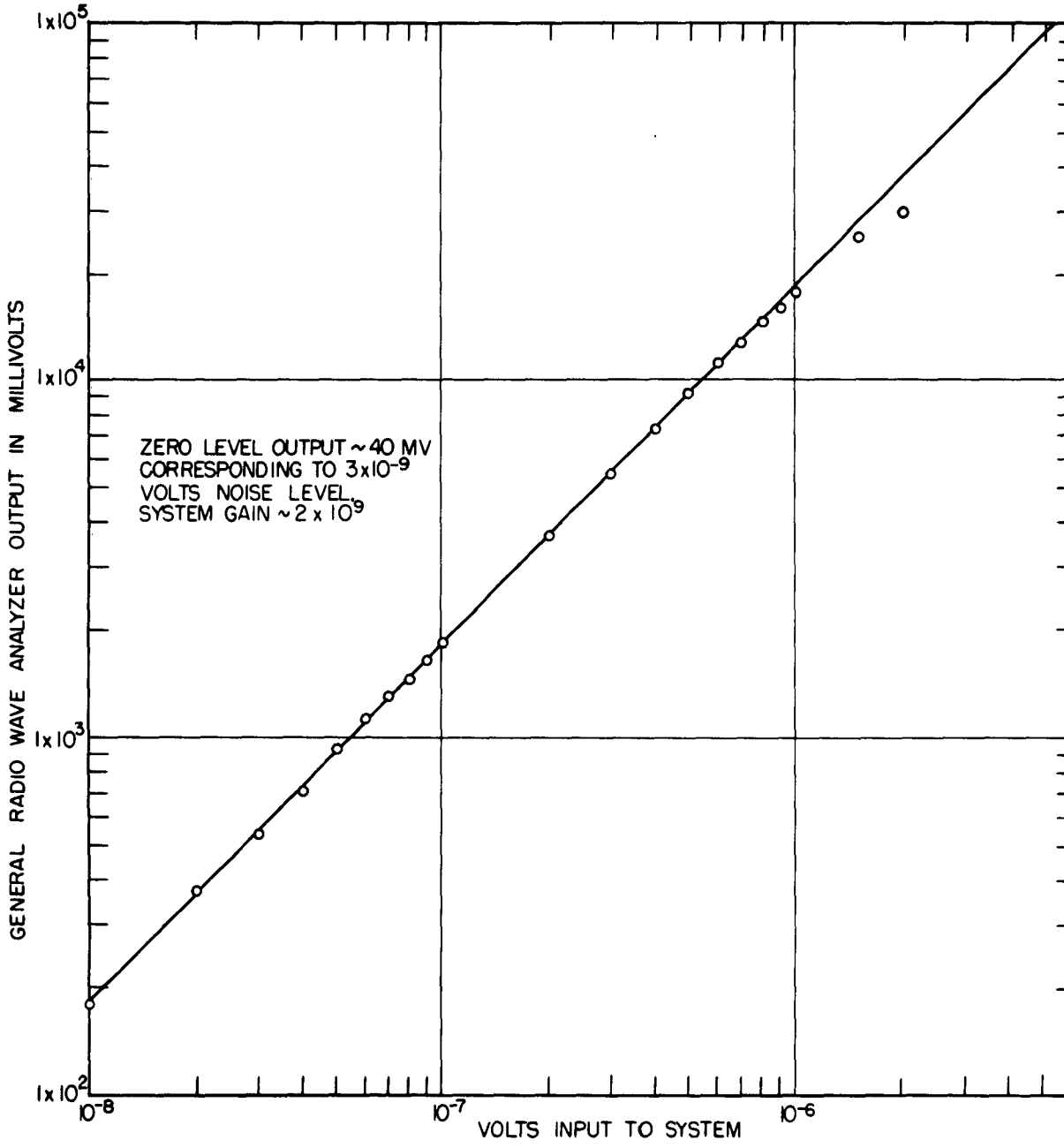

FIG. 3-3 THE SYSTEM LINEARITY

obtaining both the sample current and the bucking voltage from the same transformer. Furthermore, the stability requirement of 2 parts in 10^5 precluded the use of amplifying stages. The #1 and #2 units were similar but not identical because the required range of voltage and resolution was greater for the #1 unit. For example, in the Fe_3O_4 measurement, the #1 unit was used to buck out the IR drop of the order of 10^{-4} volts plus other smaller voltages, while the #2 unit was used to buck out the voltage due to the extraordinary effect of the order of 10^{-5} volts. Both units employed R-C phase shifters. In order that the output amplitude be insensitive to phase angle, the R-C phase shift network must work out of a low impedance and into a high impedance. As a consequence, considerable voltage loss occurs in these units, requiring voltages of the order of 100 volts at the input of the #1 unit. It was verified by test that after the appropriate cycling of voltages, there was no interaction between the #1 and #2 units. Figure 3-2 shows the bucking circuits as well as the adding and calibrating circuits.

The sample voltage and the #2 bucking unit voltage were added by the LS 31-X transformer. The #1 bucking unit voltage was added to the system by inserting the secondary of the LS 14-X transformer in series with the secondary of the LS 31-X transformer.

In order to calibrate the system for samples with a wide range of impedance, including values greater than the impedance of the input transformer, the calibrating signal was fed into a one-ohm wire-wound resistor in series with the sample input. The General Radio Microvolter was calibrated as well as the voltage transformation ratio of the LS 12-X coupling transformer. Since this ratio was 1.07×10^{-3}:1, voltages between 10^{-9} volts and 1 millivolt were provided for calibration purposes.

(E) The Electromagnet

The electromagnet, of laboratory design, consisted of a U-shaped section 19 inches high by 20 inches long of 6 inches square Armco iron. The poles were 7 inches in diameter. Four coils, each consisting of 980 turns of No. 12 copper wire, provided the excitation field. The end plates of the coils were water cooled. A field of 8900 oersteds was provided by 2200 watts in a 2-inch gap and 12,400 oersteds in a 1-inch gap.

The magnet supply consisted of 8 selenium rectifiers in two parallel full-wave bridge circuits. The output was smoothed with a heavy-duty L-C filter. Maximum power available was 2200 watts.

The magnetic field was calibrated with proton and lithium resonance lines and fill-in points were obtained with a flip coil and ballistic galvanometer. A Weston Model 430, 1/4 of 1 per cent ammeter was used both to calibrate the magnet and to set the magnetic field during measurements. The homogeneity, as evidenced by the proton lines, was much better than needed in this measurement.

Although magnet hysteresis causes no concern because of the method of measurement, it may be stated that negligible hysteresis existed in this magnet. Healy [44] has reported a 4-oersted hysteresis in the field at 3000 oersteds when the magnet was cycled around the 4000-gauss hysteresis loop.

Figure 3-4 is a photograph of the equipment used in this research.

3.2 Discussion of Errors

The determination of R_o requires the measurement of the sample current, the output voltage, the magnetic field, and the sample thickness. The determination of R_1 requires the measurement of the sample current, the output voltage, the saturation magnetization, and the sample thickness. All of these measurements are subjeet to random error of measurement as well as to systematic error in the calibration and reading of the instruments used to make the measurements. For example, the output meter of the General Radio Wave Analyzer could be read to about 1 per cent. Therefore, with each reading of output voltage we have a 1 per cent random error. On the other hand, the ammeter used to determine the sample current was calibrated against a laboratory standard with an accuracy of 3/4 of 1 per cent. Therefore, the values of current measured with this ammeter may be in error by 3/4 of 1 per cent but the same error will systematically occur in every determination of current. Random errors may be minimized by using the average value of several observations. Systematic errors can be reduced only by improved calibration or improved accuracy of the measuring system. However, the net effect of two or more systematic errors which are completely

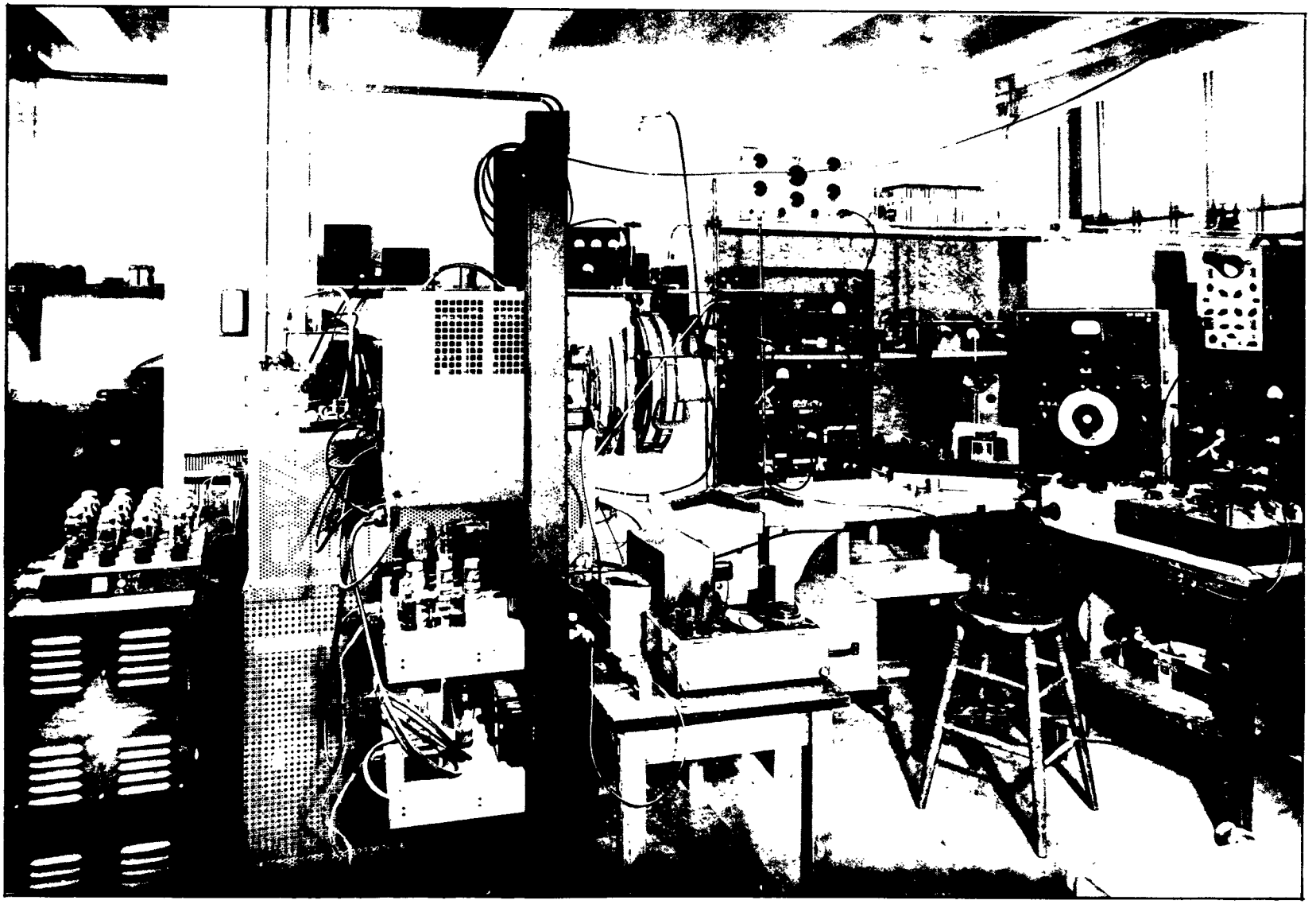

FIG. 3-4 A PHOTOGRAPH OF THE EQUIPMENT

independent is random. For example, if we have a 1 per cent systematic error in determining the current, and a 2 per cent systematic error in measuring the sample thickness, the probability that these two errors add is equal to the probability that they subtract. Therefore, we estimate their net effect by taking the square root of the sum of their squares. Random errors are compounded in the same way, and hence, with a few exceptions, we treat all errors in this manner.

In addition to the errors of measurement, error may occur because of the presence of large voltages which are temperature-and field-dependent. For example, in the measurement of R_o, a large IR drop and a large extra-ordinary Hall voltage are produced across the Hall probes. Because of the uncertainty in setting the magnetic field at each of four values in the differential measurement and because of temperature fluctuations during the time of the measurement, voltages different from the ordinary Hall voltage may be observed However, these effects gives rise to small errors (2 per cent or less), except in the case of the Fe_3O_4 measurement, which are inherently random and which can be minimized by repeated observations.

In the case of the R_o measurements on Grade A-Ni, we have 1 per cent error in determining the sample current, 1 per cent error due to the harmonics present in the current, 1.5 per cent error in reading the output voltage, 1.7 per cent error due to the signal-to-noise voltage ratio, 2.5 per cent error in the calibrating voltage, and 2 per cent error in the sample thickness. The uncertainty in the measurement of the magnetic field, along with the other errors which occur because of uncertainties in setting the magnetic field, total about 2.3 per cent. We assume about 1 per cent random error due to temperature fluctuations over the time of measurement. We estimate the total error in R_o by calculating the rms value of all the errors except the 1 per cent due to harmonics in the current. Since this is known to decrease the value of the current at 1000 cps, we prefer to add this error algebraically. The total error in R_o is then 5.7 per cent. To this we must add the uncertainty in R_o due to the change of M above saturation. We estimate that this causes about 3 per cent error at room temperature and about 5 per cent error at 140°C. Above the Curie temperature the signal-to-noise voltage error is reduced to about1 per cent, and because

the magneto-resistance effect is small in this region, the error due to the magnetic field is reduced to about 1 per cent. The error above the Curie temperature is estimated to be 5.1 per cent.

The errors estimated for the R_o measurements of Grade A Ni typify the error in the other R_o measurements, with the exception of Fe_3O_4. In the case of the 70 per cent Ni-30 per cent Cu alloy we estimate 5.7 per cent error below the Curie temperature and 5.1 per cent above. In the case of the R_o measurement of $(NiO)_{.75}(FeO)_{.25}(Fe_2O_3)$ at room temperature, we estimate about 6.3 per cent error.

In the case of the R_o measurement of Fe_3O_4, the error is larger. Because of the very large IR drop and the large extraordinary Hall voltage, uncertainties in setting the magnetic field and temperature fluctuations produced large random errors. The very small signal-to-noise ratio also produced large random errors. We estimate the effect of these random errors by calculating the standard deviation of the mean value of 31 observations and dividing by the mean value. The error estimated in this manner is 5.5 per cent. To this we add 4.5 per cent error in determining the electrical quantities and the sample thickness. We conservatively total this error to 10 per cent. However, the change of M above saturation, which is discussed more fully in Appendix B, can provide a large uncertainty in R_o.

In the case of the R_1 measurements on Grade A Ni, certain of the random errors are negligible. For example, because relatively large voltages were observed, the signal-to-noise voltage error is negligible, and the uncertainties caused by the magnetic field and temperature fluctuations are very small The uncertainties in determining the output voltage, the sample current, and the sample thickness are the same as in the R_o measurement. However, in the R_1 measurements, additional error occurs because of the uncertainty in M_s and because of the error in applying corrections to R_1. In the case of Grade A-Ni, we estimate less than 1 per cent uncertainty in M_s and about 1 per cent uncertainty in the corrections. Therefore, the error in R_1 is about 5.0 per cent at all temperatures.

In the case of the other metals, the uncertainties in M_s are somewhat

larger and the correction errors are larger in certain cases. However, in no case is error greater than 6.0 per cent estimated. In the case of Fe_3O_4, M_s is known fairly accurately and the estimated error is also less than 6.0 per cent. However, in the case of $(NiO)_{.75}(FeO)_{.25}(Fe_2O_3)$ a calculated value of M_s was used and no estimate of error can be assigned. However, all other errors in this measurement total about 6.0 per cent.

According to the Karplus-Luttinger theory, R_1 is proportional to ρ^2. In order to determine the observed proportionality, we have calculated the slope of the curve of log R_1 versus log ρ. The slope of this curve is quite sensitive to the values of R_1 and especially ρ, and hence error in the measurement of these quantities will cause marked departure from the true value. However, virtually all of the random errors are averaged out, and the systematic errors do not alter the slope of the curve. One of the more serious sources of error in this determination was the comparison of R_1 with values of ρ measured in zero magnetic field. The value of ρ which occurs in the measurement of R_1 may differ by a few per cent, because of magneto-resistance. However, it can be shown [84] that error cannot account for the observed departure from a ρ^2 dependence in the case of the high Ni concentration alloys. In the case of the 80 per cent Ni-Fe alloys, both R_1 and ρ are fairly insensitive functions of temperature, and errors in the observation of these quantities may account for some of the observed departure from a ρ^2 dependence.

3.3 The Sample Holders

As indicated in Section 2-3, and pointed out by Kevane, Levgold, and Spedding [45], the most serious difficulty in the use of an ac system is the presence of spurious voltages due to vibrations. The vibration troubles occur when the high current leads or the sample vibrate in the magnetic field, or when the vibrations of the sample holder cause relative motion between the Hall loop and the high current carriers. These were eliminated by mechanical design of the sample holder.

(A) For Metals

The method of eliminating the difficulty in the case of metal samples, dimensions of the order of 0.75" x 3.0" x 0.005", is shown in Fig. 3-5 and

Fig. 3-6, views of the high-temperature metal sample holder. The sample current was led through the magnetic field in a rigid coaxial cable. In order to prevent vibration of the sample, and in order to prevent relative motion between the sample and the Hall leads in the vicinity of the sample, both the sample and the Hall leads were clamped to the base plate by stainless flat sections, mica-insulated. Thus, although vibrations of the sample holder itself might not be eliminated, there was no voltage induced in the Hall loop. No special precautions were taken in running the Hall leads out of the magnetic field. The field due to the current was small in this region because of the use of the coaxial line and the distance from the sample.

The solid coaxial line consisted of two #304 stainless steel tubes. The outer one, 0.319 inch I.D., was spaced from the inner one, 0.125 inch O.D., by Stupakoff (Stupakoff Ceramic and Manufacturing Company, Latrobe, Pennsylvania) steatite insulating beads 0.312 inch O.D., 0.125 inch I.D. No. 78 Sauereisen (Sauereisen Cements Company, Pittsburgh 15, Pennsylvania) was used to cement the insulating beads to one another and to the inner and outer conductors. Stainless steel was used throughout the sample holder, since in the region of temperature gradient its low thermal conductivity minimized losses, and in the region of high temperature, its high-temperature structural properties were needed. Three leads were silver-soldered to all metal samples; one end of the sample was grounded to the sample holder. The holder shown in the photograph, Fig. 3-7, was used up to 500°C.

In the case of low-temperature metal measurements, similar techniques were employed. Variations were made only to conform to the requirements of the temperature range and to the space limitations imposed by the Dewar flask. Figure 3-8 shows a photograph of the low-temperature metal sample holder. The large brass rings served as clamps, in the absence of room to sink threads in the base plate, and provided a large thermal mass for the holder. The entire sample area was enclosed by a cylindrical brass case, liquid-air-tight.

(B) For Ferrites

The technique of mounting the sample in a sample block shown in the exploded view of Fig. 3-9 was used at both low and high temperatures. For

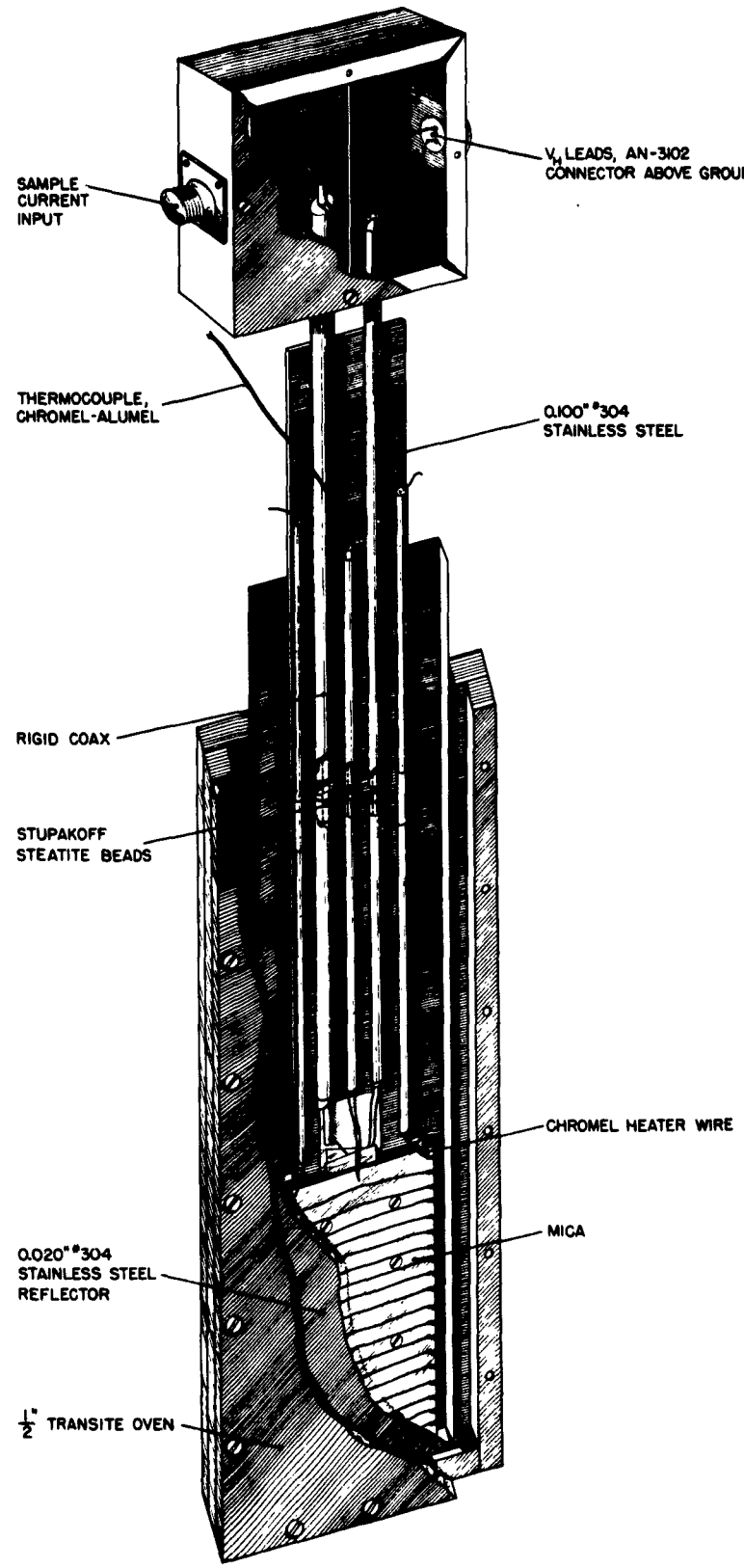

FIG. 3-5 A CUT-AWAY VIEW OF THE HIGH TEMPERATURE SAMPLE HOLDER AND FURNACE FOR METALS.

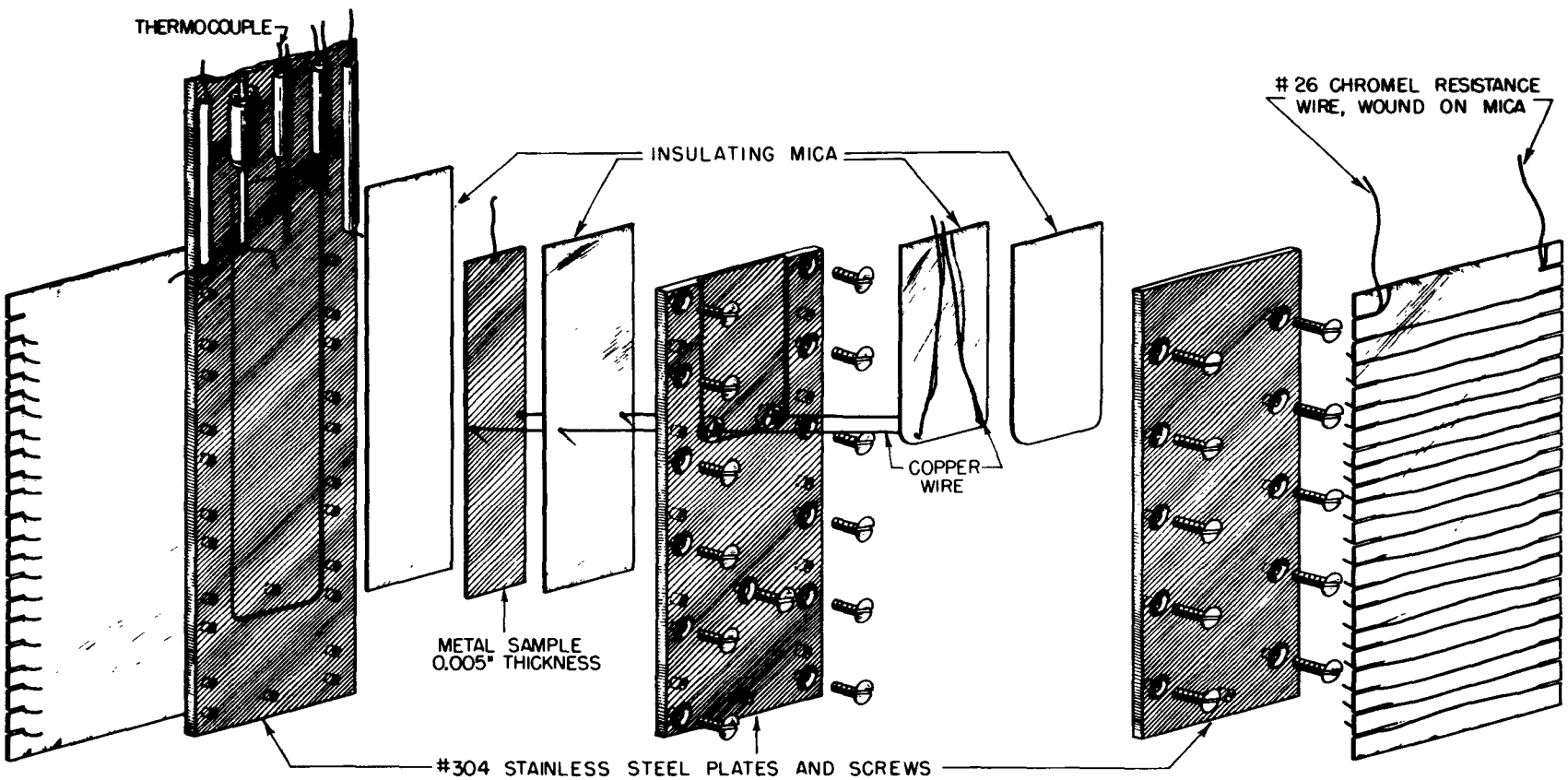

FIG. 3-6 AN EXPLODED VIEW OF THE HIGH TEMPERATURE SAMPLE HOLDER FOR METAL SAMPLES

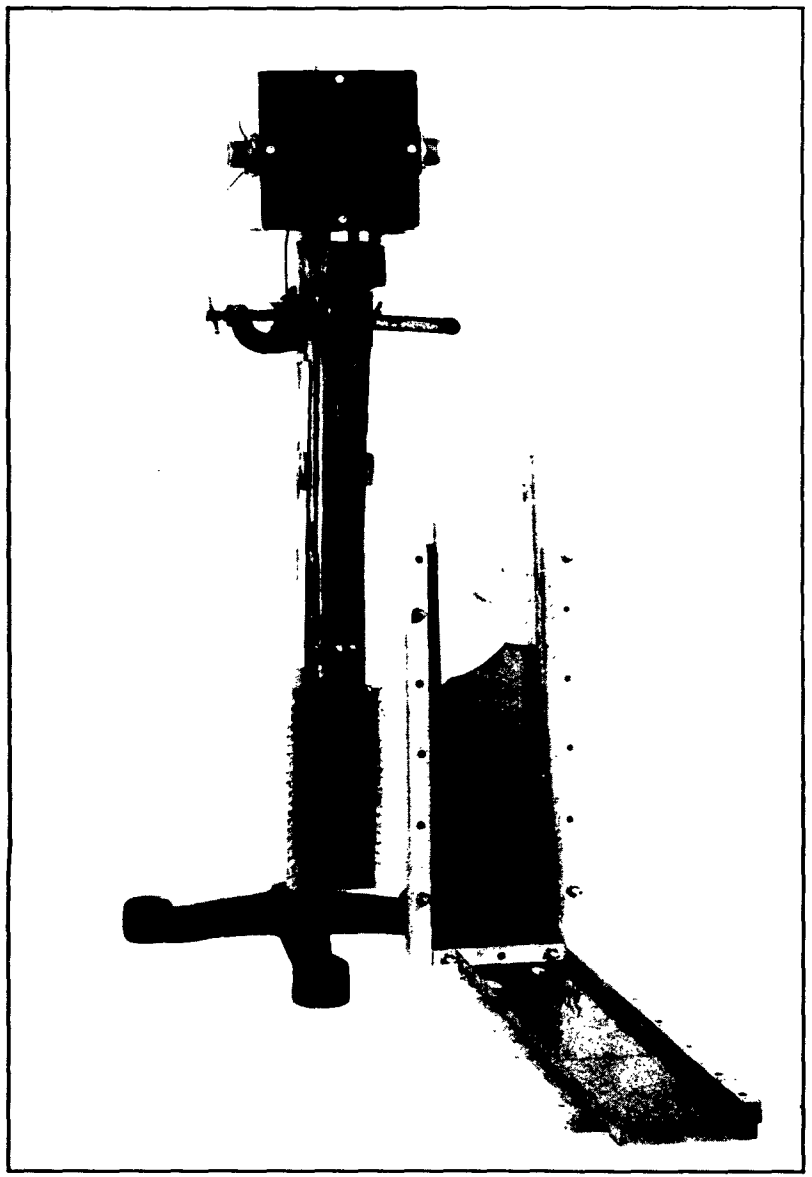

FIG. 3-7 THE HIGH TEMPERATURE SAMPLE HOLDER FOR METAL SAMPLES OUTSIDE OF THE FURNACE

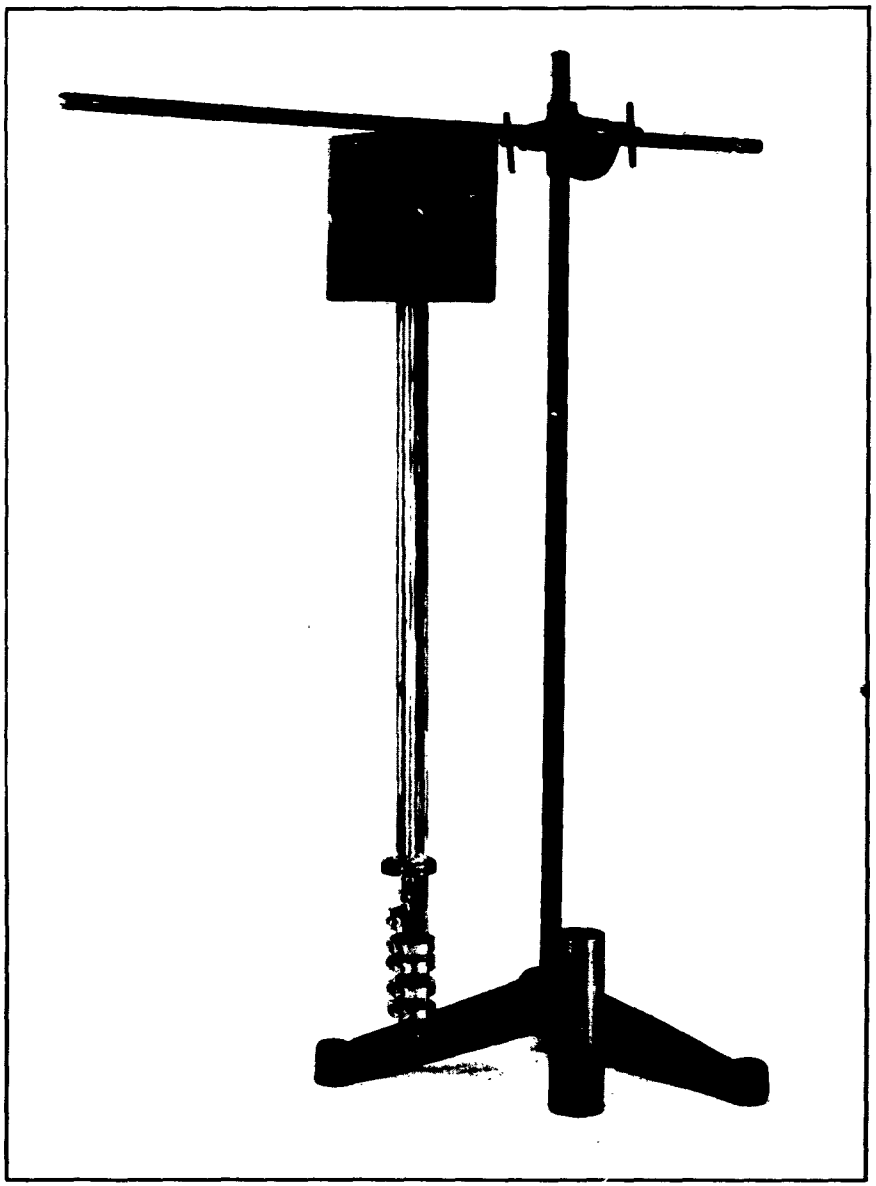

FIG. 3-8 THE LOW TEMPERATURE SAMPLE HOLDER FOR METAL SAMPLES

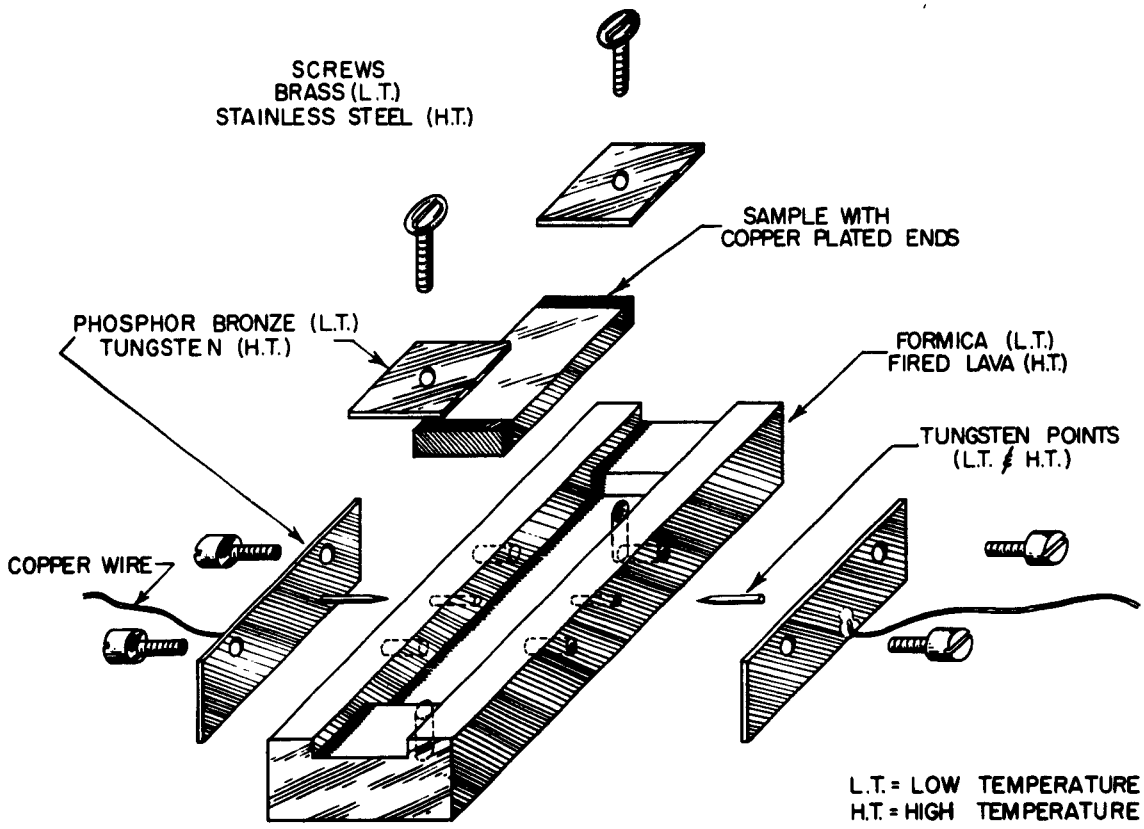

FIG. 3-9 AN EXPLODED VIEW OF THE SAMPLE BLOCK FOR THE $(NiO)_{.75}$ $(FeO)_{.25}$ (Fe_2O_3) SAMPLE

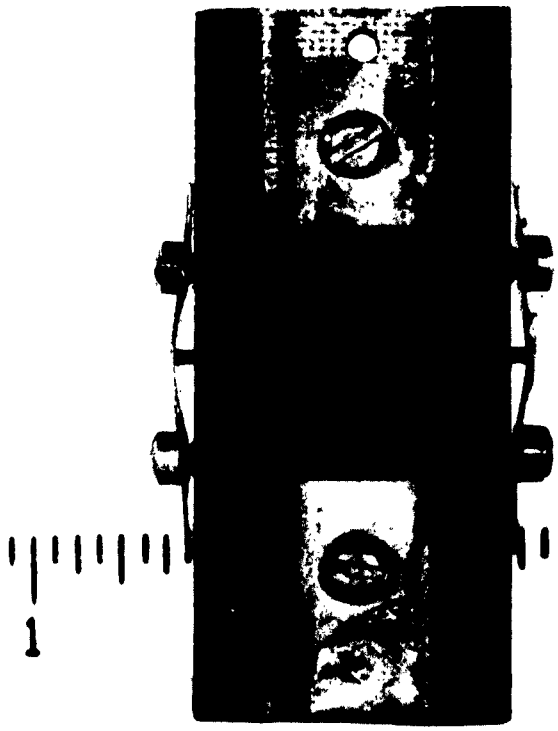

FIG. 3-10 PHOTOGRAPH OF THE SAMPLE BLOCK FOR THE $(NiO)_{.75}$ $(FeO)_{.25}$ (Fe_2O_3) SAMPLE

low-temperature work, the sample block was made of bakelite (linen-base) or formica. Pointed 0.040-inch tungsten rods backed by flat phosphor bronze springs provided the Hall contacts. The current contacts were also flat phosphor bronze springs applied to the upper end surface of the sample, and served to clamp the sample to the block, as well. The ends of the sample, extending back about 0.10-inch on four sides, were plated, first with rhodium and then with copper. The sample block and the Hall leads were solidly clamped to the base plate of the holder. Connections from the current contacts to the coaxial line and ground were made by a short, heavy copper rod and a screw passing through the sample block to the base plate.

For high temperatures, the sample blocks were machined from Grade A Lava (American Lava Corporation, Chatanooga 5, Tennessee) and fired at 1000°C. Similar tungsten points were used, and flat springs were made of 0.006 inch tungsten sheet. Figure 3-10 shows a typical ferrite sample mounting.

3.4 Temperature Techniques

Figure 3-5 shows a cut-away view of the high-temperature metal sample holder and furnace. About 8 feet of No. 26 chromel wire was wound in a bifilar winding around two supporting mica sheets, notched at the ends to space the wire. A 0.020-inch stainless steel reflector was placed around the windings and insulated from them by sheet mica. A box made of 1/2 inch transite, clamped tightly to reflector, windings, and sample holder, provided thermal insulation. Six hundred watts (dc) was adequate to raise the sample temperature to 600°C. Stabilities of the order of 0.05°C were obtained for periods of several minutes, adequate for measurements of the extraordinary effect, R_1. When R_0 measurements were made, a regulated power supply was used for additional stability.

For low-temperature measurements of R_1 in metals, the low-temperature holder shown in Fig. 3-8, was inserted in a glass dewar. Temperatures between room temperature and liquid-air temperature were obtained by adding small quantities of liquid air to the dewar, and measurements were made at the equilibrium temperature. Since the system approached equilibrium

exponentially in time, and since the sample was well lagged, a period of at least two minutes was available for each run.

Similar techniques were used for the R_1 measurements on the ferrites at both high and low temperatures. For the R_o measurements on the ferrites, made only at room temperature, it was found preferable to place the sample in a metal can in contact with the large thermal mass of the magnet. Thermal isolation, as, for example, by inserting in a dewar, did not enhance the thermal stability due to the small but finite amount of power supplied to the sample.

Temperatures were measured with chromel-alumel (high-temperature range) and copper-constant in (low-temperature range) thermocouples and a Leeds and Northrup K-2 Potentiometer. The chromel-alumel thermocouple was calibrated at the melting point of Al(659.7°C), Zn(419.45°C), Cd(320.9°C), Sn(231.85°C) and at the transition point of $Na_2SO_4 \cdot 10H_2O$ (32.384°C). The copper-constantin thermocouple was calibrated at the boiling point of liquid O_2(-183.00°C), at the CO_2(-78.51°C) point and compared at other points with a thermocouple calibrated at the National Bureau of Standards. Total error in absolute temperature measurements due to all uncertainties was less than 0.5°C for all points.

3.5 Samples

Ferrites have been made for many years by a sintering process which produces a material with a large number of grain boundaries. The grain boundaries produce excess noise, and inhomogeneity of electrical properties. The samples used in this research were single or nearly-single crystals of known composition. The writer is grateful to Professor A. R. von Hippel and Mr. J. Smiltens [46] of the Laboratory for Insulation Research, M.I.T., for the Fe_3O_4 sample supplied and to Dr. G. W. Clark and The Linde Air Products Company for the other single crystal ferrite samples measured in this work.

The impurities present in Fe_3O_4, sample 18, were Pt 1.4 parts in 10^6, Si and Al less than 0.001 per cent. The value of r, where r is the ratio of total Fe to Fe^{++} was $r = 3.012 \pm 0.012$. Stoichiometric Fe_3O_4 has a value of $r = 3.000$.

The Linde nickel iron ferrite sample 8/18/52 A was composed of 19.1 per cent Ni and 52.5 per cent Fe by weight. Assuming stoichiometric proportions for oxygen, this calculated out to be $(NiO)_{.75}(FeO)_{.25}(Fe_2O_3)$.

Linde crystal 6/12/53 D, Ni Zn Fe ferrite, contained 14 per cent Ni, 4 per cent Zn, 55 per cent Fe and was calculated to be $(NiO)_{.56}(ZnO)_{.14}(FeO)_{.30}(Fe_2O_3)$.

The writer is also grateful to Mr. R.J. Pastine and the Driver-Harris Company for many of the Ni alloys provided for this research, and to Dr. R. M. Bozorth of the Bell Telephone Laboratories for the samples of Mumetal.

The following metals were obtained from the Driver-Harris Company (Harrison, New Jersey): 499 Alloy with purity of the order of 99.95 per cent; Grade A Ni, purity of the order of 99.4 per cent, with 0.2 per cent Mn, 0.15 per cent Fe, 0.1 per cent Cu, 0.1 per cent C, 0.05 per cent Si, 0.005 per cent S, given as nominal composition by the Metals Handbook [32]; R-63 alloy consisting of 95 per cent Ni, 4 per cent Mn, and 1 per cent Si; Lucero, with composition 70 per cent Ni - 30 per cent Cu.

The samples obtained from the Bell Telephone Laboratories were Mumetal, with composition 77 per cent Ni, 5 per cent Cu, 2 per cent Cr, remainder Fe and impurities, and Supermalloy, with composition 79 per cent Ni, 5 per cent Mo, remainder Fe and impurities.

The Carpenter Hymu 80, obtained from the Carpenter Steel Company (Reading, Pennsylvania) contained 79 per cent Ni, 4 per cent Mo, remainder Fe and minor constituents.

IV.
THE ORDINARY HALL MEASUREMENTS ON GRADE A Ni AND 70 Ni-30 Cu

4. 1 The Experimental Results

(A) Ni

Although Hall measurements on Ni over a wide range of temperature and at high fields had been reported by Smith [6] in 1910, no precise data concerning the variation of the ordinary Hall coefficient, R_o, could be extracted from his published curves because of the need for high resolution in the region above saturation. Therefore, in order to examine the behavior of R_o as a function of temperature, in order to verify the existing temperature data on R_1, and in order to ascertain that the measurement technique described in Chapter II and the equipment described in Chapter III would perform satisfactorily on the simpler metal measurements, the Hall measurements on Driver-Harris Grade A Ni were undertaken.

Figure 4-1 shows the curve of Hall voltage as a function of the applied magnetic field, H, at room temperature for a Grade A Ni (99.4) sample, 0.005 inch thick. The sample current was 1 ampere. It is to be noted that the demagnetizing factor for a thin sheet, perpendicular to the plane of the sheet, is 4π, and although saturation should be attained at a value of external field close to $4\pi M_s$, or 6100 oersteds for this case, the sample does not show complete saturation, or linear increase of voltage with applied field, until 7500 oersteds. This effect has been discussed in section 2-2D. The differentially measured values of voltage above 9000 oersteds are shown in the enlarged section of Fig. 4-1. From the slope of this curve, the value of the ordinary Hall coefficient, R_o, is obtained.

The value of R_o deduced from Fig. 4-1 is $R_o = -6.02 \times 10^{-13} \frac{\text{volt-cm}}{\text{amp.-oersted}}$. This compares favorably with the value $R_o = -6.11 \times 10^{-13} \frac{\text{volt-cm}}{\text{amp-oersted}}$ obtained by Pugh, Rostoker, and Schindler [10] at room temperature on Ni (99.6) and a value of $R_o = -6.07 \times 10^{-13} \frac{\text{volt-cm}}{\text{amp-oersted}}$ obtained by Schindler and Pugh [47] on Ni (high purity) at room temperature, both measured with dc systems.

Figure 4-2 shows a representative group of curves of Hall voltage as

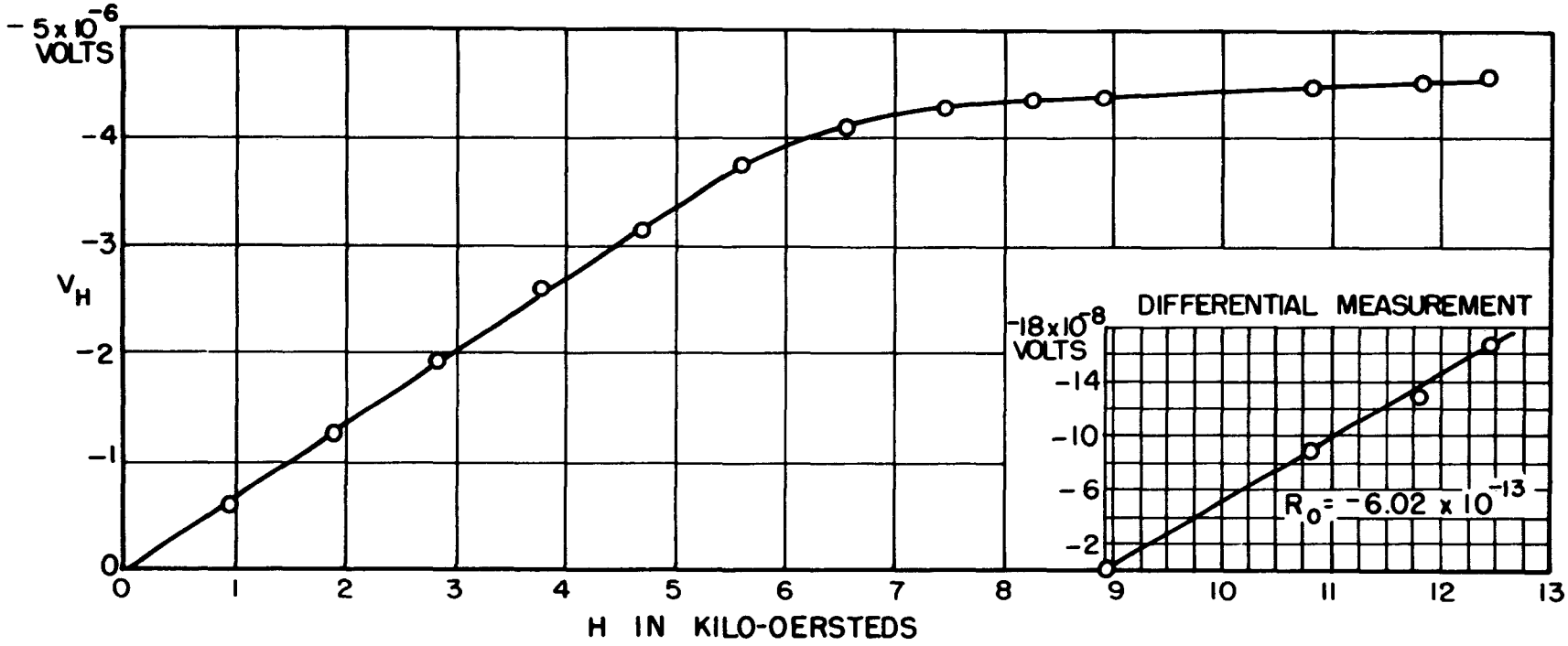

FIG. 4–1 THE HALL VOLTAGE AS A FUNCTION OF APPLIED MAGNETIC FIELD FOR GRADE A Ni. SAMPLE THICKNESS, t =.005 INCHES; I = 1 AMP.; T=27°C

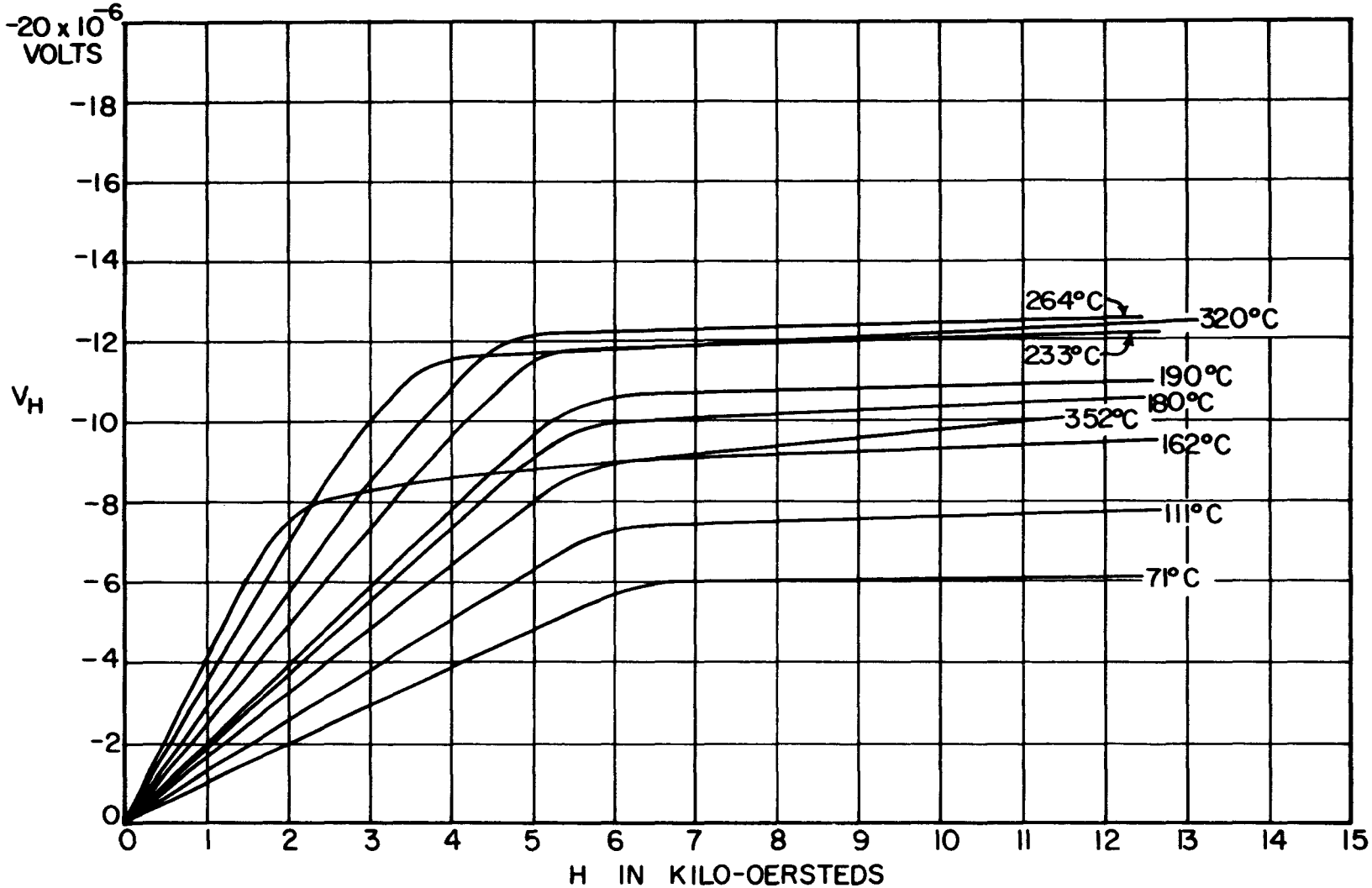

FIG. 4-2 THE HALL VOLTAGE AS A FUNCTION OF APPLIED MAGNETIC FIELD FOR GRADE A Ni AT TEMPERATURES BETWEEN 71°C AND THE CURIE TEMPERATURE. SAMPLE THICKNESS, t = .005 INCHES ; I = 1 AMP.; T_c = 358 °C

a function of applied magnetic field with temperature as a parameter. From these curves it can be seen that the voltage proportional to $R_1 M_s$ increases with temperature to within 100°C of the Curie temperature (358°C), although M_s decreases with increase of temperature. The decrease of M_s is directly evidenced by the shift of the knee of the curve to lower values of applied field, indicating decreasing values of $4\pi M_s$. The increase of the slope above saturation with increase of temperature cannot be directly attributed to a change in R_o. The change of magnetization with applied field above saturation due to the K_o term discussed in section 2-2D, increases with increase of temperature and provides the major contribution to the slope of the curve in the vicinity of the Curie temperature. This effect may be described in the following manner. When technical saturation has been reached, at temperatures different from absolute zero, some of the spins are not oriented in the direction of the applied field because of thermal agitation. The K_o term may then be ascribed to the progressive alignment of the temperature-disoriented spins by the increasing magnetic field. Although Holstein and Primakoff [31] have calculated the order of magnitude of this effect, in good agreement with experiment, by explicit consideration of the dipole-dipole interactions between spins, their theory is essentially a low-temperature theory applicable only where $M_o - M_s$ is small. M_o is the 0°K saturation magnetization. Since $\frac{M_s}{M_o} = 0.78$ at 200°C for Ni, the effect of the K_o term upon R_o cannot be calculated at this temperature with the Holstein and Primakoff formulation. Furthermore, K_o has been measured for Ni only to 140°C [ref. 12, p. 487]. Therefore, the K_o effect cannot be adequately subtracted from the total slope of the curve, and hence no significant R_o information can be obtained from these curves above 200°C.

The measurements on Grade A Ni were carried well into the paramagnetic region to observe the behavior of R_o above the Curie temperature. Figure 4-3 shows the curves of Hall voltage as a function of applied magnetic field for temperatures above the Curie temperature. Since the extraordinary Hall effect probably still exists in this region, the strong paramagnetism of Ni in this temperature range probably contributes to the observed slope. However, the paramagnetic susceptibility obeys Curie's law, and we would expect that the contribution of the

extraordinary effect would vary as $\frac{1}{T-\theta}$, where θ is the paramagnetic Curie temperature, and disappear at sufficiently high temperature. Analysis of the data above the Curie temperature by plotting the observed values of R_o as a function of $\frac{1}{T-\theta}$, where $\theta = 374^{\circ}C$, shown in Fig. 4-4, indicates the predicted behavior over a portion of the temperature range. However, between 528°C and 568°C the values of R_o do not vary with temperature. The value of R_o observed in this region is $R_o = -8.40 \times 10^{-13} \frac{\text{volt-cm}}{\text{amp-oersted}}$. The value of R_o deduced by extrapolating the linear portion of the curve of R_o versus $\frac{1}{T-\theta}$ to infinite temperature is $R_o \cong -5.5 \times 10^{-13} \frac{\text{volt-cm}}{\text{amp-oersted}}$. However, since R_1 has an unknown temperature dependence in this region, the slope of the curve will be altered by this dependence and the extrapolated value of R_o will probably be smaller in absolute value. Therefore, we may only infer that in the temperature range 528°C to 568°C $|R_o| \leq 8.40 \times 10^{-13} \frac{\text{volt-cm}}{\text{amp-oersted}}$, with a value approximately equal to the room temperature value not to be excluded.

Figure 4-5 shows the observed values of R_o over the temperature range from room temperature to 568°C. Between room temperature and 200°C the values of R_o are constant within experimental error. Rough estimates indicate that between 200°C and 300°C the apparent increase of R_o is due entirely to the change of magnetization. In the region between the Curie temperature and 528°C, the extraordinary effect undoubtedly influences the observed values of R_o. In the region between 528°C and 568°C, as indicated above, we cannot assign an exact value to R_o, but we may only place an upper bound on the absolute value.

Listed below in Table 4-1 are some of the physical properties of Grade A Ni to be used in the following discussions.

(B) 70 Ni - 30 Cu

In order to observe the behavior of R_o both above and below the Curie temperature in another ferromagnetic metal, measurements were made on Driver-Harris Lucero, a 70 Ni-30 Cu alloy. The choice of this alloy was suggested by its availability in thin sheet (0.005 inch) permitting reasonably large voltages to be observed with the available current, its low saturation magnetization permitting the linear region of the V_H, H curve to be examined with the available magnetic field (12,400 oersteds), and its relatively

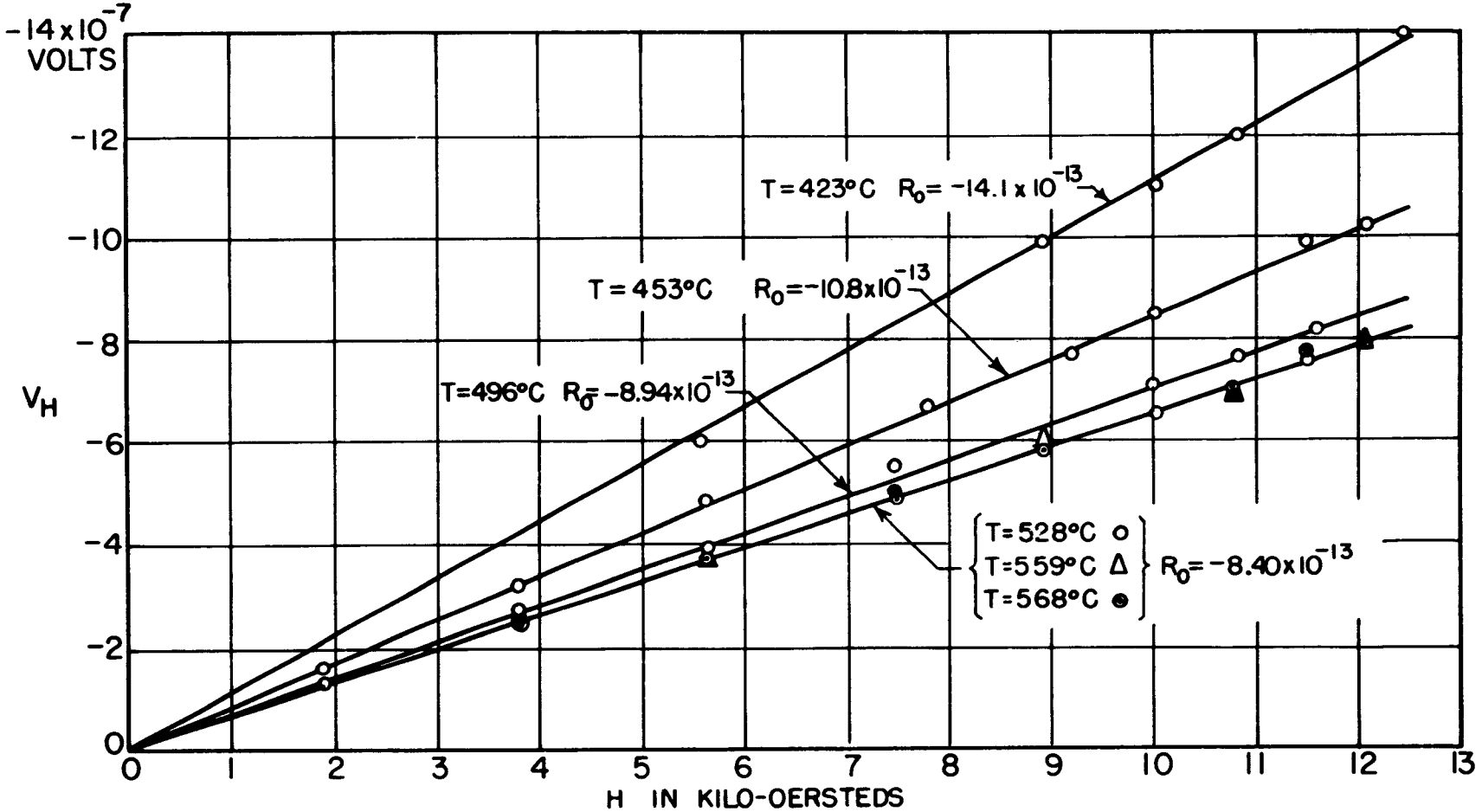

FIG. 4 – 3 THE HALL VOLTAGE AS A FUNCTION OF APPLIED MAGNETIC FIELD FOR GRADE A Ni AT TEMPERATURES ABOVE THE CURIE TEMPERATURE. SAMPLE THICKNESS, t = .005 INCHES; I = 1 AMP.; T_c = 358°C

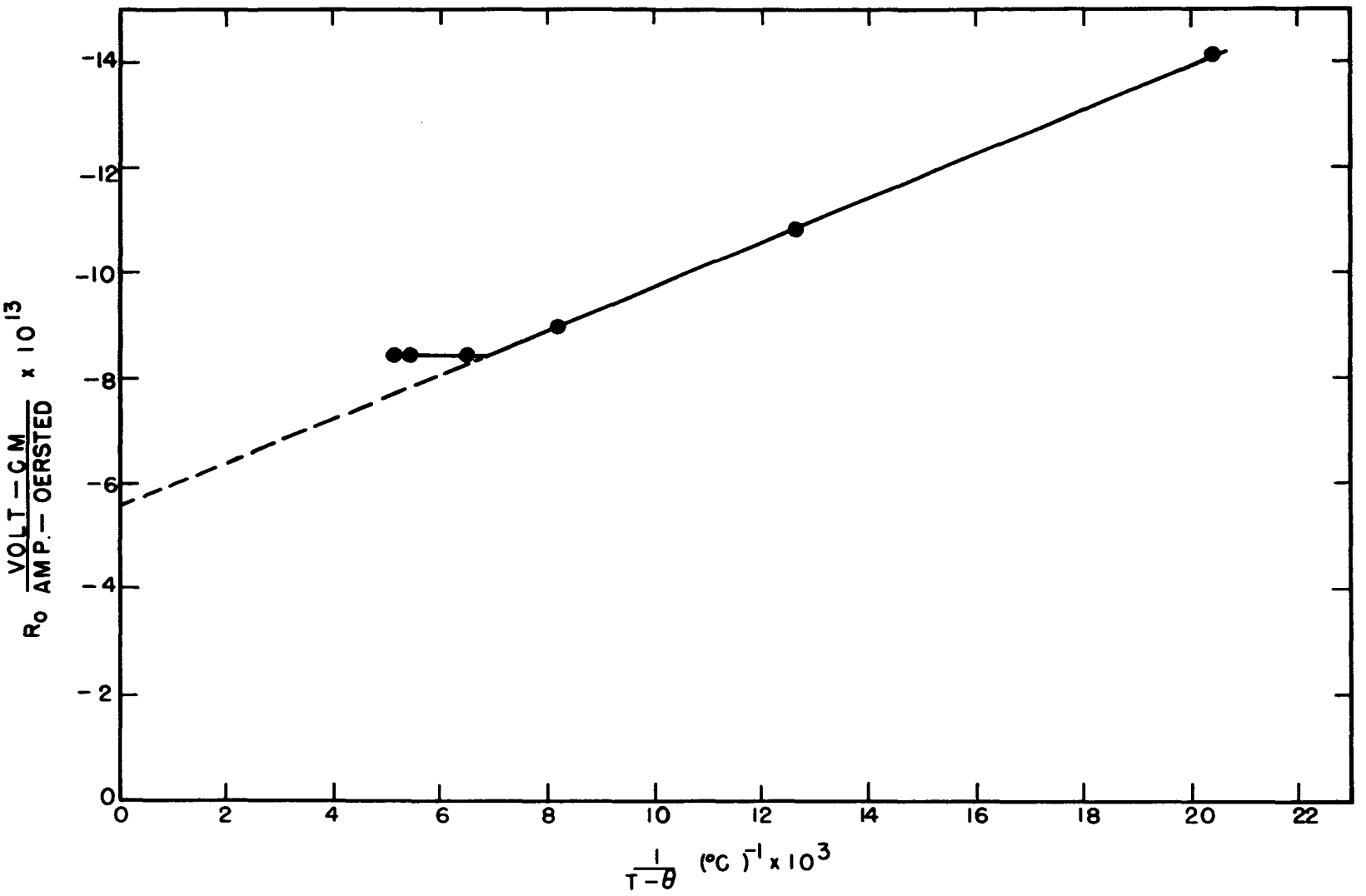

FIG. 4-4 THE VALUES OF R_0 OBSERVED ABOVE THE CURIE TEMPERATURE AS A FUNCTION OF $\frac{1}{T-\theta}$ FOR GRADE A Ni. $\theta = 374°C$

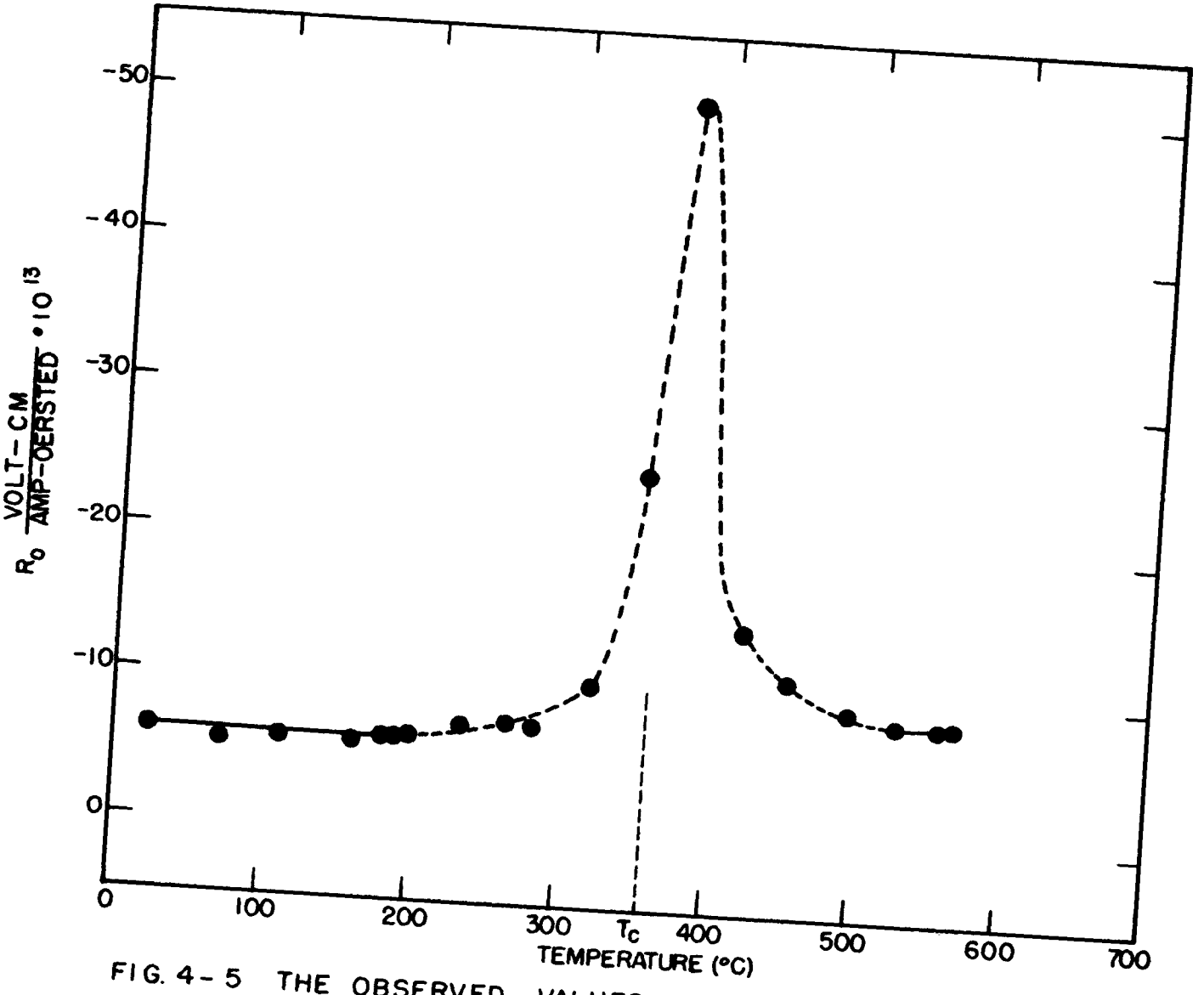

FIG. 4-5 THE OBSERVED VALUES OF R_0 AS A FUNCTION OF TEMPERATURE FOR GRADE A Ni

TABLE 4-1

SOME PHYSICAL PROPERTIES OF GRADE A Ni

At 27°C

The density	$d = 8.885\ gm/cm^3$
The number of atoms/cm^3	$n_o = 9.12 \times 10^{22}/cm^3$
The ordinary Hall coefficient	$R_o = -6.02 \times 10^{-13}\ \frac{volt\text{-}cm}{amp\text{-}oersted}$
The effective number of electrons/cm^3	$N^* = 1.04 \times 10^{23}/cm^3$
The effective number of electrons/atom	$n^* = 1.14/atom$
The extraordinary Hall coefficient (corrected)	$R_1' = -1.23 \times 10^{-10}\ \frac{volt\text{-}cm}{amp\text{-}gauss}$
The saturation magnetization	$M_s = 474.5\ gauss$
The resistivity	$\rho = 8.88 \times 10^{-6}\ ohm\text{-}cm$

At 568°C

The density	$d = 8.68\ gm/cm^3$
The number of atoms/cm^3	$n_o = 8.91 \times 10^{22}/cm^3$
The ordinary Hall coefficient (observed)	$R_o = -8.40 \times 10^{-13}\ \frac{volt\text{-}cm}{amp\text{-}oersted}$
The effective number of electrons/cm^3 deduced from the observed value of R_o	$N^* = 7.44 \times 10^{22}/cm^3$
The effective number of electrons/atom deduced from the observed value of R_o	$n^* = 0.84/atom$
The atomic weight	$W = 58.69\ gm/mole$
The saturation magnetization at 0°K	$M_o = 508.8\ gauss$
The ferromagnetic Curie temperature	$T_c = 358°C$
The paramagnetic Curie temperature [48]	$\theta = 374°C$
The number of Bohr magnetons in the ferromagnetic region	$\beta = 0.61/atom$
The number of Bohr magnetons in the paramagnetic region deduced from susceptibility measurements	$\beta = 0.87/atom$

low Curie temperature (42°C) permitting easy access to the paramagnetic region. In order to determine the value of R_o below the Curie temperature in this material, a measurement was made at liquid-air temperature, approximately 235°C below T_c. Figure 4-6 shows the curve of V_H as a function of applied magnetic field, H, for the 70 Ni-30 Cu alloy at liquid-air temperature. The enlarged view shows the high field slope from which a value of $R_o = -15.5 \times 10^{-13} \frac{\text{volt-cm}}{\text{amp-oersted}}$ is obtained.

Figure 4-7 shows the V_H, H curves in the paramagnetic region for this material. A similar decrease of slope with increase of temperature is observed, as in Ni. The values of R_o observed above 115°C are for the most part smaller than the value of R_o observed at -195°C. The value of R_o observed at 381°C is $R_o = -10.9 \times 10^{-13} \frac{\text{volt-cm}}{\text{amp-oersted}}$. Figure 4-8 shows the values of R_o observed above the Curie temperature plotted as a function of $\frac{1}{T-\theta}$, where $\theta = 52°C$. The value of R_o obtained by extrapolating this curve to infinite temperature is $R_o \simeq -9.8 \times 10^{-13} \frac{\text{volt-cm}}{\text{amp-oerste}}$ We note that the unknown temperature dependence of R_1 will tend to alter the slope of the curve, and probably tend to decrease the absolute value of R_o thus obtained. Therefore, the value of R_o deduced above the Curie temperature is only an approximate value, but it is definitely smaller in absolute value than the value observed at -195°C.

The convenient system in which to examine this effect is the Ni-Cu alloy series, because of low saturation magnetization, low Curie temperature, solid solubility without phase change in the entire series, and the existence of a large amount of experimental data on their electric and magnetic properties At the time this work was performed, it was learned that low-temperature Hall measurements were being made at Carnegie Institute of Technology on this series of alloys. Therefore, in order not to duplicate this work, and because the main purpose of this research was not an examinatio of the Ni-Cu series, no further measurements were made.

Listed below in Table 4-2 are some of the physical properties of 70 Ni - 30 Cu to be used in the following discussions.

4.2 Discussion of the Experimental Results

(A) The Two-Band Model

(1) Ni. The data are analyzed in terms of the effective number of conduction electrons/atom, n^*, where

$$n^* = \frac{N^*}{n_o} \tag{4.1}$$

and N^* is obtained from

$$N^* = \frac{10^{-8}}{R_o e_L} \tag{4.2}$$

where R_o is in units of $\frac{\text{volt-cm}}{\text{amp-oersted}}$, and $e_L = -1.60 \times 10^{-19}$ coulombs. The number of atoms/cm^3, n_o, is obtained from

$$n_o = \frac{Ad}{W} \tag{4.3}$$

where A is Avogadros number, $A = 6.025 \times 10^{23}$ mole^{-1}, d is the density of the material in gm/cm^3, and W is the atomic weight. From the room temperature Ni data, we obtain a value of $n^* = 1.14$ electrons/atom.

If we employ a simple band model [49] for Ni, the 10 electrons of the free atom which are in a $3d^8 4s^2$ state, are redistributed over four bands, two 3d bands and two 4s bands in the solid state (ref. 12, p.435). The two 3d bands are shifted in energy by an amount proportional to the exchange interaction in such a manner [50] that one 3d band with spins parallel is completely filled with electrons at 0°K and the other 3d band with spins antiparallel has 0.6 vacancies or holes/atom. Since each 3d band holds five electrons/atom, there is an excess of 0.6 spins/atom in the parallel direction, providing 0.6 Bohr magnetons/atom in Ni$^+$. Figure 4-9 shows a simple picture of this band scheme with no attempt made to draw the correct band shape or energy separation. Mott [51] was the first to suggest such a band arrangement, and Slater [52], has made semiquantitative calculations on this model.

Since there are 9.4 electrons/atom in the two 3d bands, the remaining 0.6 electrons/atom are distributed equally in the 4 s bands. Both the 0.6 4s electrons/atom and the 0.6 3d holes/atom can contribute to the electric

- - - - - - -

*In this simple model we neglect a 10 per cent correction of the orbital motion to the total magnetic moment and hence the number of d holes is about 10 per cent too large.

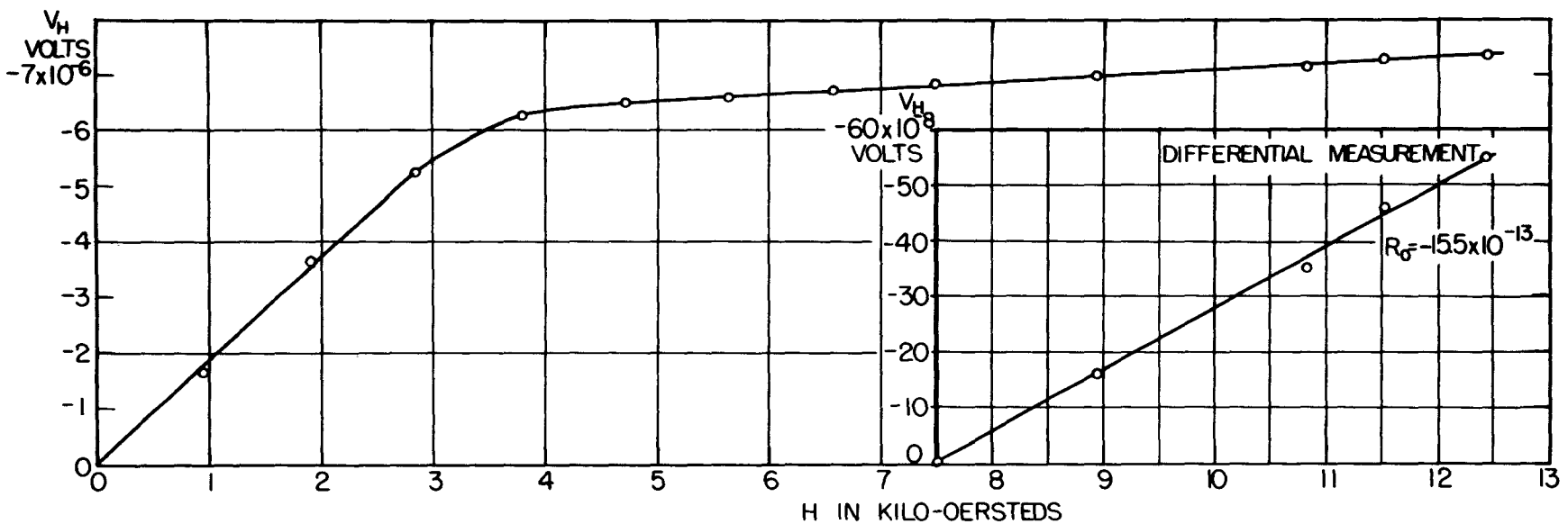

FIG. 4-6 THE HALL VOLTAGE AS A FUNCTION OF APPLIED MAGNETIC FIELD FOR 70 Ni – 30 Cu. SAMPLE THICKNESS, t=.0055 INCHES; I= 1 AMP.; T=-195° C

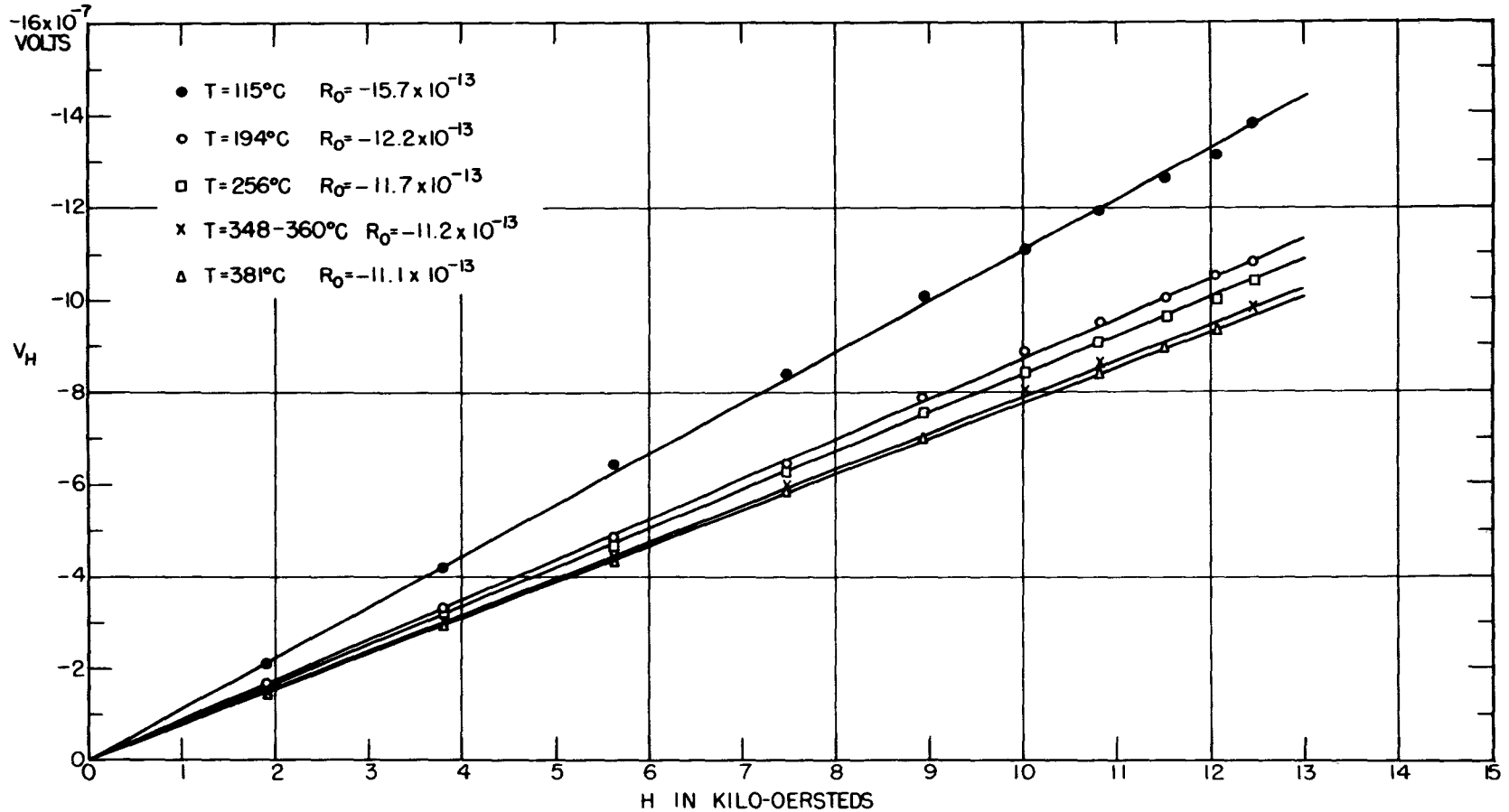

FIG. 4-7 THE HALL VOLTAGE AS A FUNCTION OF APPLIED MAGNETIC FIELD FOR 70 Ni-30 Cu AT TEMPERATURES ABOVE THE CURIE TEMPERATURE. SAMPLE THICKNESS, t=.0055 INCHES; I = 1 AMP.; T_c = 42° C

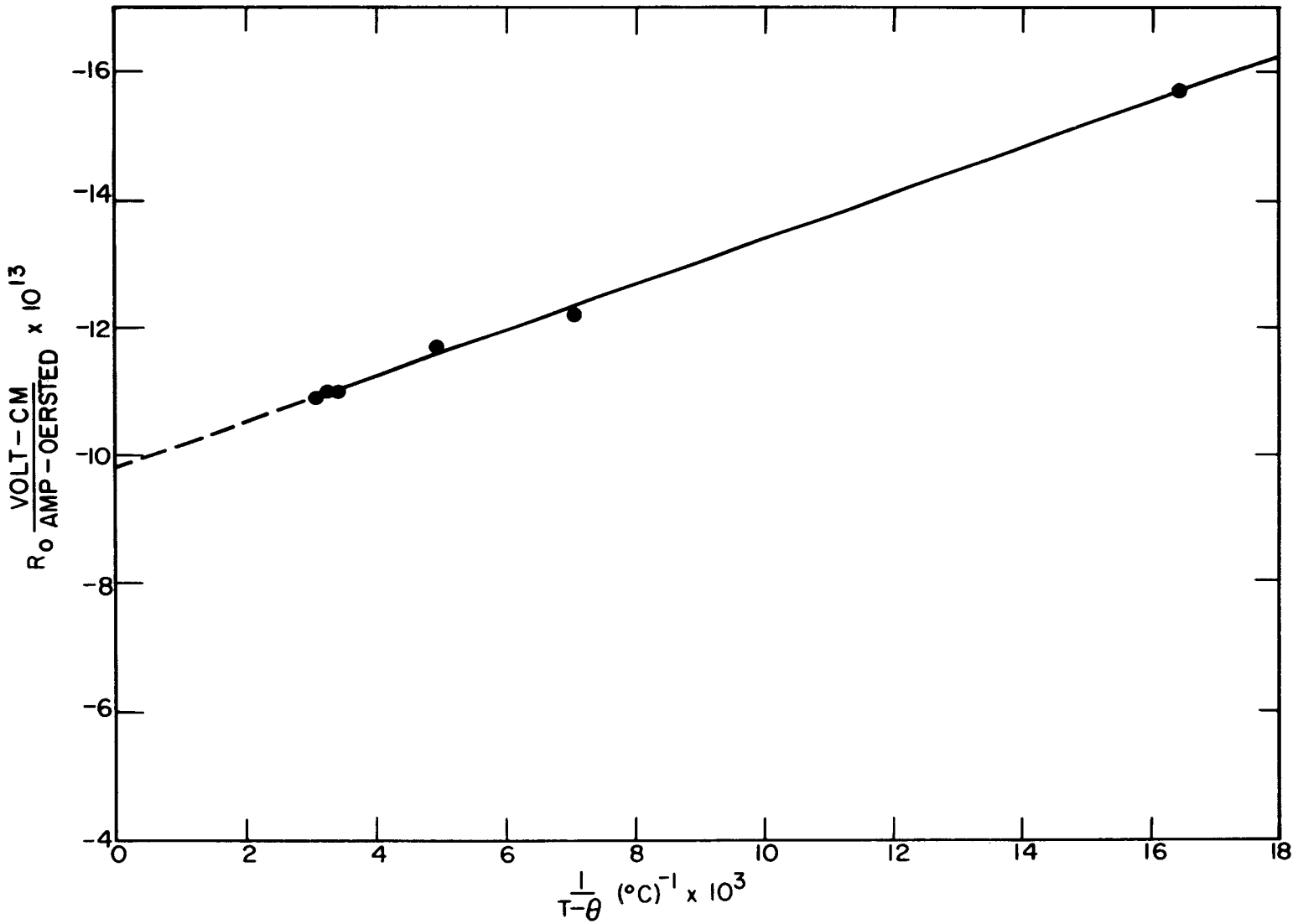

FIG. 4-8 THE VALUES OF R_o OBSERVED ABOVE THE CURIE TEMPERATURE AS A FUNCTION OF $\frac{1}{T-\theta}$ FOR 70 Ni- 30 Cu. $\theta \simeq 52°C$

TABLE 4-2

SOME PHYSICAL PROPERTIES OF 70 Ni - 30 Cu

At -195°C

The density	$d = 8.99\ gm/cm^3$
The number of atoms/cm^3	$n_o = 9.00 \times 10^{22}/cm^3$
The ordinary Hall coefficient	$R_o = -15.5 \times 10^{-13}\ \frac{volt\text{-}cm}{amp\text{-}oersted}$
The effective number of electrons/cm^3	$N^* = 4.03 \times 10^{22}/cm^3$
The effective number of electrons/atom	$n^* = 0.45/atom$
The extraordinary Hall coefficient	$R_1 = -3 \times 10^{-10}\ \frac{volt\text{-}cm}{amp\text{-}gauss}$

At 381°C

The density	$d = 8.79\ gm/cm^3$
The number of atoms/cm^3	$n_o = 8.80 \times 10^{22}/cm^3$
The ordinary Hall coefficient (observed)	$R_o = -10.9 \times 10^{-13}\ \frac{volt\text{-}cm}{amp\text{-}oerstec}$
The effective number of electrons/cm^3 obtained from the observed value of R_o	$N^* = 5.73 \times 10^{22}/cm^3$
The effective number of electrons/atom obtained from the observed value of R_o	$n^* = 0.65/atom$
The extrapolated value of R_o above the Curie temperature	$R_o \simeq -9.8 \times 10^{-13}\ \frac{volt\text{-}cm}{amp\text{-}oersted}$
The effective number of electrons/cm^3 obtained from the extrapolated values of R_o	$N^* \simeq 6.5 \times 10^{22}/cm^3$
The effective number of electrons/atom obtained from the extrapolated value of R_o and the value of n_o at 381°C	$n^* \simeq 0.7/atom$

The atomic weight	$W = 60.15\ gm/mole$
The ferromagnetic Curie temperature obtained from resistivity data [see Fig. 6-1]	$T_c = 42°C$
The paramagnetic Curie temperature	$\theta \simeq 52°C$
The number of Bohr magnetons in the ferromagnetic region	$\beta \simeq 0.3/atom$

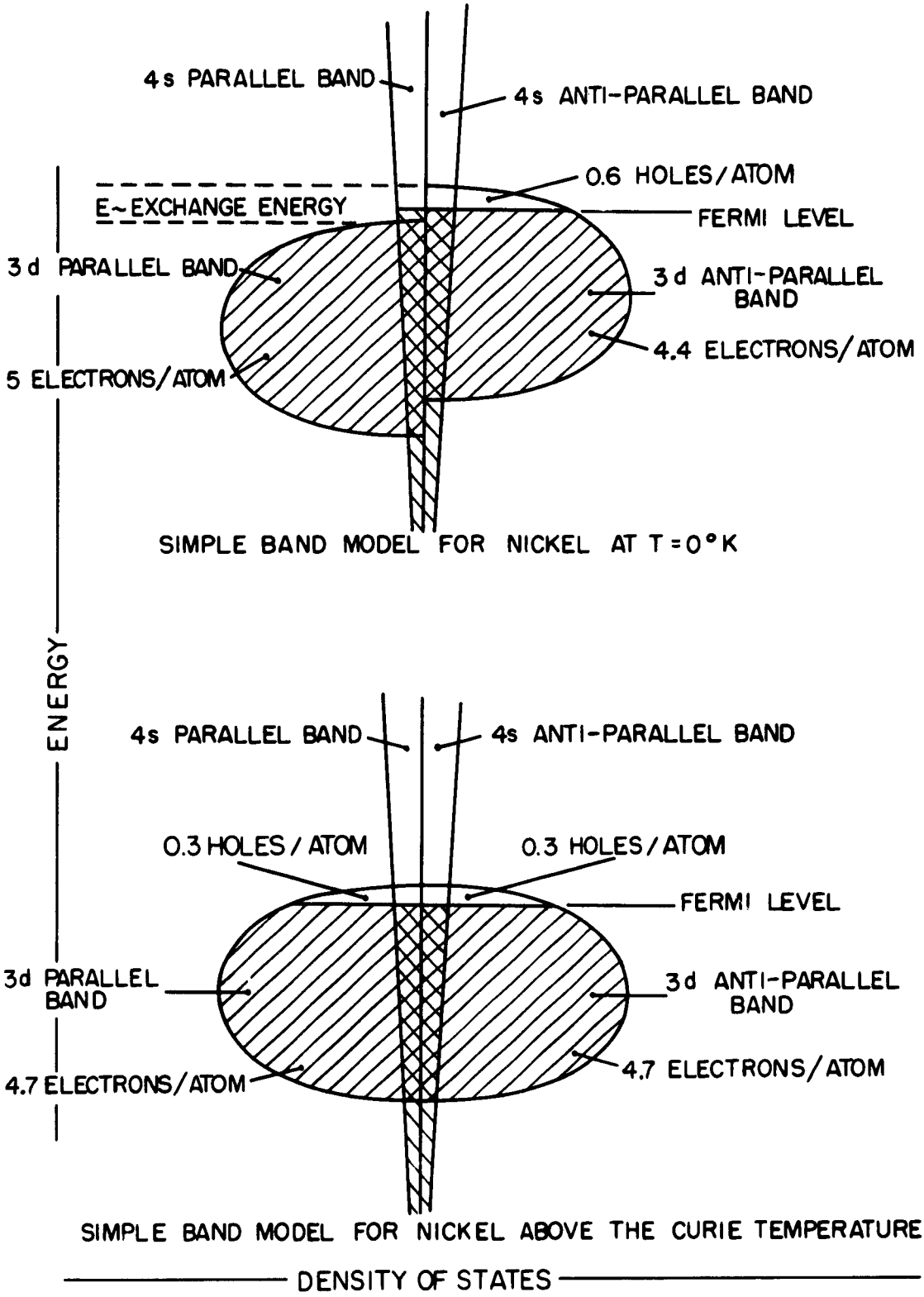

FIG. 4-9 A SIMPLE BAND MODEL FOR Ni

current. However, specific heat measurements [see 26, p. 157] indicate that the 3d holes have a large effective mass compared to the 4s electrons, and hence a low mobility. We would expect, therefore, that the major contribution to the current, and hence to the ordinary Hall coefficient, R_d would come from the 0.6 4s electrons. The value of n* = 1.14 electrons/atom is approximately twice the number we expect. A value of n* greater than 0.6 can be explained by assuming that the 0.6 3d holes contribute to the electric current and hence to R_o.

In order to take account of the hole contribution to R_o, we utilize the two-band formula for the Hall coefficient [see 10] normalized with respect to n_o, the number of atoms/cm^3, and obtain

$$\frac{1}{n^*} = \frac{1}{n_s}\left(\frac{\sigma_s}{\sigma}\right)^2 - \frac{1}{n_d}\left(\frac{\sigma_d}{\sigma}\right)^2 \qquad (4.4)$$

where $n_s = \frac{N_s}{n_o}$ = the number of s electrons/atom, and $n_d = \frac{N_d}{n_o}$ = the number of d holes/atom. If we assume that both 0.6 4s electrons and 0.6 3d holes contribute to n*, and substitute $n_s = n_d = 0.6$ into Eq. (4.4) and make use of the fact that

$$\sigma = \sigma_s + \sigma_d, \qquad (4.5)$$

we obtain

$$\frac{\sigma_s}{\sigma_d} = 3.2 \text{ and } \frac{\sigma_d}{\sigma} = 0.24, \qquad (4.6)$$

a result which has been previously obtained by Pugh, Rostoker, and Schindler [10].

From the observed value of R_o at 568°C a value of n* = 0.84 electrons/atom is deduced. If we analyze these data using Eq. (4.4) and retain $n_s = n_d = 0.6$, we obtain

$$\frac{\sigma_s}{\sigma_d} = 6.0 \text{ and } \frac{\sigma_d}{\sigma} = 0.14 \qquad (4.7)$$

(2) 70 Ni-30 Cu The simple band model discussed above and shown in Fig. 4-9 provides a means of accounting for the distribution of electrons in the Ni-Cu alloy series consistent with magnetization results. Cu with 29 electrons/atom has 1 more electron/atom than Ni. As the per-cent Ni in Cu increases from zero to 40 per cent, the number of 4s electrons/atom, n_s, decreases from 1.0 to 0.6. There are no 3d holes throughout this

range and hence ferromagnetism is not observed. As the Ni content is increased beyond 40 per cent, the 3d band with antiparallel spins begins to empty while the number of 4s electrons remains constant at 0.6. Between 40 per cent Ni and 100 per cent Ni, there is a linear increase in Bohr magneton number corresponding to the linear decrease of 3d antiparallel electrons. For each 0.1 electrons removed, an increase of 0.1 Bohr magnetons is observed. We therefore expect that the 70 Ni - 30 Cu alloy with 0.3 Bohr magnetons and with 10.3 electrons/atom outside of the closed Argon configuration will have 0.3 3d holes/atom and 0.6 4s electrons/atom. Thus, on the basis of this simple model, at temperatures well below the Curie temperature, we would expect that n^* would have a minimum value of approximately 0.6 or a value somewhat larger if hole contributions were present. From the liquid-air temperature data, we obtain a value of $n^* = 0.45$ electrons/atom. Equation (4.4) cannot be used to explain this departure from 0.6 electrons/atom.

From the value of R_o observed at 381°C, we obtain a value of $n^* = 0.65$ electrons/atom and from the value of R_o extrapolated at infinite temperature, we obtain a value $n^* \simeq 0.7$ electrons/atom. These values of n^* are approximately the value we expect from the above model.

(B) Pugh's Four-Band Model

Mott [53] has suggested that the major contribution to the resistivity of Ni comes about from s-d scattering. Since electrons are scattered mostly with spin conservation, the 4s electrons with parallel spin can not be scattered into 3d holes at low temperatures, since holes exist only in the antiparallel 3d band. The 4s electrons with antiparallel spin can, on the other hand, be scattered into 3d holes, and it is this scattering which predominates. Thus, at low temperatures, the current is carried mostly by one half of the 4s electrons, those with parallel spin. At higher temperatures, the number of holes in the parallel 3d band increases so that the 4s electrons with parallel spin are increasingly scattered. With this idea, Mott has been able to account for the difference in shape of the ρ, T curve of Ni compared with a similar nonmagnetic transition metal (Pd).

Using the same hypothesis, Pugh [54,55] has qualitatively explained the results of low-temperature Hall measurements on the Ni-Cu series made by Cohen [56]. Pugh suggests that as Ni is added to Cu, the value of n^* decreases from the value obtained in Cu ($n^* \neq 1$ in Cu for reasons not very well understood) to a value of $n^* = 0.6$ at 40 per cent Ni. This decrease of n^*, corresponding to an increase of the absolute value of R_o, has been observed by Cohen and is shown in Fig. 4-10, taken from Pugh's Final Report [54]. The value of n^* at 40 per cent Ni is near 0.6 electrons/atom. As the concentration of Ni is increased from 40 per cent, the number of holes in the antiparallel 3d band increases from zero at 40 per cent Ni to 0.6 at 100 per cent Ni. Since the Mott scattering is roughly proportional to the cube root of the number of d holes,* Pugh suggests that the increaseof scattering with the increase of the number of holes in the antiparallel d-band will result in a decreasing contribution to the conductivity from the 0.3 4s electrons with antiparallel spin. Pugh then proposes a four-band model which treats all four bands independently. With this model, n^* is given by

$$\frac{1}{n^*} = \frac{1}{n_1}\left(\frac{\sigma_1}{\sigma}\right)^2 + \frac{1}{n_2}\left(\frac{\sigma_2}{\sigma}\right)^2 - \frac{1}{n_3}\left(\frac{\sigma_3}{\sigma}\right)^2 - \frac{1}{n_4}\left(\frac{\sigma_4}{\sigma}\right)^2, \qquad (4.8)$$

where n_1 and n_2 are the number of 4s electrons with spin parallel and antiparallel, and n_3 and n_4 are the number of holes in the parallel and antiparallel 3d band. The σ_i are the corresponding conductivities.

At very low temperatures there are no holes throughout the series in the parallel 3d band and therefore $n_3 = \sigma_3 = 0$. In order to account for values of n^* less than 0.6, and in particular in order to account for a value of $n^* = 0.3$ at 80 per cent Ni, Pugh assumes that between 40 per cent Ni and 80 per cent Ni in Cu, hole contributions are relatively unimportant. Thus, with the assumption that $\frac{\sigma_4}{\sigma} \ll 1$, and $\frac{\sigma_3}{\sigma} = 0$, Eq. (4.8) reduces to

$$\frac{1}{n^*} = \frac{1}{n_1}\left(\frac{\sigma_1}{\sigma}\right)^2 + \frac{1}{n_2}\left(\frac{\sigma_2}{\sigma}\right)^2 \qquad (4.9)$$

where $n_1 = n_2 = 0.3$ for the ferromagnetic Ni-Cu alloys. Now as the Ni

*If we assume the scattering is proportional to the density of states, n(E), at the Fermi level of the antiparallel 3d band, then $n(E) \sim E^{1/2}$, and $n(E_{od}) \sim E_{od}^{1/2}$ where E_{od} is the Fermi level for holes. The number of holes, n_4, is obtained by integrating over the unoccupied distribution. Thus, $n_4 \sim \int_0^{E_{od}} n(E)dE \sim E_{od}^{3/2}$, and $n(E_{od}) \sim n_4^{1/3}$.

content is increased from 40 per cent to 80 per cent, the decrease of n^* from 0.6 to 0.3 can be accounted for by assuming that $\frac{\sigma_2}{\sigma}$ varies from 1/2 to zero (actually to $\frac{\sigma_2}{\sigma} \ll \frac{\sigma_1}{\sigma}$) as the 4s electrons with antiparallel spin are increasingly scattered. As the temperature is increased, holes appear in the parallel 3d band, i.e., $n_3 \neq 0$. This model then indicates that the ratio $\frac{\sigma_1}{\sigma}$ will approach $\frac{\sigma_2}{\sigma}$ at high temperatures with an increase of n^* with increase of temperature. This has been observed by Cohen.

At temperatures above the Curie temperature, there are presumably equal numbers of holes in both 3d bands and we expect $\frac{\sigma_1}{\sigma} = \frac{\sigma_2}{\sigma}$. Under this condition, with no hole contributions, we would expect to obtain a value of $n^* = 0.6$ in the range between 40 per cent and 80 per cent Ni. The value of n^* of the order of 0.6 observed in this research for 70 Ni - 30 Cu at $T > T_c$ fits this model.

The value of $n^* = 0.45$ electrons/atom obtained at liquid-air temperature for 70 Ni - 30 Cu is not in very good agreement with Cohen's data, as is shown in Fig. 4-10. The deviation is considerably greater than the experimental error. However, the value of $n^* = 0.45$ electrons/atom is still allowable with Pugh's model.

Thus, the four-band model can qualitatively account for the observed values of n^* less than 0.6 in the range from 40 per cent to 80 per cent Ni, and does suggest a reason for the observed temperature dependence of R_o in this alloy range. In order to account for the decrease in the absolute value of R_o between 80 per cent and 100 per cent Ni, Pugh suggests that hole contributions become increasingly important in these concentrations. Analysis of the room temperature Ni data using Eq. (4.8) and assuming that only one half of the 4s electrons contribute to the current, and assuming $n_3 = 0$, suggests that $\frac{\sigma_d}{\sigma} = 0.41$. Thus, the four-band model indicates an even larger d hole contribution to the current than the two-band model. Furthermore, the relatively constant values of R_o observed by Cohen between 4.2°K and 300°K, and observed in this research between 300°K and 500°K require that the contributions from the d holes compensate the temperature dependence of the s-d scattering which produces a temperature-dependent R_o in the other ferromagnetic Ni-Cu alloys. Above the Curie temperature, the analysis of the Ni data with the four-band model is identical

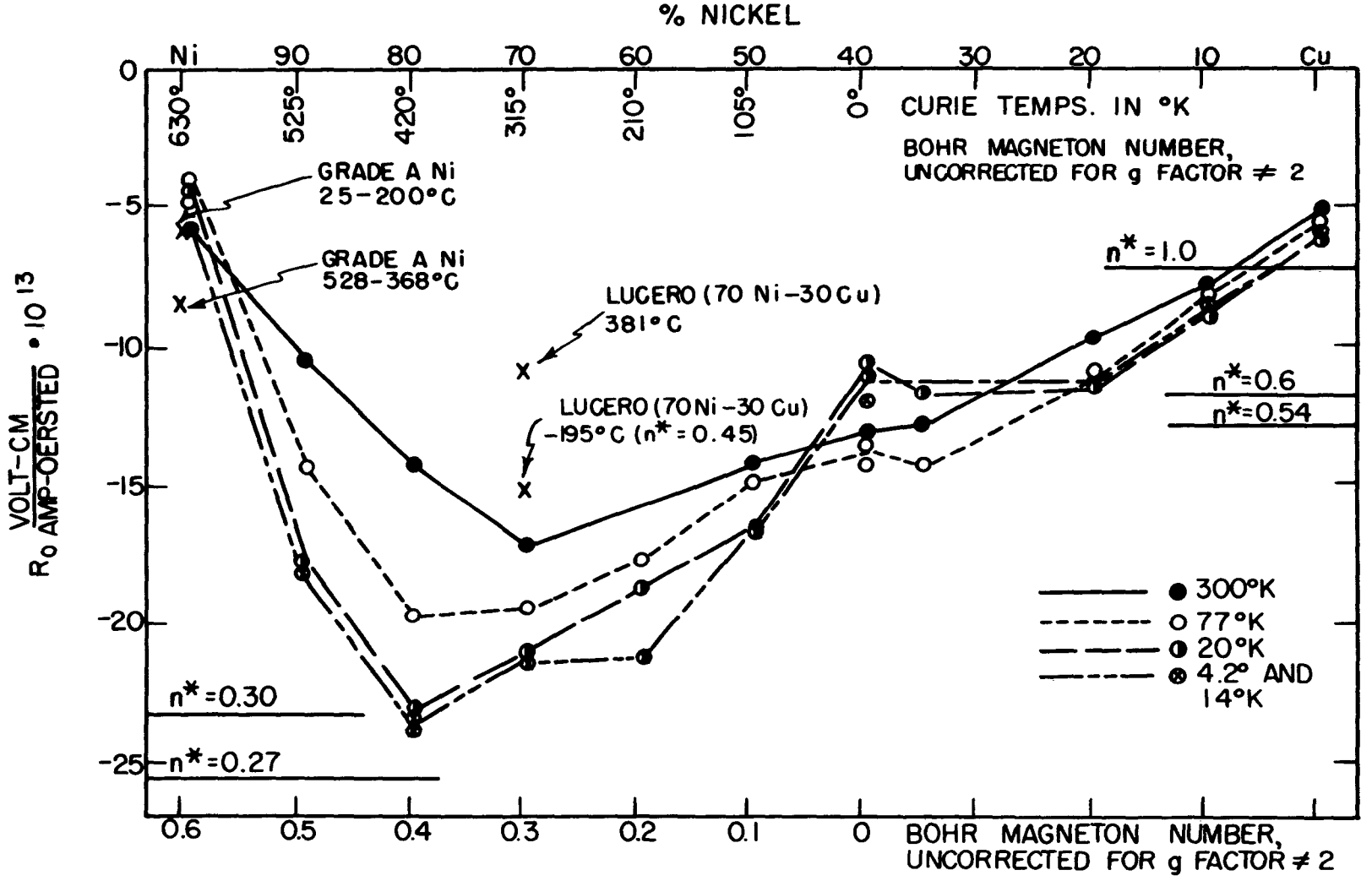

FIG. 4-10 R_0 AS A FUNCTION OF COMPOSITION FOR Ni-Cu ALLOYS. DATA TAKEN FROM PUGH'S FINAL REPORT. VALUES FOR GRADE A Ni AND 70 Ni - 30 Cu SUPERPOSED.

to that using the two-band model.

(C) Concluding Remarks

The above band models for discussing the 3d transition metals are a very crude picture of the true situation. The main justification for their use here, is that it permits a simple qualitative discussion of the observed effects. A more rigorous treatment of the collective electron or band model of the 3d transition elements has been given by Stoner [57, 58,59] and improved upon by Wohlfarth [60]. While this treatment permits analysis of magnetization data below T_c, susceptibility data above T_c, and specific heat data, and does correlate much information about the ferromagnetic metals, it offers no simple framework within which to treat the conduction properties of these materials. One aspect of the Stoner-Wohlfarth treatment should be pointed out in connection with the high-temperature Hall data. This concerns the transfer effect described by Wohlfarth [60,61] for Ni and for Ni-Cu alloys which involves a redistribution of electrons over both the s and d bands such that the number of 4s electrons increases at high temperatures and hence the number of 3d holes also increases. Wohlfarth has used this mechanism to account for the curvature of the reciprocal of the susceptibility-versus-T data observed at high temperatures, especially in Ni. The transfer effect suggests a very small increase in the value of n^* with increase of temperature.

Analysis of the room-temperature Ni data with either the two-band or four-band model indicates a rather large contribution to the conductivity from the d holes. As pointed out by Wilson [62], the large effective mass of the d holes should result in a small contribution to the current from the d holes compared with that of the s electrons. Thus the analyses presented above are not in complete agreement with the evidence from specific heat data. In this respect, Brooks [63] has suggested the possibility that perhaps one of the degenerate sub-d bands of Ni is a low-density band with a low effective mass for holes and hence a high mobility. A simple analysis then suggests that the contribution of the d holes may be more heavily weighted, perhaps by a factor of 2, in the determination of R_o than in the determination of σ.

The lack of temperature dependence of R_o in Ni observed from 4.2°K to 500°K is not by itself, surprising. One would expect that a measurement involving the density of electrons in a metal would be fairly temperature-independent. However, the behavior of Ni is completely different from the behavior of the other ferromagnetic Ni-Cu alloys, as observed by Cohen. This may then suggest that fundamental changes in the electronic structure of Ni occur with Cu alloying.

Although an exact value of R_o in Ni above the Curie temperature cannot be deduced from the observed results, the failure of the data above 528°C to follow a $\frac{1}{T-\theta}$ dependence may suggest that R_o is changing in this temperature region. If,on the other hand, the value of R_o observed in this region represents the true value of R_o, then the value of n^* deduced from R_o, $n^* = 0.84$ electrons/atom, is close to the value of 0.87 electrons/atom deduced from susceptibility data [see 12, p. 433].

The data observed for the 70 Ni-30 Cu alloy very definitely indicate different values of the ordinary Hall coefficient above and below the Curie temperature. While the simple model suggested by Pugh does give a qualitative explanation of the data, a more exact analysis awaits a more detailed theoretical examination of the electrical properties of the transition metals.

The ordinary Hall coefficient observed in the ferromagnetic transition elements and alloys may ultimately provide an additional source of information about electron densities in these materials. However, the present state of the theory of the ordinary Hall coefficient in metals does not permit reliable interpretation of these data.

V.

THE ORDINARY HALL MEASUREMENTS ON THE FERRITES

5. 1 The Experimental Results

(A) Fe_3O_4

The sample of Fe_3O_4 used in this research was grown by J. Smiltens [46], and was one of the first large synthetic ferrite crystals grown. With respect to stoichiometry and impurities, it was substantially better than natural crystals. It was not, however, a single crystal, but was composed of several large grains. Figure 5-1 is a photograph of the sample, after etching in HCl.

It has been shown in Chapter II that the ordinary Hall measurement on Fe_3O_4 is considerably more difficult than the measurement on Ni. Because of the small signal-to-noise ratio and because of temperature fluctuations, there was a large spread in the observed values of Hall voltage. No resolution of the Hall voltage, as a function of applied magnetic field, was obtained above saturation because the ratio of the spread to the average value of the observed voltage was large. Thus, the value of R_o is deduced from a two-point measurement. In addition to the uncertainty in the measured voltage, there may be large uncertainty in the value of R_o deduced from this voltage because of the change of magnetization in the region of measurement. This effect is discussed more fully in Appendix B. The effect of the change of magnetization above saturation makes the apparent value of R_o too large. Thus the measured value represents an upper limit of the true value of R_o and provides a lower limit to the charge carrier density provided that all the carriers are electrons.

The average value of 31 independent voltage measurements on the cylindrical sample, d = 0.25 inch, ℓ = 0. 50 inch, was $\Delta V_H = -5.04 \times 10^{-8}$ volts, for ΔH = 5000 oersteds. The uncertainty in the measured voltage is estimated to be about 10 per cent. The sample current was 300 ma. Taking into account the correction [64] for a length-to-width ratio less than 4, the value of R_o deduced from this voltage is $R_o = -1.80 \times 10^{-11} \frac{\text{volt-cm}}{\text{amp-oersted}}$

The value of N^*, the effective number of conduction electrons/cm^3, obtained from the relation

$$R_o = \frac{10^{-8}}{N^* e_L} \qquad (5.1)$$

where $e_L = -1.60 \times 10^{-19}$ coulombs, is $N^* = 3.47 \times 10^{21}$ electrons/cm^3. Thermoelectric power measurements [see Fig. 6-13] also indicate that the sign of the carrier is negative. Figure 5-2 shows the curve of Hall voltage as a function of applied magnetic field at room temperature for this sample.

The upper limit of the room temperature Hall mobility, obtained from the relation

$$\mu_L = R_o \sigma 10^{+8}, \qquad (5.2)$$

where $\sigma = 250$ (ohm-cm)$^{-1}$, is $\mu_L = 0.450$ cm^2/volt-sec.

Listed below are some of the physical properties of Fe_3O_4 sample No. 18 grown by J. Smiltens. All temperature-dependent values are room temperature (300°K) values unless otherwise stated.

(B) $(NiO)_{.75}(FeO)_{.25}(Fe_2O_3)$

The sample of $(NiO)_{.75}(FeO)_{.25}(Fe_2O_3)$ was obtained from the Linde Air Products Company and was a single crystal. The measurements on this sample were subject to less uncertainty than in the case of Fe_3O_4 because the signal-to-noise ratio was larger. Figure 5-3 shows the curve of the Hall voltage as a function of applied magnetic field at room temperature for this sample. The estimated uncertainty in the values of voltage measured above saturation is 6.3 per cent. The value of R_o deduced from the differential measurement is $R_o = -1.40 \times 10^{-10} \frac{\text{volt-cm}}{\text{amp-oersted}}$. The uncertainty in R_o due to the change of magnetization is probably small. The value of N^* obtained from R_o is $N^* = 4.46 \times 10^{20}$ electrons/cm^3. The room-temperature Hall mobility is calculated to be $\mu_L = 0.0476$ cm^2/volt-sec.

Listed below are some of the physical properties of Linde Air Products Company sample 8/18/52 A, $(NiO)_{.75}(FeO)_{.25}(Fe_2O_3)$. All temperature-dependent values are room-temperature (300°K) values unless otherwise stated.

TABLE 5-1

SOME PHYSICAL PROPERTIES OF Fe_3O_4

The density (20°C)	$d = 5.185$ gm/cm^3
The molecular weight	$w = 231.55$ gm/mole
The number of molecules/cm^3	$n_o = 1.35 \times 10^{22}$/cm^3
The conductivity	$\sigma = 250$ (ohm-cm)$^{-1}$
The activation energy obtained from conductivity data below room temperature	$E = 0.039$ electron volts
The upper limit of the ordinary Hall coefficient	$R_o = -1.80 \times 10^{-11} \frac{\text{volt-cm}}{\text{amp-oersted}}$
The lower limit of the effective number of electrons/cm^3 obtained from R_o	$N^* = 3.47 \times 10^{21}$/cm^3
The lower limit of the effective number of electrons/Fe_3O_4 molecule	$n^* = 0.257$/molecule
The upper limit of the Hall mobility	$\mu_L = 0.450$ cm^2/volt-sec
The extraordinary Hall coefficient	$R_1 = -3.28 \times 10^{-8} \frac{\text{volt-cm}}{\text{amp-gauss}}$
The saturation magnetization at 0°K	$M_o = 510$ gauss
The saturation magnetization	$M_s = 472.3$ gauss
The Curie temperature	$T_c = 574$°C
The transition temperature	$T = -153.8$°C

FIG. 5-1 A PHOTOGRAPH OF THE Fe_3O_4 SAMPLE AFTER ETCHING

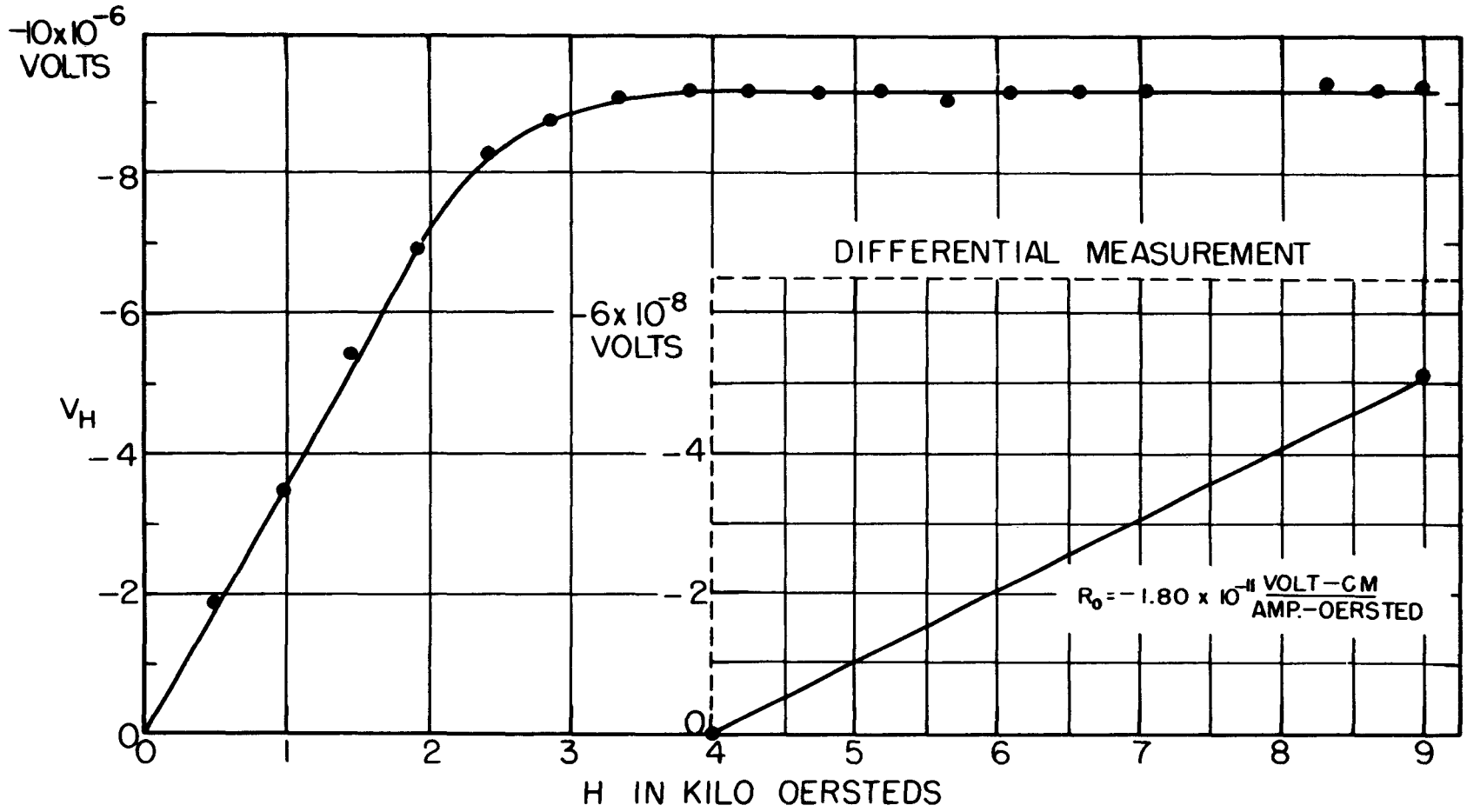

FIG. 5-2 THE HALL VOLTAGE AS A FUNCTION OF APPLIED MAGNETIC FIELD FOR Fe_3O_4 AT ROOM TEMPERATURE

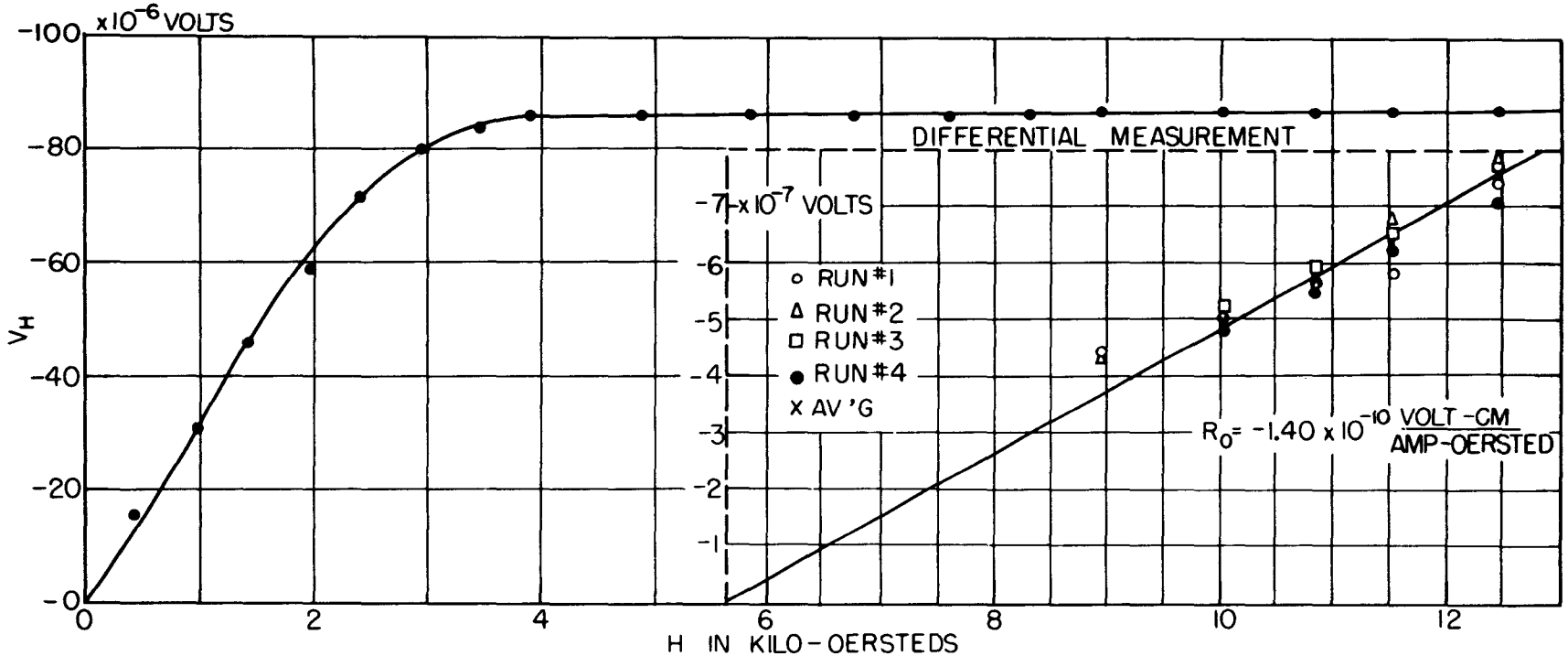

FIG. 5-3 THE HALL VOLTAGE AS A FUNCTION OF APPLIED MAGNETIC FIELD FOR $(NiO)_{.75}(FeO)_{.25}$ (Fe_2O_3) AT ROOM TEMPERATURE. SAMPLE THICKNESS, t = .100 INCHES; I = 200 MA

TABLE 5-2

SOME PHYSICAL PROPERTIES OF $(NiO)_{.75}(FeO)_{.25}(Fe_2O_3)$

The density	$d = 5.35\ gm/cm^3$
The molecular weight	$w = 233.68\ gm/mole$
The number of molecules/cm^3	$n_o = 1.38 \times 10^{22}/cm^3$
The conductivity	$\sigma = 3.40\ (ohm\text{-}cm)^{-1}$
The activation energy obtained from conductivity data below room temperature	$E = 0.078$ electron volts
The ordinary Hall coefficient	$R_o = -1.40 \times 10^{-10}\ \frac{volt\text{-}cm}{amp\text{-}oersted}$
The effective number of electrons/cm^3 obtained from R_o	$N^* = 4.46 \times 10^{20}/cm^3$
The effective number of electrons/ Fe_3O_4 molecule	$n^* = 0.129$/molecule
The Hall mobility	$\mu_L = 0.0476\ cm^2/volt\text{-}sec$
The extraordinary Hall coefficient	$R_1 = -16.4 \times 10^{-8}\ \frac{volt\text{-}cm}{amp\text{-}gauss}$
The saturation magnetization at 0^oK	$M_o = 338$ gauss
The saturation magnetization	$M_s = 308$ gauss
The Curie temperature	$T_c = 597^oC$

(C) $(NiO)_{.56}(ZnO)_{.14}(FeO)_{.30}(Fe_2O_3)$

The sample of $(NiO)_{.56}(ZnO)_{.14}(FeO)_{.30}(Fe_2O_3)$ was obtained from the Linde Air Products Company and was also a single crystal. No Hall measurements were made on this sample, but the resistivity was measured as a function of temperature. Some of the physical properties of Linde Air Products Company crystal 6/12/53 D, $(NiO)_{.56}(ZnO)_{.14}(FeO)_{.30}(Fe_2O_3)$, at room temperature ($300^oK$) are listed below.

TABLE 5-3

SOME PHYSICAL PROPERTIES OF $(NiO)_{.56}(ZnO)_{.14}(FeO)_{.30}(Fe_2O_3)$

The density	$d = 5.24$ gm/cm^3
The molecular weight	$w = 234.49$ gm/mole
The number of molecules/cm^3	$n_o = 1.35 \times 10^{22}$/cm^3
The conductivity	$\sigma = 6.67$ (ohm-cm)$^{-1}$
The activation energy obtained from the conductivity data below room temperature	E = 0.066 electron volt

5.2 Discussion of the Experimental Results

(A) Fe_3O_4

The number of molecules/cm^3 in Fe_3O_4 at room temperature is $n_o = 1.35 \times 10^{22}$/cm^3. On the basis of Verwey's simple picture of one electron per Fe_3O_4 molecule contributing to the current, we expect a value of N^* close to n_o. The value of N^* observed, $N^* = 3.47 \times 10^{21}$/cm^3, represents a lower limit of the true value of N^* and is about 1/4 the value of n_o. Thus, unless the small value of R_o is due to partial compensation by carriers of opposite sign, the observed value of N^* suggests a large carrier density roughly in accord with Verwey's hypothesis.

The conductivity of synthetic single crystals of Fe_3O_4 grown by Smiltens has been measured by Calhoun [18]. Between -100°C and 200°C, the conductivity data have been fitted by the equation

$$\sigma = AT^{-3/2} e^{-E/kT} , \tag{5.3}$$

where E = 0.039 electron volts. If we rewrite Eq. (5.3)

$$\sigma = n_o e^{-E/kT} e_L \mu_L(T) = n e_L \mu_L(T) \tag{5.4}$$

where e_L is the charge of the electron, $\mu_L(T)$ is the temperature-dependent mobility, then n, the number of electrons/cm^3 contributing to the conductivity

is given by

$$n = n_o e^{-E/kT}. \qquad (5.5)$$

If we insert the value of $n_o = 1.35 \times 10^{22}/cm^3$ and E = 0.039 electron volts, at room temperature we obtain $n = 2.98 \times 10^{21}/cm^3$, in good agreement with $N^* = 3.47 \times 10^{21}/cm^3$.

(B) $(NiO)_{.75}(FeO)_{.25}(Fe_2O_3)$

The resistivity of stoichiometric $NiOFe_2O_3$ is greater than 10^6 ohm-cm. In $NiOFe_2O_3$ the ions in the octahedral sites are not identical, and hence the distribution of electrons on the octahedral ions is not random. Because of its low conductivity, we may assume that the Ni^{2+} ion does not readily contribute an electron to the conduction process.

In the sample of $(NiO)_{.75}(FeO)_{.25}(Fe_2O_3)$, however, 1/4 of the molecules are Fe_3O_4 molecules. Therefore, on the basis of the simple Verwey model we would expect a number of electrons equal to the number of Fe_3O_4 molecules in this sample. The value of n_o of this sample is $n_o = 1.38 \times 10^{22}/cm^3$, and the number of Fe_3O_4 molecules is $3.45 \times 10^{21}/cm^3$. The observed value of $N^* = 4.46 \times 10^{20}/cm^3$ is roughly 1/10 of the number of Fe_3O_4 molecules. However, if we calculate a value of n using Eq. (5.5) with a value of E = 0.078 electron volts derived from conductivity data [see Fig. 5-4] we obtain,

$$n = \frac{n_o}{4} e^{-E/kT} = 1.68 \times 10^{20}/cm^3, \qquad (5.6)$$

which is roughly 1/3 of the observed value of N^*.

In the case of Fe_3O_4, we assume that the electron conducts by hopping along Fe^{3+} ions in the octahedral sites. In the case of $(NiO)_{.75}(FeO)_{.25}(Fe_2O_3)$ we expect that the mobility will be reduced because we do not have similar ions in all of the octahedral sites. If we assume that the mobility of $(NiO)_{.75}(FeO)_{.25}(Fe_2O_3)$ is about 1/4 the mobility of Fe_3O_4 because, on the average, each Fe_3O_4 molecule will be 3/4 surrounded by NiO Fe_2O_3 molecules, and compare the ratio of the conductivities of Fe_3O_4 and $(NiO)_{.75}(FeO)_{.25}(Fe_2O_3)$ using the values of n obtained from Eqs. (5.5) and (5.6), we obtain at room temperatu

$$\frac{\sigma(Fe_3O_4)}{\sigma[(NiO)_{.75}(FeO)_{.25}(Fe_2O_3)]} = \frac{1.35 \times 10^{22}\, e^{-\frac{0.039}{kT}}\, e_L \mu_L(T)}{\frac{1.38}{4} \times 10^{22}\, e^{-\frac{0.078}{kT}}\, e_L \frac{1}{4} \mu_L(T)} = 70.8 \qquad (5.7)$$

The observed ratio of the conductivities at room temperature is 73.5.

(C) $\underline{(NiO)_{.56}(ZnO)_{.14}(FeO)_{.30}(Fe_2O_3)}$

In the case of $(NiO)_{.56}(ZnO)_{.14}(FeO)_{.30}(Fe_2O_3)$, we expect the conductivity to be roughly the same order of magnitude as the conductivity of $(NiO)_{.75}(FeO)_{.25}(Fe_2O_3)$ since the number of Fe_3O_4 molecules is about the same. The conductivity observed at room temperature, $\sigma = 6.67\ (\text{ohm-cm})^{-1}$, is about a factor of 2 larger than the conductivity of $(NiO)_{.75}(FeO)_{.25}(Fe_2O_3)$ at room temperature. We then compare the conductivity of $(NiO)_{.56}(ZnO)_{.14}(FeO)_{.30}(Fe_2O_3)$ with the conductivity of Fe_3O_4 at room temperature. We obtain n from Eq. (5.5) assuming that n_o is equal to the number of Fe_3O_4 molecules, and we assume that the mobility is 3/10 the mobility of Fe_3O_4. Using a value of E = 0.066 electron volts derived from the data of Fig. 5-4, we obtain,

$$\frac{\sigma(Fe_3O_4)}{\sigma[(NiO)_{.56}(ZnO)_{.14}(FeO)_{.30}(Fe_2O_3)]} \qquad (5.8)$$

$$= \frac{1.35 \times 10^{22}\, e^{-\frac{0.039}{kT}}\, e_L \mu_L(T)}{\frac{3}{10}(1.35 \times 10^{22})\, e^{-\frac{0.066}{kT}}\, e_L \frac{3}{10} \mu_L(T)} = 31.4$$

The observed ratio of the conductivities at room temperature is 37.5.

(D) Concluding Remarks

The conduction mechanism of the metal oxides, of which the ferrites are a special case, is presently not very well understood. The conductivity of most transition metal oxides is very low, $\sigma < 10^{-7}\ (\text{ohm-cm})^{-1}$, in contradiction to the normally expected high conductivity of solids with incompletely filled bands. DeBoer and Verwey [65] and Mott [66] have suggested that these

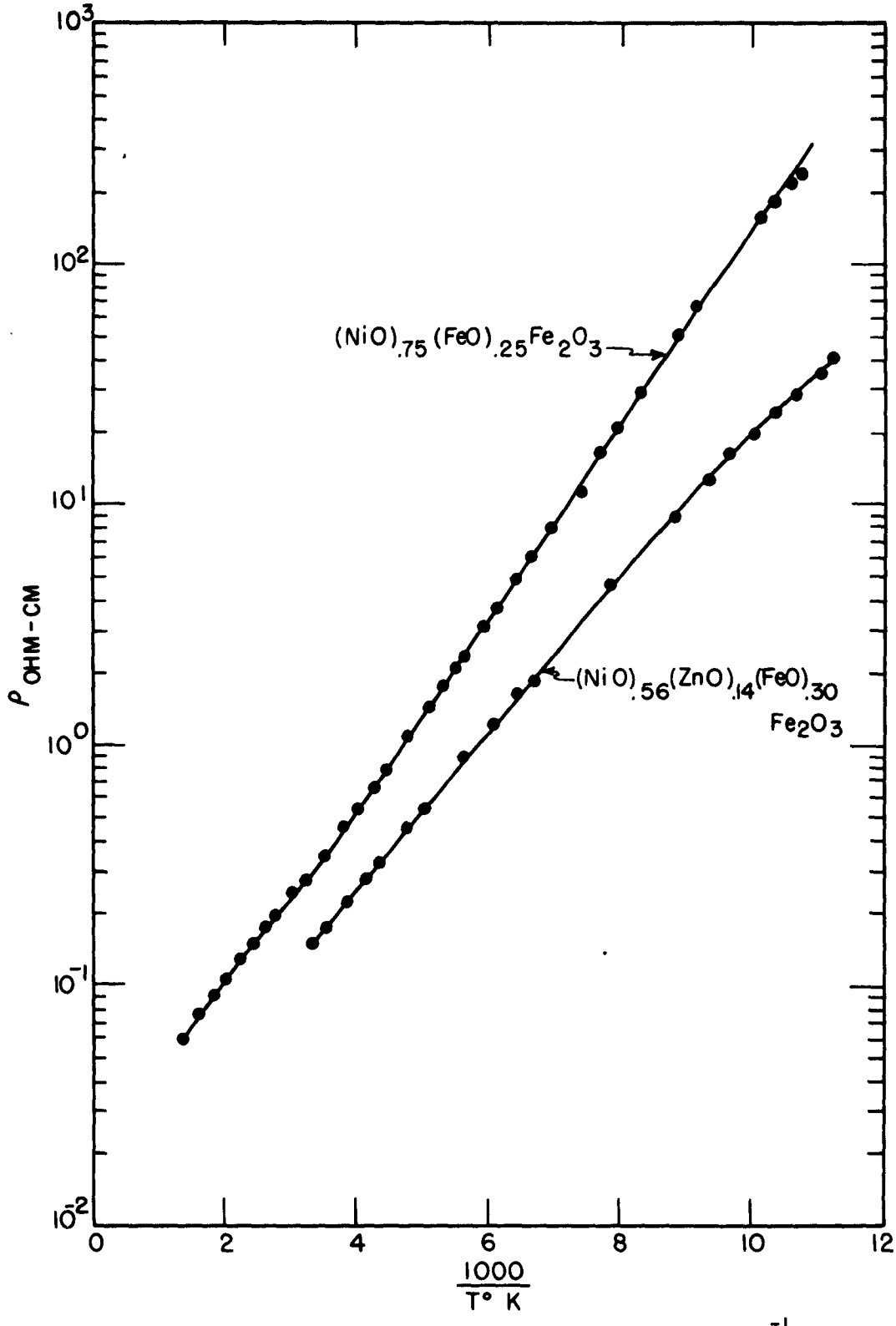

FIG. 5-4 THE RESISTIVITY AS A FUNCTION OF T^{-1} FOR $(NiO)_{.75}(FeO)_{.25}(Fe_2O_3)$ AND $(NiO)_{.56}(ZnO)_{.14}(FeO)_{.30}(Fe_2O_3)$

materials be treated in a way deviating fundamentally from the Wilson theory [67,68]. They have proposed that a suitable approximation to the state of such a system be obtained by starting with atomic wave functions and forming lattice wave functions analogous to the Heitler-London treatment of molecules. The transport of electricity is then associated with certain excited states of the metal ion.

The usual example of this mechanism is the conductivity of NiO. The Ni ion in the normal state is Ni^{2+}. An excited state giving rise to an electric current would be a state in which two Ni^{2+} are converted to one Ni^{3+} and one Ni^{+}. As may be expected, such a mechanism results in a negligibly small current, and the conductivity of pure, stoichiometric NiO is of the order of $10^{-8}(ohm\text{-}cm)^{-1}$. However, if an excess of oxygen is introduced into the lattice, resulting in metallic deficiencies, then around each missing Ni^{2+} ion, two Ni^{3+} ions are created. Under these conditions, when a normal Ni^{2+} ion is excited to an Ni^{3+} state plus an electron, and if this electron becomes trapped by an Ni^{3+} ion in the vicinity of the metal deficit, then the electron deficit may propagate through the crystal. This mechanism can then provide a current as well as an activation energy for the process, which is observed. Thus, the presence of identical ions with different valence in identical lattice sites is seen to be a condition for conduction in this oxide.

In the case of Fe_3O_4, we have a similar but not identical situation. The presence of Fe^{2+} and Fe^{3+} ions in octahedral sites occurs as a consequence of the inverted spinel structure. Under these conditions, we would expect that an electron would be free to wander through the crystal with zero activation energy. Thus the presence of a small but finite activation energy in the region above the transition requires explanation, which has not been forthcoming.

With regard to the conductivity of oxide materials, and Fe_3O_4 in particular, a few of the pertinent papers should be mentioned. Verwey and Haayman [19] have measured the conductivity of sintered bars of Fe_3O_4 with deviations from stoichiometry resulting in deficiencies of Fe^{2+} ions in octahedral sites. Their data indicate that above the transition the conductivity of Fe_3O_4, unlike that of NiO, decreases with increasing number of deficits,

while the activation energy increases. They have associated the increase of activation energy with an increase of the average energy needed to prevent the electrons from being trapped somewhere in the lattice. They suggest that the octahedral holes act as negative charge centers which tend to surround themselves with Fe^{3+} ions and hence disturb the random distribution of the electrons on the octahedral ions.

This may then suggest that in pure stoichiometric Fe_3O_4 the activation energy may approach zero. While this is a possibility, it is more than likely that Smilten's crystals contain few octahedral ion deficiencies.

Below the transition, the work of Verwey [69], Verwey and Haayman [19,20] supported by the work of Calhoun [18] has indicated that Fe_3O_4 is in an ordered state. The activation energy observed below the transition may then be associated with the observed order. One may then speculate upon the existence of short-range order in the region above the transition. However, the order of magnitude of the activation energy below the transition does not agree very well with the energy difference between the ordered and disordered state calculated for an ionic crystal, and no calculations have been carried out above the transition.

Morin [70,71] has made measurements on sintered samples of αFe_2O_3 and NiO with deviations from stoichiometry. His Hall effect measurements were inconclusive, but he has inferred a value of N^* from thermoelectric measurements. The thermoelectric and conductivity data then indicate that an activation energy is to be associated with the mobility. At high temperature, this activation energy tends toward 0.1 electron volts for both the αFe_2O_3 and NiO samples. He has then suggested that the 0.1 electron volts may be the energy required for the fundamental transfer of an electron from the potential well of one cation to the potential well of the next cation.

It may be proper to associate the observed activation energy of Fe_3O_4 above the transition with the mobility, but no conclusive arguments for doing this have yet been presented. On the other hand, the association of the activation energy with the carrier density is also without supporting argument and was done to best fit the data. In this respect, the measurements reported in this chapter are inconclusive because they have not been made as a function of temperature.

Jonker and Van Santen [72,73] have made measurements on the system $La_{1-x}A_xMnO_3$, where A represents Ca, Sr or Ba. They have attributed the good conductivity observed in a limited range of x to the transfer of electrons from Mn^{3+} to Mn^{4+} ions. In discussing these data, Zener [74] also suggests the inappropriateness of describing the electronic states in terms of the customary band representation. However, he notes that in the case of the perovskite structure ($LaMnO_3$), unlike the case of the inverted spinel, the Mn ions are sufficiently far apart as to have no appreciable overlap of wave functions. He then suggests a double exchange mechanism in which an electron is transferred from a Mn^{3+} to an O^{2-} ion with the simultaneous transfer of an electron from the O^{2-} to the Mn^{4+} ion. The double exchange will not, however, provide an activation energy. Its applicability to the case of the inverted spinels has not been established, and it requires a collinear array of Fe^{2+}, O^{2-}, Fe^{3+} ions which does not occur in the inverted spinel. In this paper, however, Zener makes an interesting suggestion concerning the relationship between the conductivity and the ferromagnetism which is observed for a limited range of x. He suggests that the electron will prefer to exchange if the spins of the Mn^{3+} and Mn^{4+} ion are in the same direction. Thus the mobility and the conductivity are improved by a ferromagnetic alignment of Mn ions. A linear relation between ρ and $\frac{T}{T_c}$ is developed.

This effect may account for some of the increase of ρ of Fe_3O_4 observed by Smith [75] [see Fig. 6-7] between room temperature and 60°C below the Curie temperature, and may account for some of the $T^{3/2}$ dependence observed by Calhoun.

These remarks simply point out the lack of a coherent picture of the conductivity of the metal oxides. The condition of similar ions with different valence in identical lattice sites seems to be a rather general condition for an appreciable conductivity, as has been pointed out by Verwey [76], but even the mechanism by which the electron hops has not been clarified.

While the measurements reported in this chapter shed no light upon the problem of the oxides, they do suggest that the number of electrons

involved in the conductivity of Fe_3O_4 is large. While the possibility that the observed value of R_o is small because of partial compensation by positive carriers is not to be ignored, nevertheless, the low conductivity of Fe_3O_4 with respect to metals is probably due to a low mobility. The limited data reported in this chapter and the low conductivity of $NiOFe_2O_3$ may also suggest that the condition of equivalent ions with different valence in identical sites is obtained in $NiOFe_2O_3$ by the addition of Fe_3O_4 molecules.

VI.

THE EXTRAORDINARY HALL MEASUREMENTS ON Ni, Ni ALLOYS, AND THE FERRITES

6.1 The Experimental Results

Measurements of R_1 were made by the field reversal technique described in Chapter II. The voltages measured were for the most part much larger than the ordinary Hall voltages observed for Grade A Ni and the ferrites, and therefore the measurements were considerably easier to perform. For example, the lowest value of voltage observed, in the 499 Alloy at -195°C, was of the order of 7×10^{-7} volts, and comparable with values of the order of 3×10^{-7} volts observed in the Grade A Ni R_o measurements, but at higher temperatures in the case of the 499 Alloy and at all temperatures in the case of the other metals, voltages greater than 1 microvolt and in many cases greater than 10 microvolts were observed. The voltages observed in the R_1 measurements on the ferrites were, for the most part, also large voltages for the measuring system.

The value of R_1 was deduced from the voltage observed at a point slightly above technical saturation. For example, in Grade A Ni (see Fig. 4-1) the value of R_1 at room temperature was deduced from the voltage observed at an applied field of about 7500 oersteds. As indicated in Eq. (2.2), the Hall voltage above technical saturation is given by

$$V_H = (R_1 M_s + R_o H) \frac{I}{t} \tag{6.1}$$

When the ratio $\frac{R_o H}{R_1 M_s}$ is small, the error in the approximation

$$V_H \simeq R_1 M_s \frac{I}{t} \tag{6.2}$$

is small, and the value of R_1 may be calculated from Eq. (6.2) with measured values of I, t, and M_s.

In this research, values of M_s were not measured. The values of M_s for 499 Alloy and Grade A Ni were obtained from the known value of

M_o, the saturation magnetization at 0°K [ref. 12, p. 270], and a universal curve of $\frac{M_s}{M_o}$ vs $\frac{T}{T_c}$ obtained from Jan's [11] data. The Curie temperature, T_c, was obtained, for the 499 Alloy, the Grade A Ni, and the other metal samples, from the observed resistivity-versus-temperature data, in the manner shown in Fig. 6-1. The value of M_o for R-63 Alloy was deduced from data presented by Bozorth [ref. 12, p. 317] which indicated a linear increase of M_o for small concentration of Mn in Ni, with a value about 10 per cent larger than Ni suggested for R-63 Alloy (95 Ni, 4 Mn, 1 Si). This value was in reasonable agreement with the value deduced from the V_H, H curve of this alloy. The temperature dependence of M_s was obtained from the $\frac{M_s}{M_o}$ vs $\frac{T}{T_c}$ curve for Ni. The values of M_s at room temperature for Supermalloy and Mumetal were obtained from Bozorth [ref. 12, p.870] and the value of M_s at room temperature for Carpenter Hymu 80 was obtained from the Carpenter Steel Company. The temperature dependence of Ms for these alloys was obtained from the universal curve for Ni. Since the curves of $\frac{M_s}{M_o}$ vs $\frac{T}{T_c}$ for Ni and Fe are very nearly coincident for small values of $\frac{T}{T_c}$, this procedure probably introduces small error in the values of M_s between liquid-air temperature and room temperature ($\frac{T}{T_c} < 0.4$). Both the value of M_o and the values of M_s for Fe_3O_4 were obtained from Pauthenet's [77] data on a natural crystal. In the case of $(NiO)_{.75}(FeO)_{.25}(Fe_2O_3)$, the value of M_o was obtained from the sum of $\frac{1}{4}$ of the value of M_o for Fe_3O_4 and $\frac{3}{4}$ of the value of M_o for $NiOFe_2O_3$, both taken from Pauthenet's [77] data. This procedure is somewhat justified by the fact that the net magnetization of the ferrites can be accounted for by the spin of the bivalent metal ion plus a small addition due to orbital contributions (i.e., g-factor greater than 2), or due to failure of some of the bivalent ions to be situated in octahedral sites [78]. In the case of both $NiOFe_2O_3$ and Fe_3O_4, the departure of the observed Bohr magneton value from the spin only value of the bivalent ion is small and can be roughly accounted for by the g-factor. Therefore, it is reasonable to assume that in $(NiO)_{.75}(FeO)_{.25}(Fe_2O_3)$ the effective Bohr magneton value may be deduced from the sum of $\frac{3}{4}$ of the observed Bohr magneton number of $NiOFe_2O_3$ and $\frac{1}{4}$ of the observed Bohr magneton number of Fe_3O_4. The value of M_o for $(NiO)_{.75}(FeO)_{.25}(Fe_2O_3)$ obtained from the M_o values of $NiOFe_2O_3$ and Fe_3O_4 is essentially equal to the value deduced

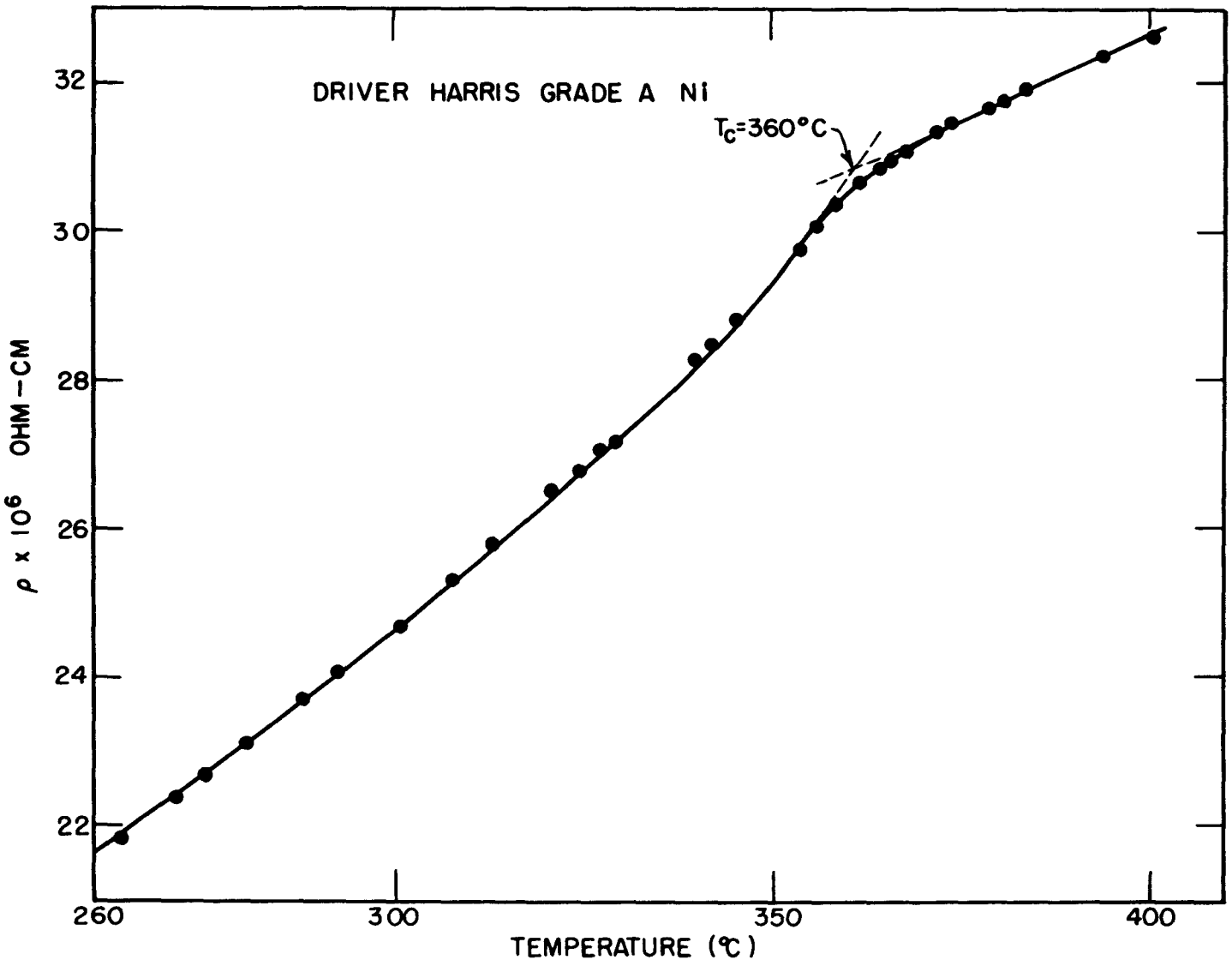

FIG. 6-1 THE METHOD OF DETERMINING THE CURIE TEMPERATURE FOR GRADE A Ni

from the composite Bohr magneton number for the material ($\beta = 2.689$). The temperature dependence of M_s for this sample was deduced from a calculated curve of $\frac{M_s}{M_o}$ vs $\frac{T}{T_c}$ using $\frac{3}{4}$ of the value of M_s for $NiOFe_2O_3$ and $\frac{1}{4}$ of the value of M_s for Fe_3O_4. This procedure is probably not justified since the exchange interactions which determine the temperature dependence probably do not average in this manner. The value of T_c used was the value for $NiOFe_2O_3$, but it is noted that T_c for Fe_3O_4 lies within 25°C of T_c for $NiOFe_2O_3$. Since the $(NiO)_{.75}(FeO)_{.25}(Fe_2O_3)$ sample is mostly $NiOFe_2O_3$, it is reasonable to assume that the true $\frac{M_s}{M_o}$ vs $\frac{T}{T_c}$ curve for this sample lies close to that for $NiOFe_2O_3$ and is probably displaced in the direction of the universal curve for Fe_3O_4. Thus, in the absence of apparatus for measuring M_s, the above procedure was used. Therefore, with the exception of $(NiO)_{.75}(FeO)_{.25}(Fe_2O_3)$, for which case the uncertainty cannot be estimated, the errors in M_s are estimated to be small.

In the case of the low temperature R_1 measurements on the metals, the ratio $\frac{R_oH}{R_1M_s}$ was not small, and corrections have been applied by calculating the H field inside the sample from the value of the applied magnetic field and the demagnetizing factor of the sample. In addition to this correction, where R_1 is small, the effective field acting on the conduction electrons must be taken into account in order to compare the observed results with the Karplus-Luttinger theory. As indicated in Eq. (1.7), the Hall voltage above technical saturation may be written

$$V_H = \left\{ R_o[H + 2\pi(1+p)M_s] + R_1'M_s \right\} \frac{I}{t} \qquad (6.3)$$

where $H + 2\pi(1+p)\,M_s$ is the effective field acting on the conduction electrons, and p has been estimated by Wannier [14] to be very nearly equal to zero. R_1' is the quantity calculated by Karplus and Luttinger [13]. In those cases where R_oH/M_s and $2\pi R_o$ were not small compared with R_1, R_1' has been deduced from the relation

$$R_1' = R_1 - \frac{R_oH}{M_s} - 2\pi R_o \qquad (6.4)$$

(A) The measurements on Grade A Ni, 499 Alloy, R-63 Alloy, Supermalloy, Mumetal, and Carpenter Hymu 80

R_1 measurements on Grade A Ni above room temperature were made simultaneously with the R_o measurements. The behavior of R_1 in Grade A

Ni was sufficiently different from the behavior of R_1 in Ni observed by Jan[11], that it seemed worthwhile, in view of the R_1 dependence upon ρ suggested by the Karplus-Luttinger theory, to explore the dependence of R_1 upon impurity and hence upon resistivity in a small region near pure Ni. Of the several commercial samples available, most possessed a liquid air temperature resistivity fairly close to that of Grade A Ni and hence were not investigated. The resistivities of Driver-Harris 499 Alloy (99.9 Ni) and R-63 Alloy (95 Ni, 4 Mn, 1 Si) were respectively three times smaller and six times larger than the resistivity of Grade A Ni (99.4 Ni) at liquid air temperature. The ρ, T curves of these alloys between liquid air temperature and temperatures slightly above their Curie temperatures are shown in Fig. 6-2. Thus, measurements were made on Driver-Harris 499 Alloy and R-63 Alloy from liquid air temperature to temperatures near their Curie temperatures, and measurements on Grade A Ni were extended from room temperature down to liquid air temperature. Figure 6-3 compares the values of R_1' of 499 Alloy, Grade A Ni, and R-63 Alloy with Jan's data. At liquid air temperature, the absolute values of R_1' for 499 Alloy and Grade A Ni are roughly 1/10 and 1/2 the absolute value of R_1' observed by Jan. On the other hand, the absolute value of R_1 (uncorrected) for R-63 Alloy at liquid air temperature, is about seven times larger than the absolute value of R_1' observed by Jan and roughly 65 times larger than the absolute value of R_1' for 499 Alloy at the same temperature. Thus, the magnitude of R_1' for these materials is significantly different at liquid air temperature. The sign of R_1', however, is negative in all of these materials. With increase of temperature, the magnitude of R_1' increases to temperatures near the Curie temperature. At about 140°C, the magnitude of R_1' of 499 Alloy and Grade A Ni is roughly the same as that observed by Jan, but only about 1/2 the absolute value of R_1 for R-63 Alloy. The difference in the behavior of Grade A Ni and Jan's data in the vicinity of 300°C may be due in part to the uncertainty in the determination of M_s in this region. Thus, over most of the observed temperature range, the absolute values of R_1' for these materials are significantly different. These data, listed in Tables 6-1, 6-2 and 6-3 will be compared with the resistivity data in Section 6.2.

While the number of ferromagnetic metals and alloys on which to test the Karplus-Luttinger theory was essentially unlimited, the equipment

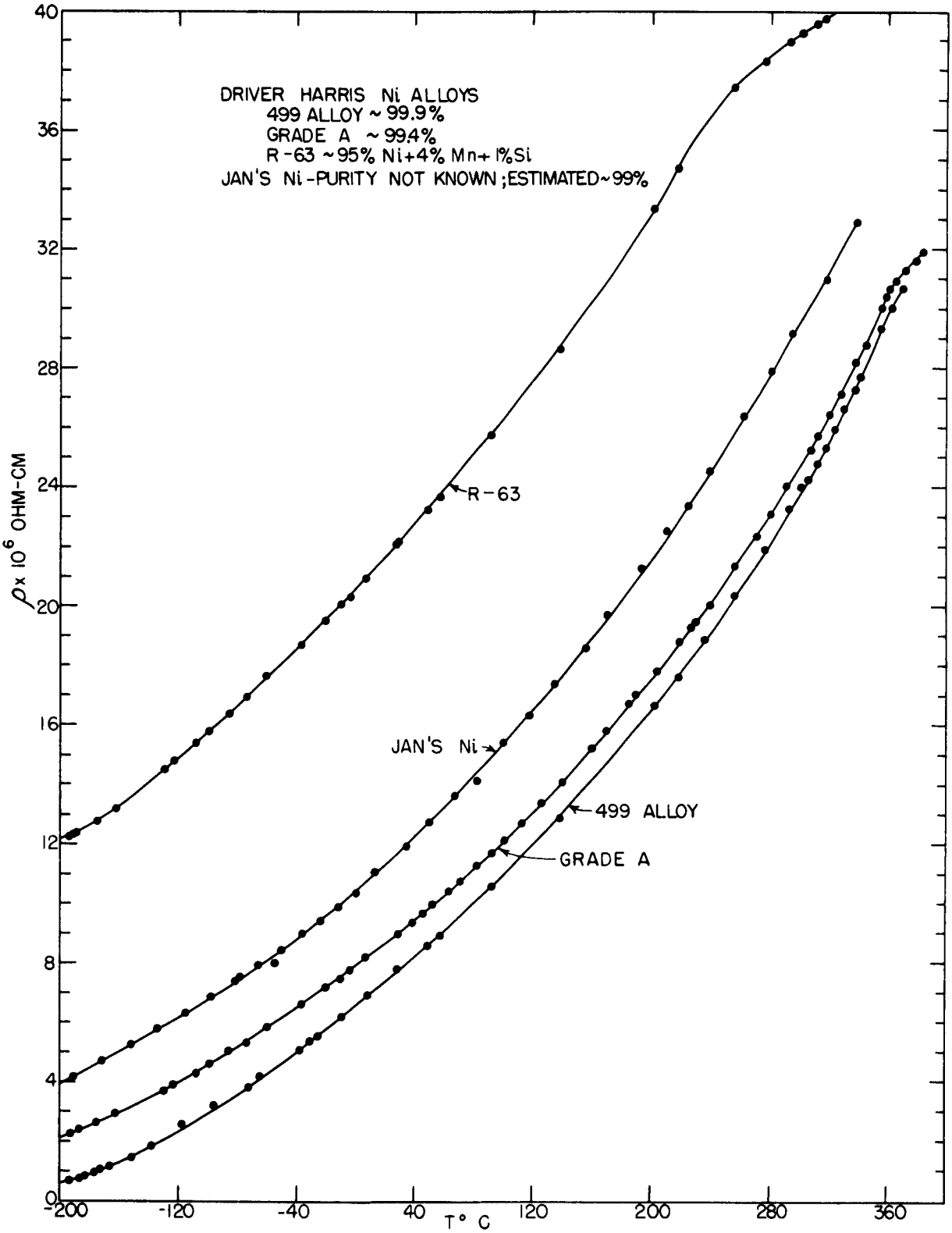

FIG. 6-2 THE RESISTIVITY OF 499 ALLOY, GRADE A Ni AND R-63 ALLOY AS A FUNCTION OF TEMPERATURE BETWEEN LIQUID AIR TEMPERATURE AND TEMPERATURES ABOVE THEIR CURIE TEMPERATURES, COMPARED WITH JAN'S DATA

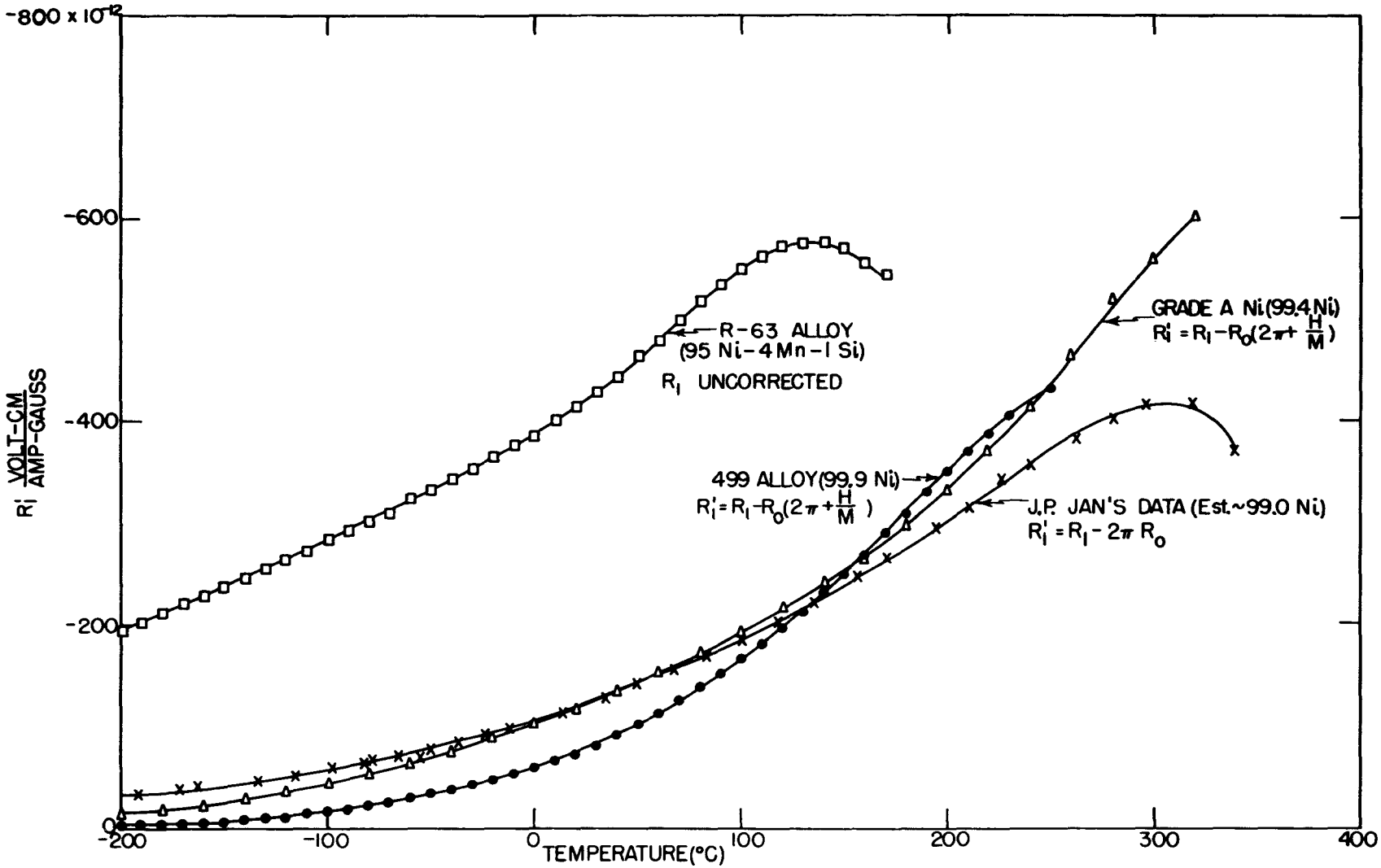

FIG. 6-3 R_i' OF 499 ALLOY, GRADE A Ni AND R-63 ALLOY AS A FUNCTION OF TEMPERATURE BETWEEN LIQUID AIR TEMPERATURE AND TEMPERATURES NEAR THEIR CURIE TEMPERATURES, COMPARED WITH JAN'S DATA

TABLE 6-1

VALUES OF M_s, R_l, R_l', ρ, AND r AS A FUNCTION OF TEMPERATURE FOR GRADE A Ni

T	M_s	$-R_l$	$-R_l'$	ρ	-r
^oK	gauss	$\frac{\text{volt-cm}}{\text{amp-gauss}}$	$\frac{\text{volt-cm}}{\text{amp-gauss}}$	ohm-cm	$\frac{(\text{ohm-cm})}{\text{gauss}}$
		$X10^{12}$	$X10^{12}$	$X10^{6}$	
73	506.3	21.3	15.4	2.08	3.56
93	505.2	24.9	19.0	2.52	2.99
113	503.7	29.8	23.9	2.97	2.71
133	502.2	35.7	29.9	3.44	2.53
153	500.7	42.6	36.9	3.97	2.34
173	499.1	50.9	45.2	4.52	2.22
193	496.1	60.4	54.8	5.12	2.09
213	493.0	70.9	65.3	5.75	1.97
233	489.5	82.0	76.5	6.42	1.86
253	485.4	94.7	89.3	7.14	1.75
273	480.8	108.	103.	7.84	1.67
293	476.2	123.	118.	8.60	1.59
313	471.1	139.	134.	9.39	1.52
333	464.5	157.	152.	10.3	1.43
353	457.4	177.	172.	11.1	1.40
373	449.8	198.	193.	12.1	1.32
393	440.6	221.	216.	13.0	1.28
413	431.5	247.	241.	14.0	1 23
433	420.8	272.	266.	15.2	1.15
453	408.6	301.	296.	16.4	1.10
473	394.8	337.	332.	17.5	1 08
493	379.6	376.	371.	18.8	1.05
513	360.2	420.	414.	20.1	1.02
533	337.8	469.	463.	21.6	0.994
553	312.9	525.	520.	23.1	0.983
573	281.9	565.	560.	24.6	0.926
593	240.7	606.	601.	26.4	0.862
613	178.1	709.	704.	28.3	0.879

$$T_c = 631^oK$$

$$M_o = 508.8 \text{ gauss}$$

$$R_l' = R_l - R_o\left(2\pi + \frac{H}{M_s}\right)$$

$$r = \frac{R_l'}{\rho^2} \quad \frac{(\text{ohm-cm})^{-1}}{\text{gauss}}$$

TABLE 6-2

VALUES OF M_s, R_l, R_l', ρ, AND r AS A FUNCTION OF TEMPERATURE FOR 499 ALLOY

T	M_s	$-R_l$	$-R_l'$	ρ	$-r$
^oK	gauss	$\frac{\text{volt-cm}}{\text{amp-gauss}}$	$\frac{\text{volt-cm}}{\text{amp-gauss}}$	ohm-cm	$\frac{(\text{ohm-cm})^{-1}}{\text{gauss}}$
		$X10^{10}$	$X10^{12}$	$X10^{6}$	
73	506.3	8.97	3.01	0.65	7.12
93	505.2	10.3	4.38	0.88	5.66
113	503.7	12.1	6.27	1.25	4.02
133	502.2	14.5	8.68	1.72	2.93
153	500.7	17.9	12.2	2.31	2.28
173	499.1	22.1	16.5	2.96	1.88
193	496.1	28.0	22.4	3.65	1.68
213	493.0	35.6	30.0	4.32	1.60
233	489.5	44.0	38.5	4.99	1.55
253	485.4	54.0	48.6	5.74	1.48
273	480.8	65.6	60.3	6.53	1.41
293	476.2	79.1	73.7	7.38	1.35
313	471.1	97.2	91.9	8.20	1.37
333	464.5	119.	114.	9.04	1.40
353	457.4	144.	139.	9.97	1.40
373	449.8	172.	166.	10.9	1.39
393	440.6	201.	196.	12.0	1.36
413	431.5	236.	230.	13.0	1.36
433	420.8	273.	268.	14.1	1.35
453	408.6	314.	308.	15.3	1.32
473	394.8	355.	350.	16.5	1.29
493	379.6	393.	388.	17.8	1.22
513	360.2	426.	420.	19.2	1.14

$$T_c = 631^oK$$

$$M_o = 508.8 \text{ gauss}$$

$$R_l' = R_l - R_o\left(2\pi + \frac{H}{M_s}\right)$$

$$r = \frac{R_l'}{\rho} \frac{(\text{ohm-cm})^{-1}}{\text{gauss}}$$

TABLE 6-3

VALUES OF M_s, R_l, ρ, AND r AS A FUNCTION OF TEMPERATURE FOR R-63 ALLOY

T ^{o}K	M_s gauss	$-R_l$ $\frac{\text{volt-cm}}{\text{amp-gauss}}$ $\times 10^{-10}$	ρ ohm-cm $\times 10^{6}$	$-r$ $\frac{(\text{ohm-cm})^{-1}}{\text{gauss}}$
73	548.1	1.95	12.1	1.34
93	546.5	2.12	12.6	1.33
113	544.3	2.29	13.2	1.32
133	542.1	2.46	14.0	1.26
153	539.3	2.64	14.8	1.21
173	535.4	2.83	15.7	1.15
193	531.0	3.01	16.6	1.09
213	525.5	3.23	17.5	1.06
233	519.4	3.43	18.5	1.00
253	512.8	3.65	19.5	0.961
273	510.0	3.85	20.6	0.908
293	494.6	4.15	21.7	0.881
313	484.1	4.43	22.7	0.860
333	472.5	4.79	23.9	0.839
353	458.7	5.18	25.1	0.822
373	442.7	5.49	26.2	0.800
393	425.0	5.71	27.4	0.760
413	401.9	5.75	28.7	0.698
433	375.4	5.55	30.1	0.613
443	359.4	5.43	30.9	0.569

$$T_c = 519^{o}K$$

$$M_o = 552 \text{ gauss}$$

$$r = \frac{R_l}{\rho^2} \frac{(\text{ohm-cm})^{-1}}{\text{gauss}}$$

imposed certain limitations upon the choice of samples. The magnet gap for low-temperature measurements was limited to two inches because of the size of the dewar, and thus samples with a magnetic induction less than 9000 gauss were required. Because the voltages measured were proportional to the current density, thin samples were needed in order to obtain reasonable voltages with the available current supply. The inherent difficulties in alloying and rolling suitable samples called for the use of commercially available products or those available from other laboratories. Thus it was decided to make measurements on some of the high-permeability Ni-Fe alloys with about 80 per cent Ni content because they fulfilled the above requirements and because it was of interest to observe the behavior of R_1 in alloys in which ρ was an insensitive function of temperature. As is well known, the resistivity of an alloy is composed of two parts; a residual resistance which is temperature independent and a temperature-dependent part. If the residual resistance, which increases with increase of alloying constituent, is large compared with the temperature-dependent part, then the total resistivity has a fairly insensitive temperature dependence. The resistivity data of the 80 per cent Ni-Fe alloys, Supermalloy, Mumetal, and Carpenter Hymu 80, as a function of temperature between liquid air temperature and temperatures above their Curie temperatures, are shown in Fig. 6-4. Between liquid air temperature and room temperature, the resistivities of these alloys increase by less than 25 per cent compared with changes by factors of 10, 4, and 2 for 499 Alloy, Grade A Ni, and R-63 Alloy, over the same temperature range.

Figure 6-5 shows both the observed values of R_1 and the corrected values of R_1' as a function of temperature, between liquid air temperature and room temperature, for these alloys. The corrections were made using a value of R_o obtained by Foner [79] on 75 Ni - 25 Fe, and therefore may be in error. The values of R_1' observed for the 80 per cent Ni-Fe alloys are roughly the same order of magnitude as the value observed for Grade A Ni at room temperature. However, R_1' in these alloys is positive, in contrast with the negative values of R_1' observed in the high-concentration Ni alloys. The values of R_1' increase by less than a factor of 2 from liquid air temperature to room temperature compared with increases by about a factor of 2

for the R-63 Alloy, and by factors of about 7 and 15 for the Grade A Ni and 499 Alloy over the same temperature range. These data are listed in Tables 6-4, 6-5, and 6-6.

(B) The Measurements on Fe_3O_4 and $(NiO)_{.75}(FeO)_{.25}(Fe_2O_3)$

As suggested in Chapter I, it was significant to observe the behavior of R_1 in Fe_3O_4 because of the R_1 dependence upon ρ suggested by the Karplus-Luttinger theory. The resistivity of Fe_3O_4 is strongly temperature dependent below room temperature, and at the transition temperature, $T = -153.8^{\circ}C$, there is a 100-fold increase of resistivity. Figure 6-6 shows the resistivity of Fe_3O_4 as a function of T^{-1}. The low-temperature data were obtained from Calhoun [18] and the high-temperature data are due to D. O. Smith [75]. Since the ratio R_1/R_o is large in Fe_3O_4, neither the R_oH/M_s nor the $2\pi R_o$ correction is significant and the observed values of R_1 are reported. Figure 6-7 shows R_1 as a function of temperature between $-140^{\circ}C$ and $550^{\circ}C$. Values of ρ are plotted on the same graph for comparison. R_1 at room temperature is negative and in absolute value roughly 300 times larger than the absolute values observed for both Grade A Ni and 499 Alloy at room temperature. Above room temperature, R_1 decreases in absolute value with increasing temperature and passes through zero at about $380^{\circ}C$. The sign of R_1 above $380^{\circ}C$ is positive. Below room temperature, the value of R_1 is essentially constant between $0^{\circ}C$ and $-60^{\circ}C$ and increases in absolute value with decrease of temperature between $-60^{\circ}C$ and $-140^{\circ}C$. The solid data points of Fig. 6-7 were obtained on another sample of Fe_3O_4 from the same melt, which was somewhat less homogeneous electrically because of grain boundaries. Between $-140^{\circ}C$ and liquid oxygen temperature ($-183^{\circ}C$), the absolute value of R_1 increases by about a factor of 500 while the resistivity increases by about a factor of 10^5. Between liquid oxygen and liquid air temperatures, R_1 remains essentially constant while the resistivity increases by a factor of 7.

In the case of the measurements on $(NiO)_{.75}(FeO)_{.25}(Fe_2O_3)$, the corrections are not important and the observed values of R_1 are reported. Figure 6-8 shows R_1 for $(NiO)_{.75}(FeO)_{.25}(Fe_2O_3)$ as a function of temperature between $-100^{\circ}C$ and $580^{\circ}C$. At room temperature R_1 is negative and 5 times

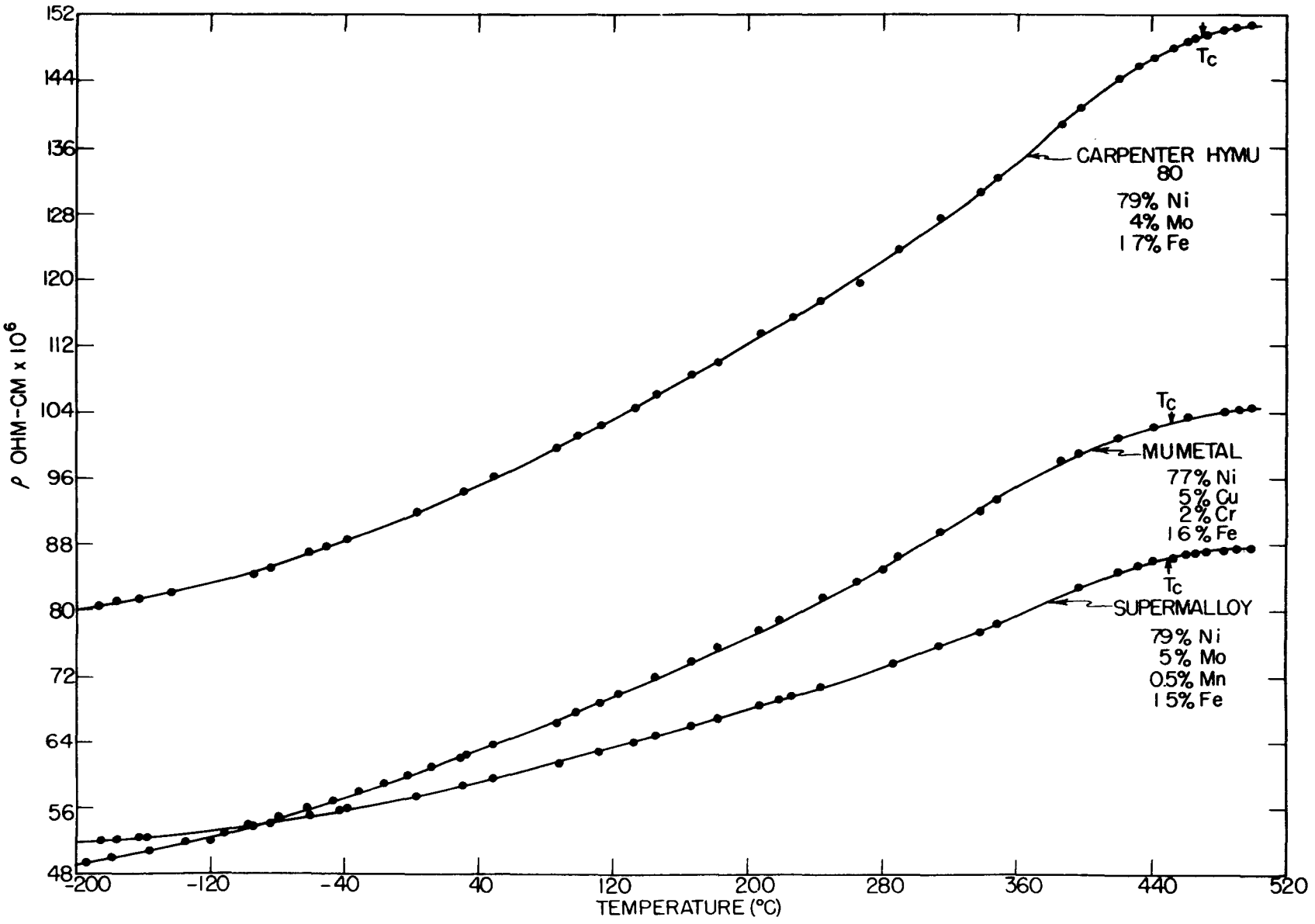

FIG. 6-4 THE RESISTIVITY OF SUPERMALLOY, MUMETAL AND CARPENTER HYMU 80, AS A FUNCTION OF TEMPERATURE BETWEEN LIQUID AIR TEMPERATURE AND TEMPERATURES ABOVE THEIR CURIE

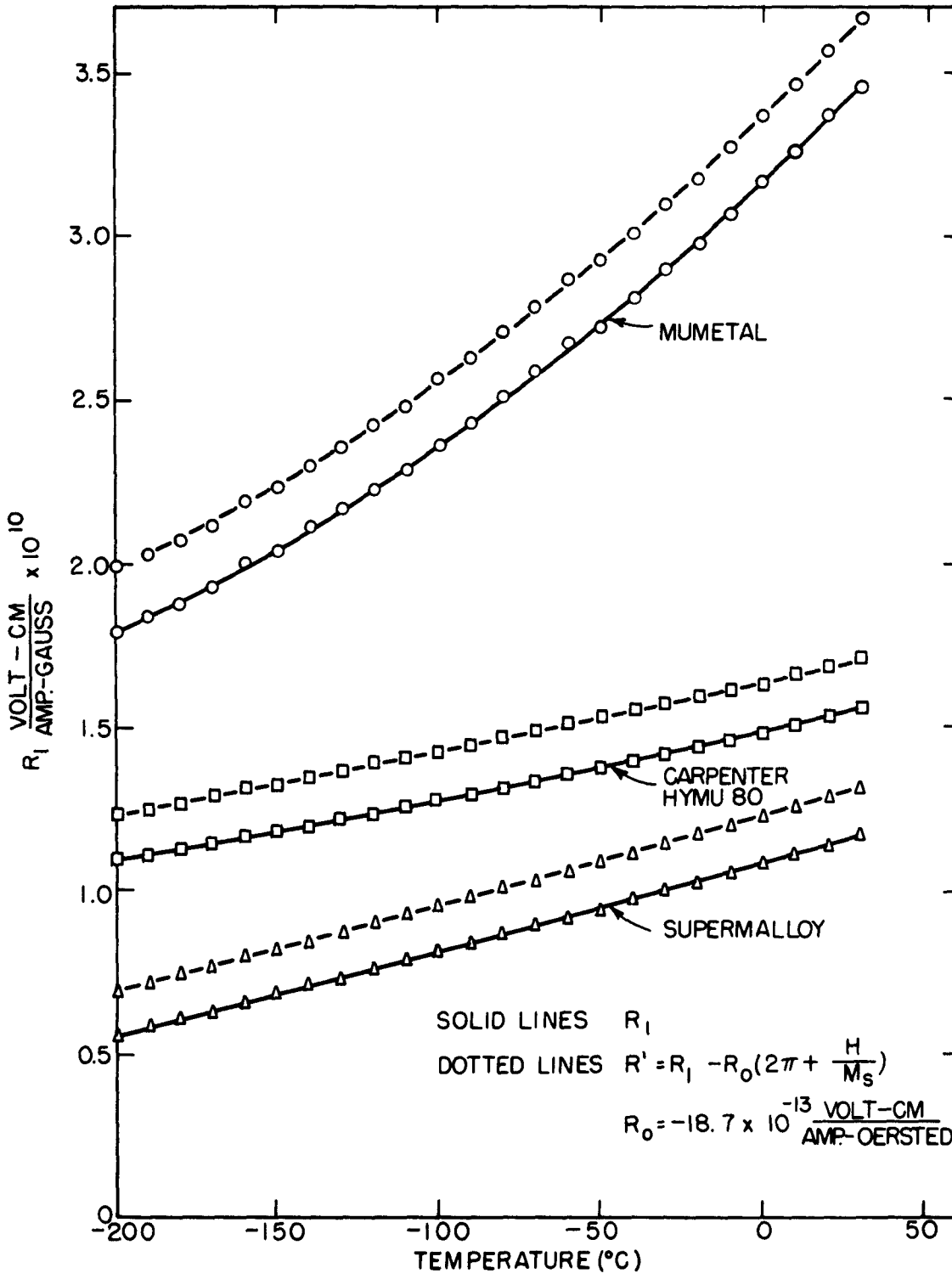

FIG. 6-5 THE OBSERVED VALUES OF R_1 AND THE CORRECTED VALUES OF R_1' AS A FUNCTION OF TEMPERATURE FOR SUPERMALLOY, CARPENTER HYMU 80, AND MUMETAL

TABLE 6-4

VALUES OF M_s, R_1, R_1', ρ, AND r AS A FUNCTION OF TEMPERATURE FOR SUPERMALLOY

T ^oK	M_s gauss	R_1 $\frac{\text{volt-cm}}{\text{amp-gauss}}$ $\times 10^{11}$	R_1' $\frac{\text{volt-cm}}{\text{amp-gauss}}$ $\times 10^{11}$	ρ ohm-cm $\times 10^{5}$	r $\frac{(\text{ohm-cm})^{-1}}{\text{gauss}}$ $\times 10^{2}$
73	659.1	5.63	6.98	5.20	2.58
93	657.8	6.11	7.47	5.22	2.75
113	656.5	6.63	8.00	5.25	2.90
133	654.8	7.12	8.50	5.29	3.04
153	653.2	7.62	9.01	5.33	3.17
173	651.2	8.12	9.52	5.38	3.29
193	649.2	8.66	10.1	5.44	3.41
213	646.6	9.17	10.6	5.50	3.50
233	643.3	9.73	11.2	5.57	3.61
253	640.0	10.3	11.7	5.66	3.66
273	635.3	10.9	12.3	5.75	3.72
293	630.7	11.5	12.9	5.84	3.78
303	628.0	11.8	13.3	5.89	3.83

$$T_c = 723^oK$$

$$M_o = 661.8 \text{ gauss}$$

$$R_1' = R_1 - R_o\left(2\pi + \frac{H}{M_s}\right)$$

$$R_o = -18.7 \times 10^{-13} \frac{\text{volt-cm}}{\text{amp-oersted}}$$

$$r = \frac{R_1}{\rho^2} \frac{(\text{ohm-cm})^{-1}}{\text{gauss}}$$

TABLE 6-5

VALUES OF M_s, R_l, R_l', and ρ, AND r AS A FUNCTION OF TEMPERATURE FOR MUMETAL

T ^oK	M_s gauss	R_l $\frac{\text{volt-cm}}{\text{amp-gauss}}$ $\times 10^{10}$	R_l' $\frac{\text{volt-cm}}{\text{amp-gauss}}$ $\times 10^{10}$	ρ ohm-cm $\times 10^{5}$	r $\frac{(\text{ohm-cm})^{-1}}{\text{gauss}}$ $\times 10^{3}$
73	542.9	1.80	1.99	4.91	8.26
93	541.8	1.88	2.07	4.99	8.31
113	540.7	2.00	2.19	5.09	8.46
133	539.6	2.11	2.30	5.18	8.58
153	538.0	2.23	2.42	5.28	8.67
173	536.4	2.37	2.57	5.39	8.83
193	534.7	2.51	2.71	5.50	8.94
213	532.6	2.67	2.87	5.62	9.08
233	529.8	2.81	3.01	5.75	9.09
253	527.1	2.98	3.18	5.88	9.19
273	523.3	3.17	3.37	6.02	9.31
293	519.5	3.37	3.57	6.16	9.42
303	517.3	3.46	3.66	6.23	9.43

$$T_c = 725^oK$$

$$M_o = 545.1 \text{ gauss}$$

$$R_l' = R_l - R_o\left(2\pi + \frac{H}{M_s}\right)$$

$$R_o = -18.7 \times 10^{-13} \frac{\text{volt-cm}}{\text{amp-oersted}}$$

$$r = \frac{R_l'}{\rho^2} \frac{(\text{ohm-cm})^{-1}}{\text{gauss}}$$

TABLE 6-6

VALUES OF M_s, R_l, R_l', ρ, AND r AS A FUNCTION OF TEMPERATURE FOR CARPENTER HYMU 80

T ^oK	M_s gauss	R_l $\frac{\text{volt-cm}}{\text{amp-gauss}}$	R_l' $\frac{\text{volt-cm}}{\text{amp-gauss}}$	ρ ohm-cm	r $\frac{(\text{ohm-cm})^{-1}}{\text{gauss}}$
		$X10^{10}$	$X10^{10}$	$X10^{5}$	$X10^{2}$
73	632.8	1.09	1.24	8.02	1.93
93	631.5	1.13	1.28	8.07	1.97
113	630.2	1.17	1.32	8.14	1.99
133	628.9	1.20	1.35	8.22	2.00
153	627.7	1.24	1.39	8.32	2.01
173	625.8	1.27	1.42	8.43	2.00
193	623.9	1.32	1.47	8.56	2.01
213	621.3	1.36	1.51	8.70	1.99
233	618.8	1.40	1.55	8.85	1.98
253	615.0	1.44	1.60	9.01	1.97
273	611.8	1.48	1.64	9.18	1.95
293	607.3	1.53	1.69	9.36	1.93
303	604.8	1.56	1.72	9.45	1.93

$T_c = 743^oK$

$M_o = 635.3$ gauss

$R_l' = R_l - R_o(2\pi + \frac{H}{M_s})$

$R_o = -18.7 \times 10^{-13} \frac{\text{volt-cm}}{\text{amp-oersted}}$

$r = \frac{R_l'}{\rho^2} \left(\frac{\text{ohm-cm})^{-1}}{\text{gauss}}\right.$

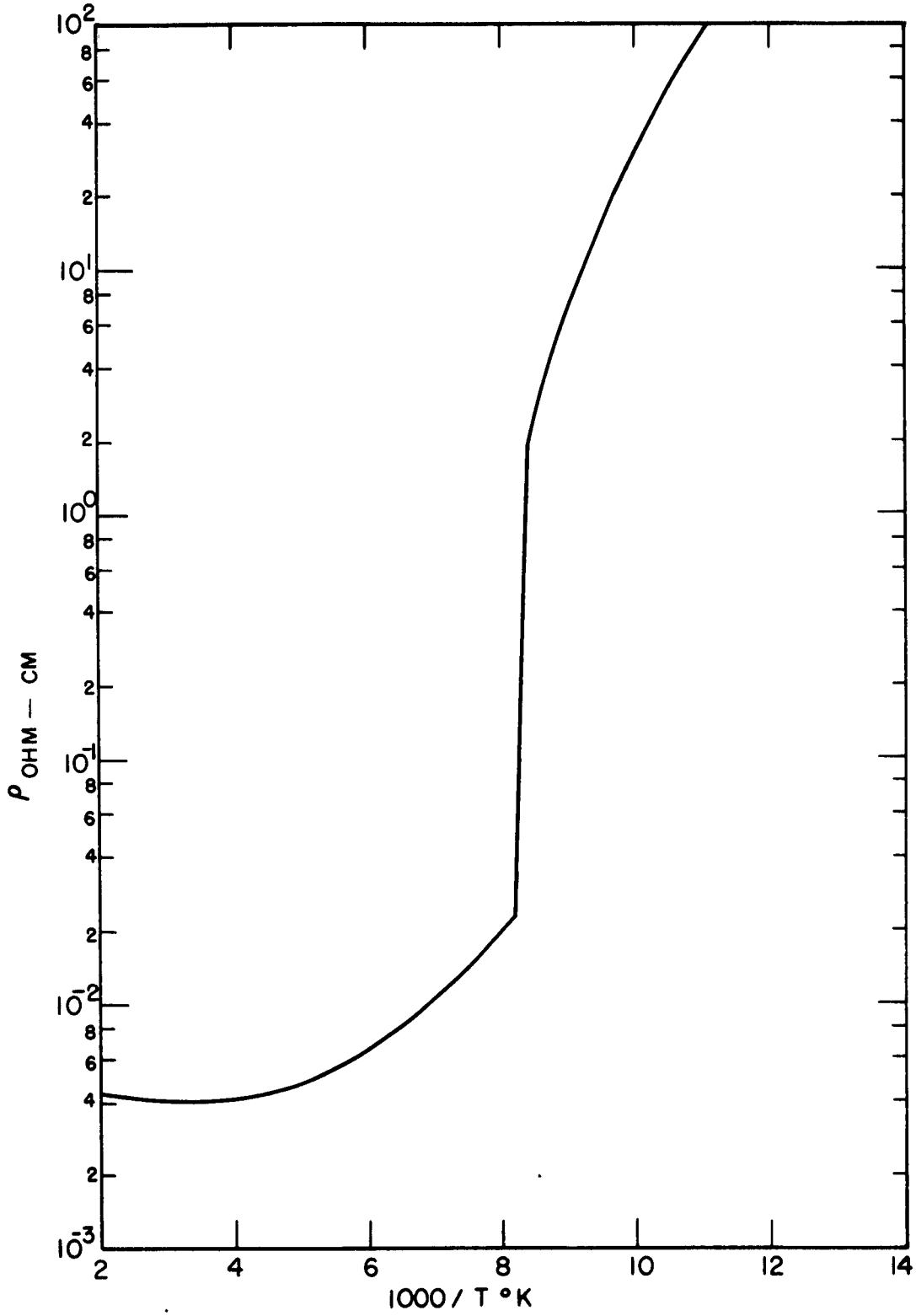

FIG. 6-6 THE RESISTIVITY OF SYNTHETIC SINGLE CRYSTAL Fe_3O_4 AS A FUNCTION OF T^{-1}

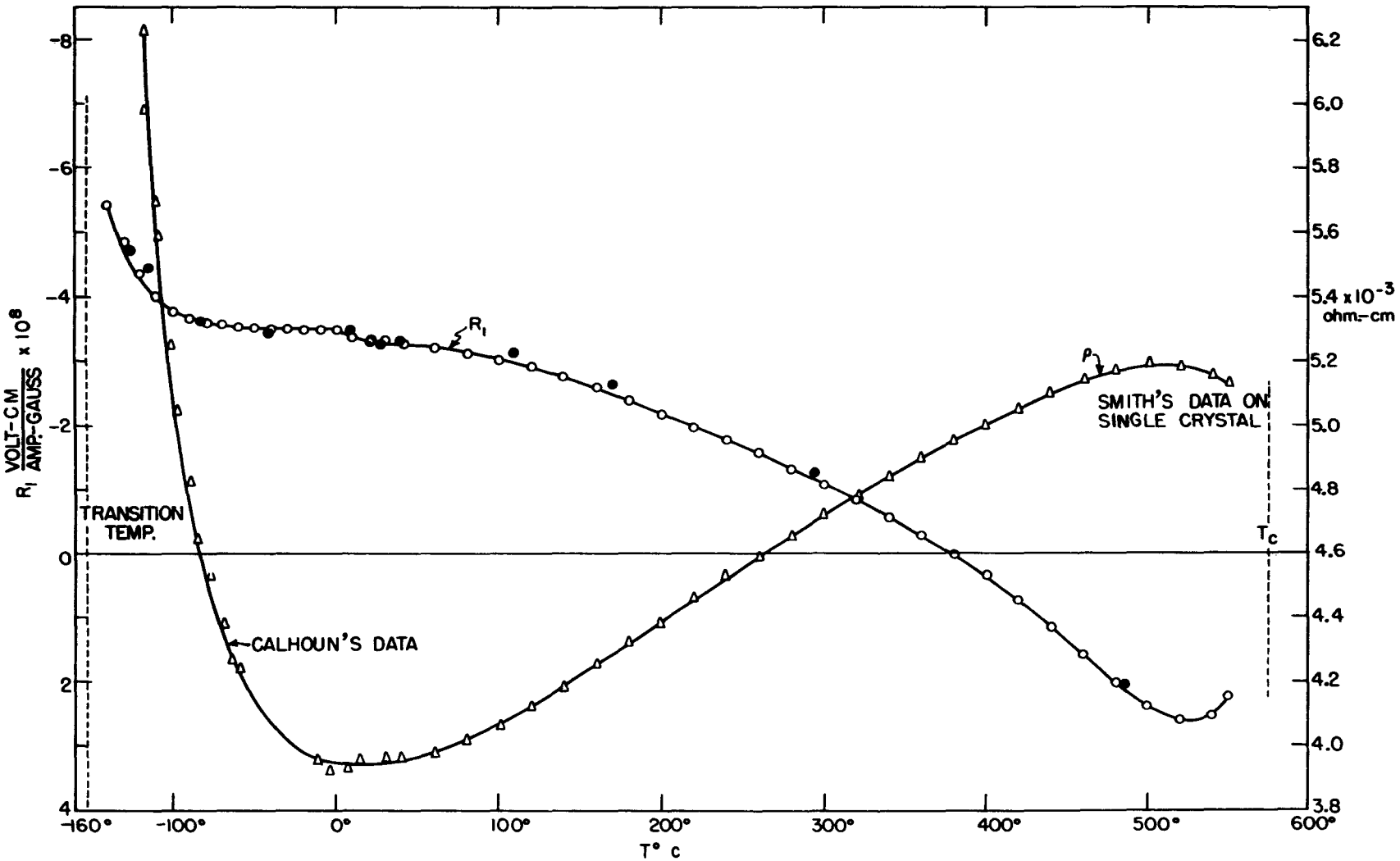

FIG. 6-7 R_I AND ρ FOR Fe_3O_4 AS A FUNCTION OF TEMPERATURE BETWEEN THE TRANSITION TEMPERATURE AND THE CURIE TEMPERATURE

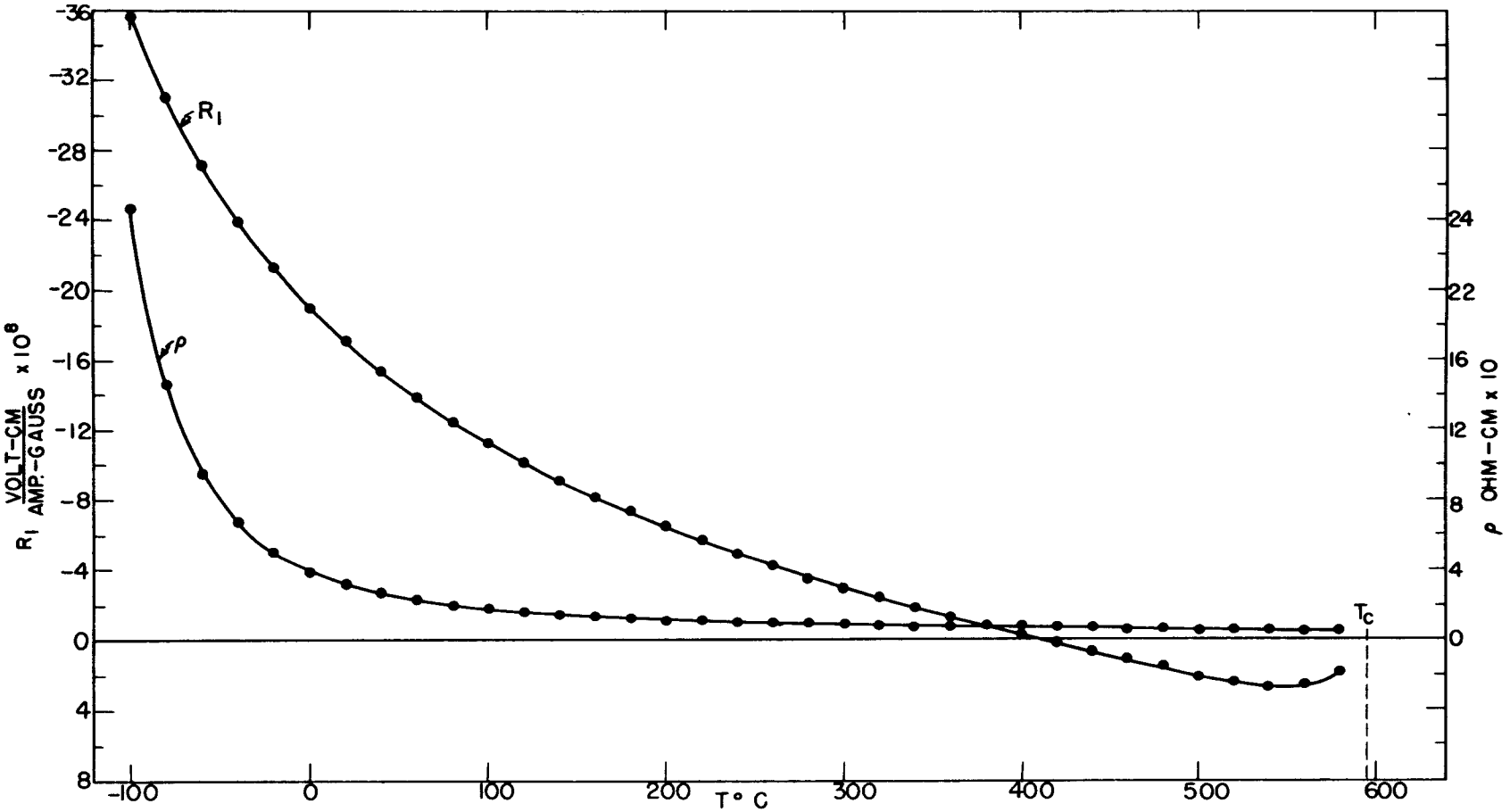

FIG. 6-8 R_1 AND ρ AS A FUNCTION OF TEMPERATURE FOR $(NiO)_{.75}(FeO)_{.25}(Fe_2O_3)$

larger in absolute value than R_1 in Fe_3O_4. R_1 decreases in absolute value with increase of temperature somewhat in the same manner as R_1 in Fe_3O_4, and passes through zero at about 410°C. Above 410°C the sign of R_1 is positive. From room temperature to -100°C, R_1 increases in absolute value with decrease of temperature. Values of ρ over the same range of temperature are plotted in Fig. 6-8 for comparison (Fig. 5-4 shows the plot of log ρ versus 1/T for this sample). The data for Fe_3O_4 and $(NiO)_{.75}(FeO)_{.25}(Fe_2O_3)$ are listed in Tables 6-7 and 6-8.

6.2 Discussion of the Experimental Results

(A) The Ni and Ni Alloys

As indicated in Chapter I, the Karplus-Luttinger theory suggests that R_1^i is proportional to the square of the resistivity. In order to observe the ρ dependence of R_1^i, values of log R_1^i are plotted as a function of log ρ, and the ρ dependence is obtained directly from the slope of the curve. The Grade A Ni data indicate a $\rho^{1.49}$ dependence over most of the observed range. The corrections discussed in Section 6.1 have small effect in the region above $\rho = 8.88 \times 10^{-6}$ ohm-cm (room temperature), but in the region around $\rho = 3 \times 10^{-6}$ ohm-cm (liquid-air temperature) the corrections tend to improve the linearity of the log R_1^i versus log ρ curve. The $\rho^{1.49}$ dependence of R_1^i observed in Grade A Ni is similar to the $\rho^{1.46}$ dependence obtained from Jan's data. Figure 6-9 compares the R_1^i, ρ data of the Grade A Ni with Jan's data. The departure of Jan's data from linearity at low values of resistivity may be due in part to the failure to apply the R_0H/M_s correction. While the slopes of the two curves are approximately the same above $\rho = 8.88 \times 10^{-6}$ ohm-cm, the curve for Grade A Ni lies about 50 per cent higher than the curve for Jan's sample.

Figure 6-9 also shows the R_1^i, ρ data for the 499 Alloy. In the region between $\rho = 6.95 \times 10^{-6}$ ohm-cm (10°C) and $\rho = 14.12 \times 10^{-6}$ ohm-cm (160°C), R_1^i is proportional to $\rho^{1.97}$, in good agreement with the Karplus-Luttinger theory. However, between $\rho = 6.95 \times 10^{-6}$ ohm-cm(10°C) and $\rho = 3.65 \times 10^{-6}$ ohm-cm(-80°C), R_1^i is proportional to $\rho^{1.70}$, and between $\rho = 2.63 \times 10^{-6}$ ohm-cm(-110°C) and $\rho = 0.65 \times 10^{-6}$ ohm-cm(-200°C), R_1^i is proportional to $\rho^{1.10}$. In the case of the 499 Alloy, the corrections indicated in Section 6.1 are necessary in order to obtain the $\rho^{1.97}$ dependence

in the region above $\rho = 6.95 \times 10^{-6}$ ohm-cm. However, the corrections do not improve the linearity of the data at low values of ρ although they are in the right direction. Thus the R_1' data for the Grade A Ni, the 499 Alloy, and Jan's sample do not exhibit a general ρ^2 dependence. However, the data over almost three decades of R_1' definitely suggest some dependence on ρ, and the wide spread of values of R_1' for these materials at liquid air temperature appears to be related to the values of resistivity observed at this temperature.

The R_1, ρ data for the R-63 Alloy are also shown in Fig. 6-9, and they suggest a $\rho^{1.20}$ dependence for R_1 (uncorrected) between $\rho = 13.2 \times 10^{-6}$ ohm-cm (-160°C) and $\rho = 22.2 \times 10^{-6}$ ohm-cm (30°C). The observed values of R_1 have been used in the analysis of these data because the value of R_o was not measured. However, even if the value of R_o for R-63 were double the value of R_o for Ni, the ρ dependence would be altered by less than 10 per cent. It is most significant that the liquid air temperature value of R_1 for R-63 Alloy which in absolute value is roughly 65 times larger than R_1' for the 499 Alloy and roughly 13 times larger than R_1' for Grade A Ni at the same temperature is equal to the value of R_1' for these materials at $\rho = 12.1 \times 10^{-6}$ ohm-cm. Thus, the large values of R_1 observed at low temperatures for R-63 Alloy appear to be a consequence of the high resistivity of this alloy at low temperatures. Moreover, the relatively small increase of R_1 in R-63 over the observed range of temperature is in marked contrast to the large variation observed in the 499 Alloy, yet, both are correlated with the temperature variation of their resisitvities.

It is noted that R_1 in these materials has been measured with a saturating magnetic field and compared with the resistivity measured at zero magnetic field. In no case, however, will the magneto-resistance alter the ρ dependence of R_1' by more than a few per cent. Thus, it is not at all probable that the deviation from a ρ^2 dependence in these materials can be attributed to experimental error.

In the Karplus-Luttinger theory, the predicted ρ^2 dependence of R_1' comes about because the physical mechanism leads to a quantity $r = \frac{J_y}{E_x M}$ whereas the conventional Hall measuring technique gives $R_1' = \frac{E_y}{J_x M}$. Strict ρ^2 dependence would thus imply a value of r which is temperature

TABLE 6-7

VALUES OF M_s, R_1, ρ, AND r AS A FUNCTION OF TEMPERATURE FOR Fe_3O_4

T	M_s	R_1	ρ	r
^oK	gauss	$\frac{\text{volt-cm}}{\text{amp-gauss}}$	ohm-cm	$\frac{(\text{ohm-cm})^{-1}}{\text{gauss}}$
		$X10^8$	$X10^3$	$X10^3$
133	502.9	-5.44	15.0	-0.242
153	500.3	-4.35	8.25	-0.639
173	497.8	-3.77	6.00	-1.05
193	494.2	-3.61	5.01	-1.44
213	490.6	-3.52	4.45	-1.78
233	487.1	-3.48	4.20	-1.98
253	483.0	-3.48	4.10	-2.07
273	478.4	-3.49	4.01	-2.17
293	473.8	-3.28	3.96	-2.09
313	468.7	-3.27	3.96	-2.08
333	463.6	-3.18	3.98	-2.01
353	457.5	-3.11	4.01	-1.93
373	451.9	-3.00	4.06	-1.82
393	445.2	-2.92	4.12	-1.72
413	438.6	-2.75	4.18	-1.57
433	431.5	-2.57	4.25	-1.42
453	423.8	-2.39	4.32	-1.28
473	416.2	-2.19	4.38	-1.14
493	407.5	-1.98	4.46	-0.995
513	398.3	-1.77	4.52	-0 868
533	392.2	-1.54	4.58	-0.733
553	378.9	-1.32	4.65	-0.611
573	368.2	-1.08	4.71	-0.486
593	357.0	-0.84	4.77	-0.37
613	345.3	-0.57	4.83	-0.24
633	334.1	-0.27	4.89	-0.11
653	320.8	+0.03	4.95	+0.01
673	307.5	0.35	5.00	0.14
693	293.8	0.72	5.05	0.28
713	278.0	1.14	5.09	0.440
733	261.1	1.59	5.13	0.605
753	241.7	2.02	5.17	0.757
773	219.3	2.40	5.19	0.892
793	193.3	2.61	5.18	0.974
813	158.1	2.55	5.15	0.962
823	134.1	2.21	5.13	0.840

$T_C = 847^oK$;

$M_o = 510$ gauss;

$$r = \frac{R_1}{\rho^2} \frac{(\text{ohm-cm})^{-1}}{\text{gauss}}$$

TABLE 6-8

VALUES OF M_s, R_1, ρ, AND r AS A FUNCTION OF TEMPERATURE FOR $(NiO)_{.75}(FeO)_{.25}(Fe_2O_3)$

T	M_s	R_1	ρ	r
^oK	gauss	$\frac{\text{volt-cm}}{\text{amp-gauss}}$	ohm-cm	$\frac{(\text{ohm-cm})^{-1}}{\text{gauss}}$
		$X10^8$		$X10^6$
173	328	-35.6	2.46	-0.059
193	325	-31.0	1.46	-0.150
213	323	-27.1	0.960	-0.294
233	320	-23.9	0.670	-0.532
253	316	-21.3	0.500	-0.852
273	313	-19.0	0.385	-1.28
293	309	-17.1	0.312	-1.76
313	306	-15.4	0.266	-2.18
333	301	-13.9	0.230	-2.63
353	296	-12.5	0.202	-3.06
373	291	-11.2	0.179	-3.50
393	285	-10.1	0.161	-3.90
413	280	- 9.1	0.145	-4.3
433	273	- 8.2	0.132	-4.7
453	267	- 7.3	0.121	-5.0
473	261	- 6.5	0.112	-5.2
493	255	- 5.7	0.105	-5.2
513	248	- 4.9	0.099	-5.0
533	241	- 4.2	0.093	-4.9
553	234	- 3.5	0.088	-4.5
573	227	- 3.0	0.084	-4.2
593	219	- 2.4	0.079	-3.9
613	211	- 1.8	0.075	-3.2
633	202	- 1.3	0.071	-2.6
653	194	- 0.8	0.068	-1.7
673	185	- 0.3	0.064	-0.73
693	176	+ 0.2	0.061	+0.54
713	166	0.7	0.059	2.0
733	156	1.1	0.057	3.4
753	146	1.5	0.055	5.0
773	134	2.1	0.054	7.2
793	122	2.5	0.052	9.3
813	108	2.7	0.049	11.
833	91	2.6	0.047	12.
853	65	1.8	0.044	9.5

$T_c = 870^oK$

$M_o = 338$ gauss

$$r = \frac{R_1}{\rho^2} \frac{(\text{ohm-cm})^{-1}}{\text{gauss}}$$

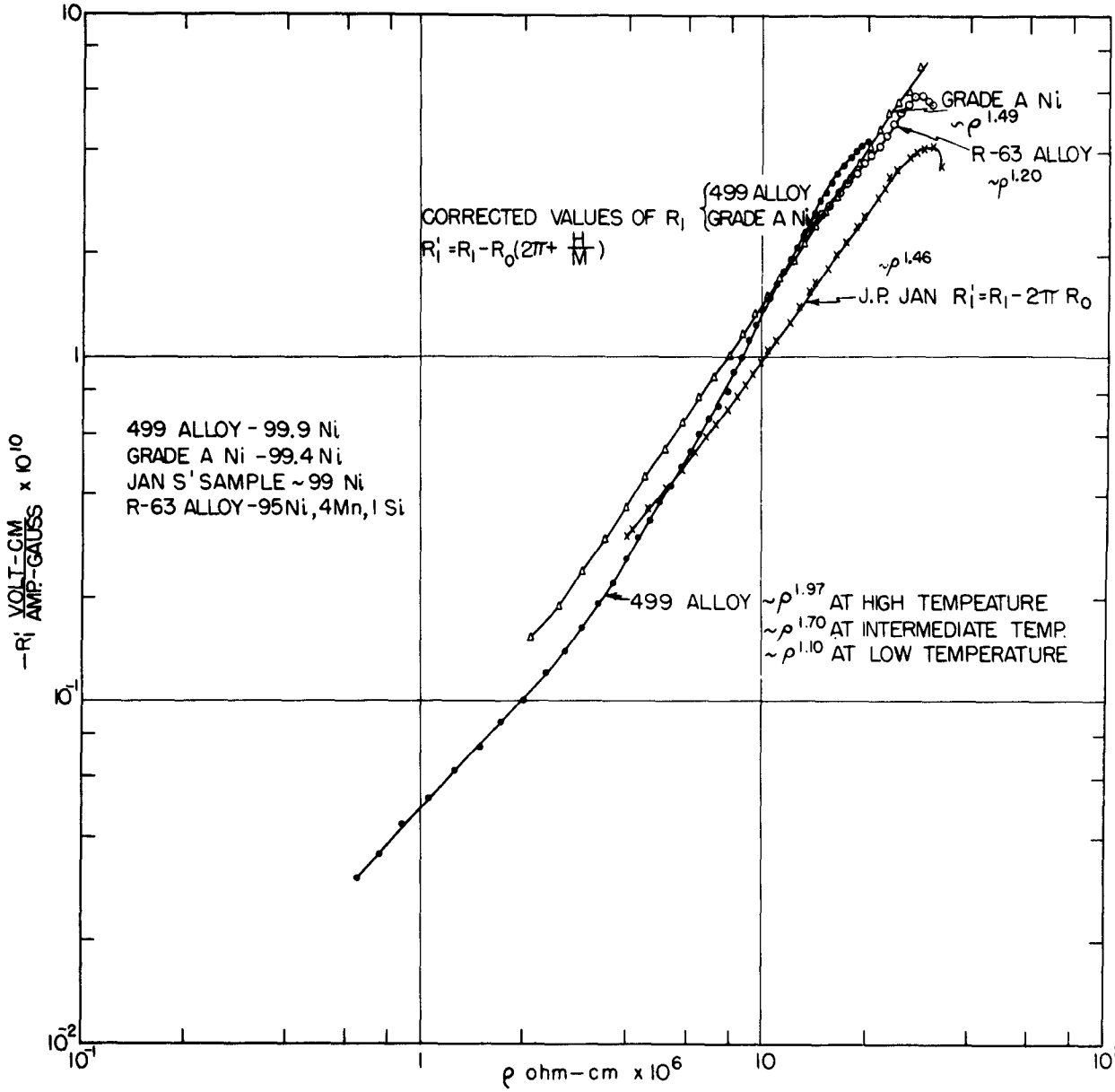

FIG.6-9 R_1' AS A FUNCTION OF ρ FOR GRADE A Ni, 499 ALLOY AND R-63 ALLOY COMPARED WITH JAN'S DATA BETWEEN LIQUID AIR TEMPERATURE AND TEMPERATURES NEAR THEIR CURIE TEMPERATURES

independent Since r depends on the manner in which the d levels are populated, it should not be very temperature dependent, especially at low temperatures where the magnetization is nearly constant. However, we cannot make a priori predictions about the behavior of r without a more detailed knowledge of the d-band structure than is available. Thus, a better test of the theory than a $\log R_1'$ vs $\log \rho$ plot, is a plot of r as a function of temperature, where $r = \frac{R_1}{\rho^2}$. Figure 6-10 compares the values of r observed for the 499 Alloy, Grade A Ni, and R-63 Alloy with Jan's data. Between liquid air temperature and room temperature r of 499 Alloy changes by about a factor of 5. However, between room temperature and 240°C, the magnitude of r decreases by only 15 per cent. The strong temperature dependence of r observed at low temperatures in the 499 Alloy (99.9 Ni) appears to decrease with increasing alloy concentration and the R-63 Alloy (95 Ni) indicates a low-temperature behavior similar to that observed at high temperatures. The reason for the observed temperature dependence of r is at present not clear, especially since most of the variation occurs at low temperatures. Although the largest errors in r occur at low temperatures, experimental error cannot possible explain the low-temperature behavior of r.

Figure 6-11 shows the $\log R_1'$, $\log \rho$ data for Supermalloy, Mumetal, and Carpenter Hymu 80 between liquid air temperature and room temperature. The ρ dependence of R_1' is completely different over different portions of the curve for each alloy, and not at all similar for the three alloys. However, because of the very small range of both $\log R_1'$ and $\log \rho$, the slopes of these curves are not very significant and a plot of r is a much better test of the theory. We note, however, that the magnetoresistance effect may alter the slopes of these curves somewhat, but since the magneto-resistance effect in these alloys is less than 3/4 per cent at liquid air temperature and changes by less than 1/2 per cent between room temperature and liquid air temperature, this effect will not be appreciable. Figure 6-12 compares the values of r for Mumetal, Carpenter Hymu 80, and Supermalloy between liquid air temperature and room temperature. In the case of Mumetal, r increases by about 15 per cent between liquid air temperature and room temperature. Over the same temperature range, r for Carpenter Hymu 80 is constant within 3 per cent. Of these three alloys, only Supermalloy exhibits an appreciable temperatu

dependence, r increasing by about 50 per cent over the range from liquid air temperature to room temperature. The magnitude of r which is a more significant measure of the magnitude of the effect is roughly 100 times smaller in these alloys than in the high concentration Ni alloys. With respect to the magnitude of r it is noted that the magnitude of r observed in Fe by Jan [11] and more recently in Fe and Fe with 1 per cent to 5 per cent Si concentration, by Kooi [80], is of the order of unity. Thus the magnitude of r in Fe and Ni does not depart appreciably from unity with alloy concentrations to 5 per cent, but about 20 per cent concentration in Ni reduces r by a factor of 100. It is noted, however, that this reduction in the magnitude of r has been observed in a very special case, namely in the case of alloys with a very small magnetic anisotropy, and this reduction of the magnitude of r may not be general.

(B) The Ferrites

The data of Figure 6-7 suggest very little correlation between R_1 and ρ for the Fe_3O_4 sample. Although both the absolute value of R_1 and ρ increase with decrease of temperature below -100°C, ρ increases more rapidly than R_1. Above room temperature, R_1 decreases in absolute value while ρ increases. The change of sign of R_1 at 380°C is also quite unusual. Although both positive and negative values of R_1 have been observed previously, in only one case, that of 70 Ni - 30 Co, reported by Smit and Volger [81] has a change of sign of R_1 with temperature been observed. The sign of R_1 has not been explained by Karplus and Luttinger.

The sign of R_1 in Fe has been observed to be positive by both Jan [11] and Foner [82], while the sign of R_1 in Ni has been observed to be negative by many investigators. Foner [82] has reported a positive R_1 in Co and has observed a transition from a positive R_1 to a negative R_1 in the Co-Ni alloy series, with R_1 passing through zero at about 30 Co - 70 Ni at room temperature. There appears to be no correlation between the sign of R_1 and the sign of R_o in the metals and alloys. For example, although both R_1 and R_o are negative in Ni and positive in Fe, Foner [82] has observed that in Co at room temperature, R_1 is positive although R_o is negative. Similarly, Foner has observed that R_1 is positive between 70 per cent Ni in Co and 100 per cent Co at room temperature, while R_o is negative throughout

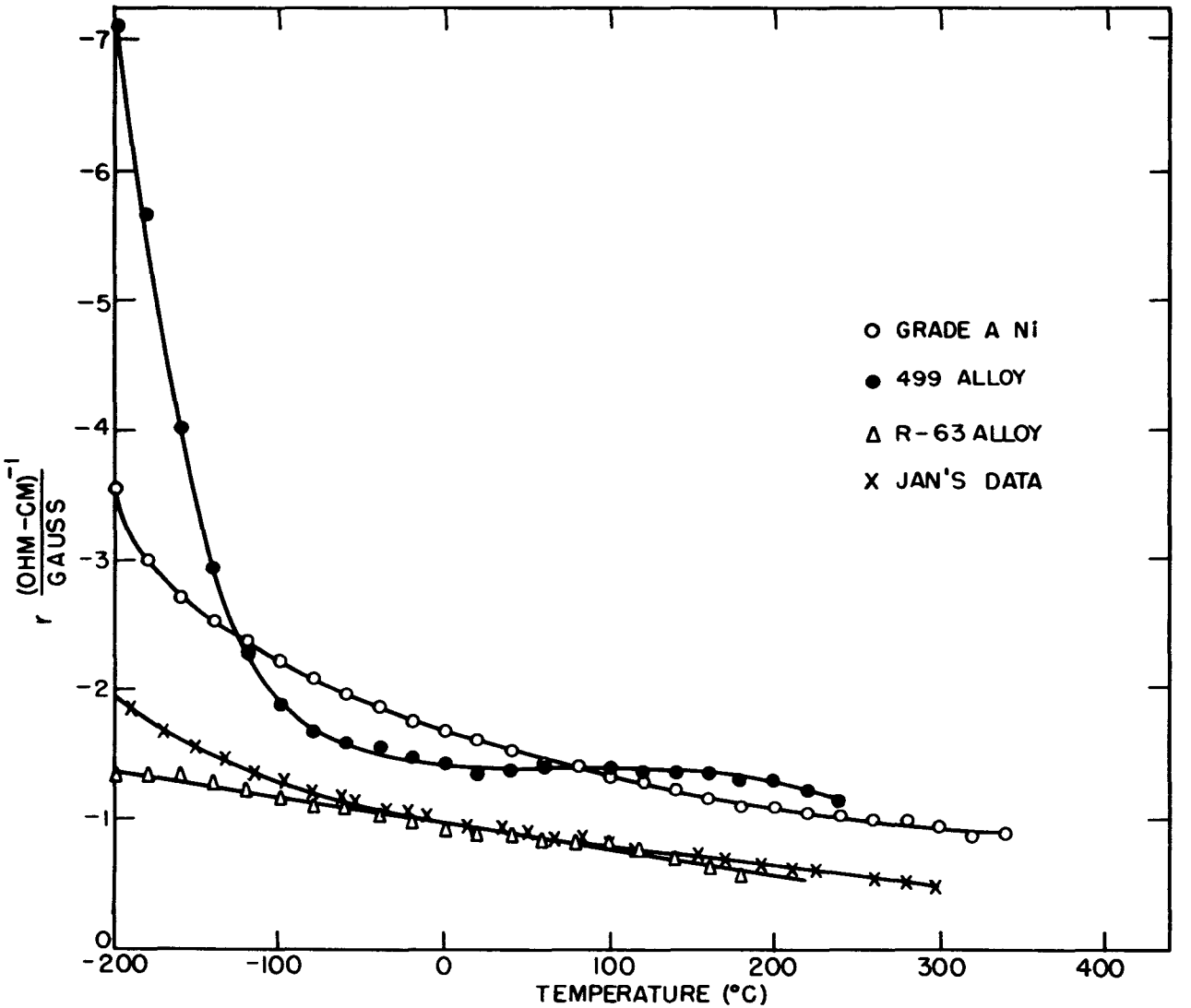

FIG. 6-10 COMPARISON OF r AS A FUNCTION OF TEMPERATURE FOR 499 ALLOY, GRADE A Ni, AND R-63 ALLOY WITH JAN'S DATA

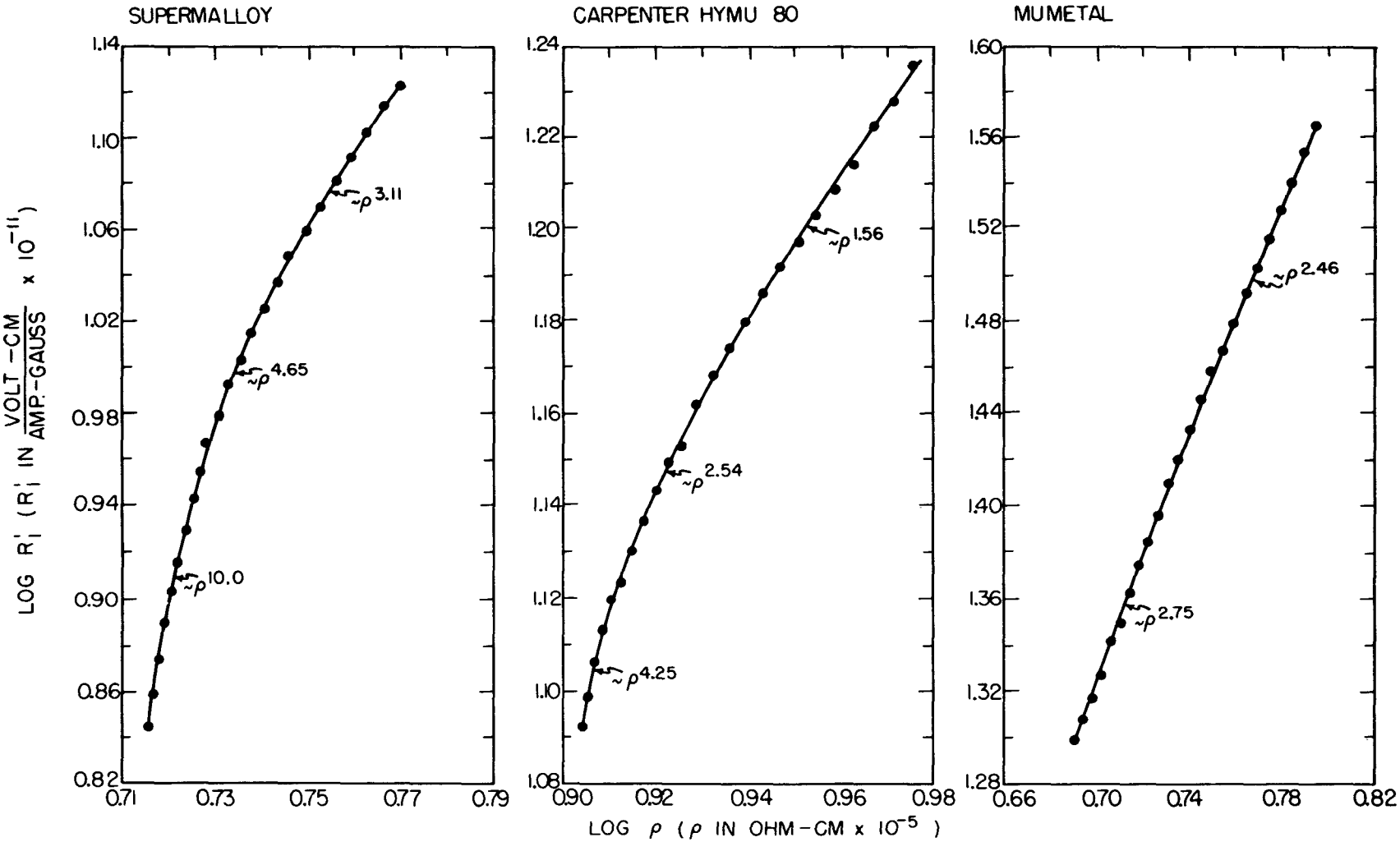

FIG. 6-11 LOG R_i' AS A FUNCTION OF LOG ρ FOR SUPERMALLOY, MUMETAL AND CARPENTER HYMU 80, BETWEEN LIQUID AIR TEMPERATURE AND ROOM TEMPERATURE

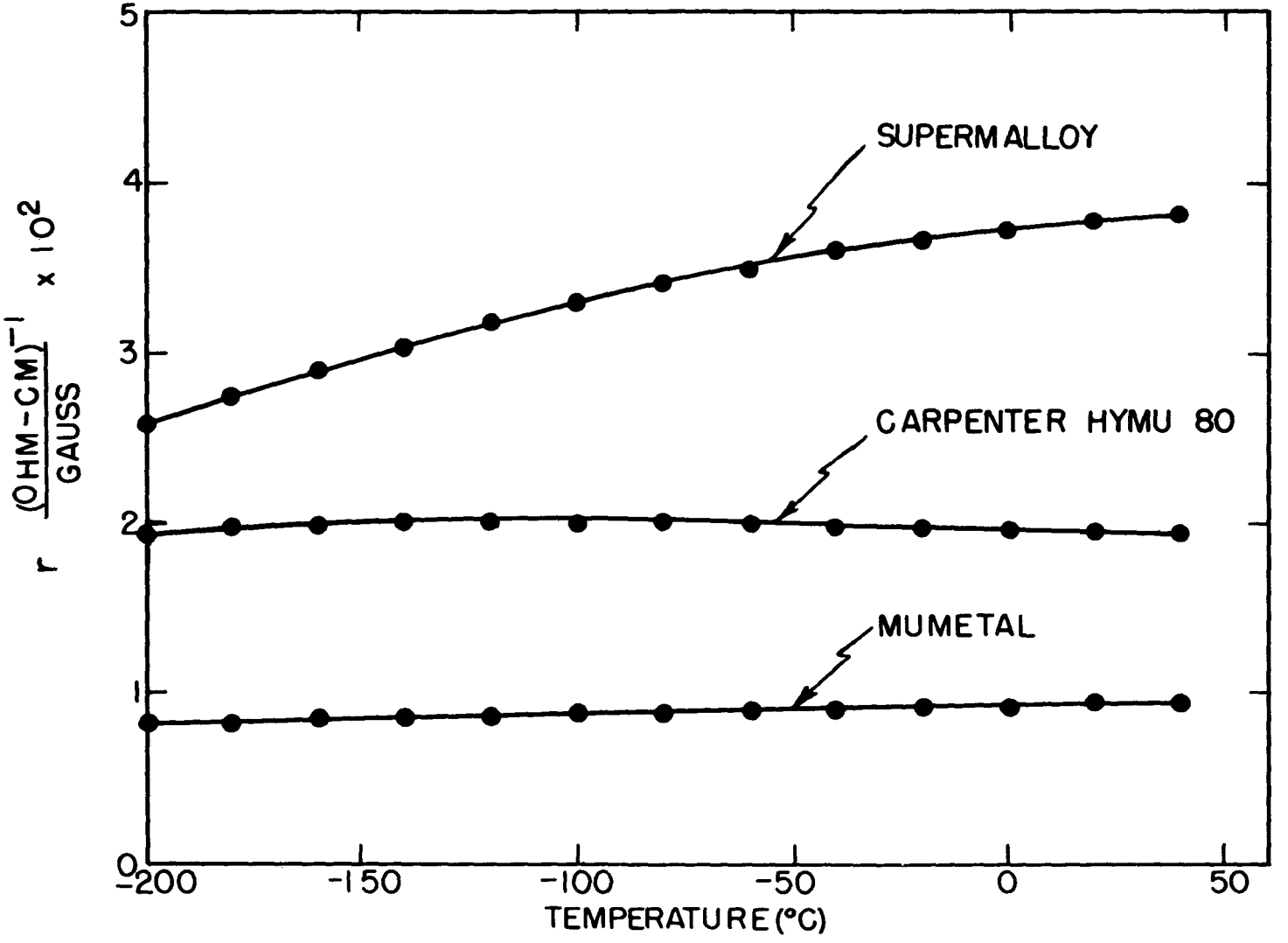

FIG. 6-12 COMPARISON OF r AS A FUNCTION OF TEMPERATURE FOR MUMETAL, CARPENTER HYMU 80 AND SUPERMALLOY

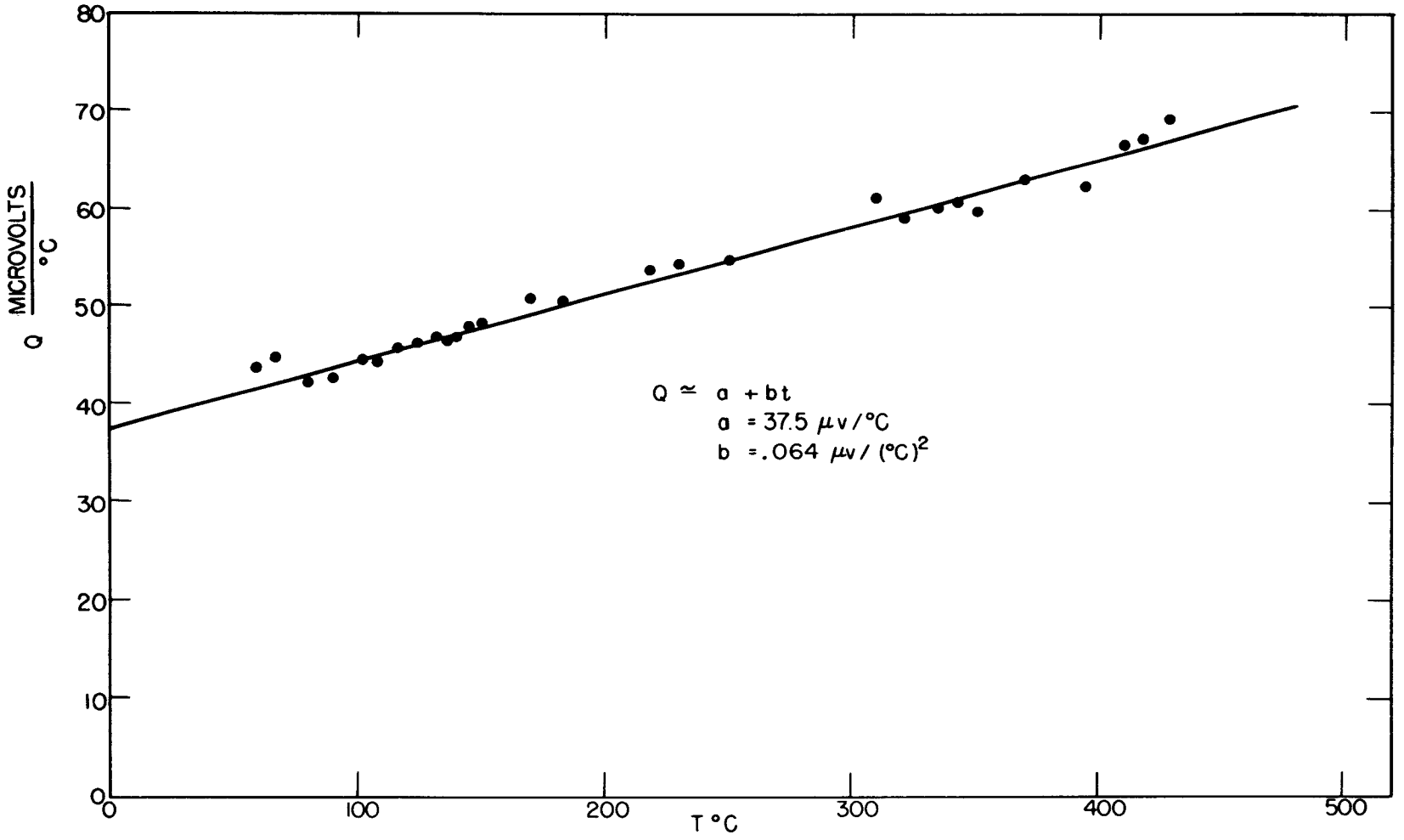

FIG. 6 –13 THE THERMOELECTRIC POWER OF Fe_3O_4 AGAINST Cu AS A FUNCTION OF TEMPERATURE

the Ni-Co Alloy series. Smit and Volger [81] have also observed a positive value of R_1 and a negative value of R_o in 84 Ni - 16 Fe. In spite of this lack of correlation between the sign of R_1 and the sign of R_o in the metals, it was of interest to investigate the sign of the current carrier in Fe_3O_4 through the region in which R_1 changes sign. Because the ordinary Hall measurement on Fe_3O_4 above room temperature was difficult to perform, a thermoelectric power measurement was made. From the sign of the thermoelectric voltage [see 62, p. 119] the sign of the current carrier may be inferred. Figure 6-13 shows the thermoelectric power of Fe_3O_4 against Cu, as a function of temperature. Between room temperature and 430°C, these data indicate that the sign of the carrier is negative. Thus, the sign reversal of R_1 in Fe_3O_4 does not seem to be related to the sign of the current carrier in Fe_3O_4. It is also noted, that the sign reversal of R_1 for Fe_3O_4 occurs at high temperature, and while a change of sign of the anisotropy constant has been reported [83] at -143°C, no anisotropy measurements have been reported above room temperature.

The values of r for Fe_3O_4 as a function of temperature between -140°C and 550°C are shown in Fig. 6-14. Above room temperature, r exhibits a temperature dependence not too different from that shown by R_1 in Fig. 6-7. It is noted that although ρ increases above room temperature, the increase is only about 25 per cent. Below room temperature, however, the data indicate that the magnitude of r decreases with decrease of temperature unlike the behavior of R_1. Thus, if the general features of the Karplus-Luttinger theory apply to the ferrites, the large effect observed below room temperature is to be attributed to the large resistivity in this region. At room temperature the magnitude of r is about 1000 times smaller in Fe_3O_4 than in Ni, although the observed magnitude of R_1 is roughly 300 times larger in Fe_3O_4 than in Ni. At liquid air temperature, about 41°C below the transition, the value of r is roughly 10^{-10} times the value observed in Ni.

In the case of $(NiO)_{.75}(FeO)_{.25}(Fe_2O_3)$, the absolute value of R_1 and ρ decrease monotonically with increase of temperature [see Fig. 6-8] between -100°C and 410°C. However, the data do not indicate any unique

dependence upon ρ in this temperature range nor over any portion of this temperature range. R_1 goes through zero at about 410°C and increases between 410°C and 550°C while ρ continues to decrease. Thus, although the resistivities of Fe_3O_4 and $(NiO)_{.75}(FeO)_{.25}(Fe_2O_3)$ are not similar over the range -100°C to 500°C, the shapes of their R_1, T curves evidence some similarity.

Figure 6-15 shows the plot of r as a function of temperature between -100°C and 560°C for the $(NiO)_{.75}(FeO)_{.25}(Fe_2O_3)$ sample. Both the Fe_3O_4 and the $(NiO)_{.75}(FeO)_{.25}(Fe_2O_3)$ data show a peak for negative values of r, although the peak occurs at about 0°C for Fe_3O_4 and at about 200°C for $(NiO)_{.75}(FeO)_{.25}(Fe_2O_3)$. The absolute value of r decreases below 0°C for both ferrites. At room temperature, the magnitude of r in $(NiO)_{.75}(FeO)_{.25}(Fe_2O_3)$ is roughly 1000 times smaller than the magnitude of r in Fe_3O_4, although R_1 is 5 times larger in $(NiO)_{.75}(FeO)_{.25}(Fe_2O_3)$ than in Fe_3O_4. The magnitude of r in $(NiO)_{.75}(FeO)_{.25}(Fe_2O_3)$ at room temperature is roughly 10^6 times smaller than r in Ni and Fe.

(C) Concluding Remarks

The large magnitude and unusual temperature dependence of the extraordinary Hall coefficient had been a puzzle for many years. The attempt to explain the effect by the effective field formulation proved totally unsatisfactory because magnetic interactions involving the conduction electrons could explain neither the magnitude nor the temperature dependence of the observed effect. Therefore, the contribution of the Karplus-Luttinger theory in pointing out that spin-orbit interactions can produce a current proportional to the magnetization and, because of the manner in which the effect has been observed, a voltage proportional to the square of the resistivity, is indeed significant. While the measurements on the metals and alloys reported in this chapter do not generally exhibit a ρ^2 dependence, they do suggest that the essential features of the Karplus-Luttinger theory are probably correct. However, the unusual temperature dependence of r in the 499 Alloy at low temperatures, and the marked reduction in the magnitude of r in the 80 per cent Ni - Fe alloys indicate a need for a better understanding of r. The failure of R_1 to exhibit a ρ dependence in the ferrites may not indicate that the general features of the Karplus-Luttinger theory do not apply to these

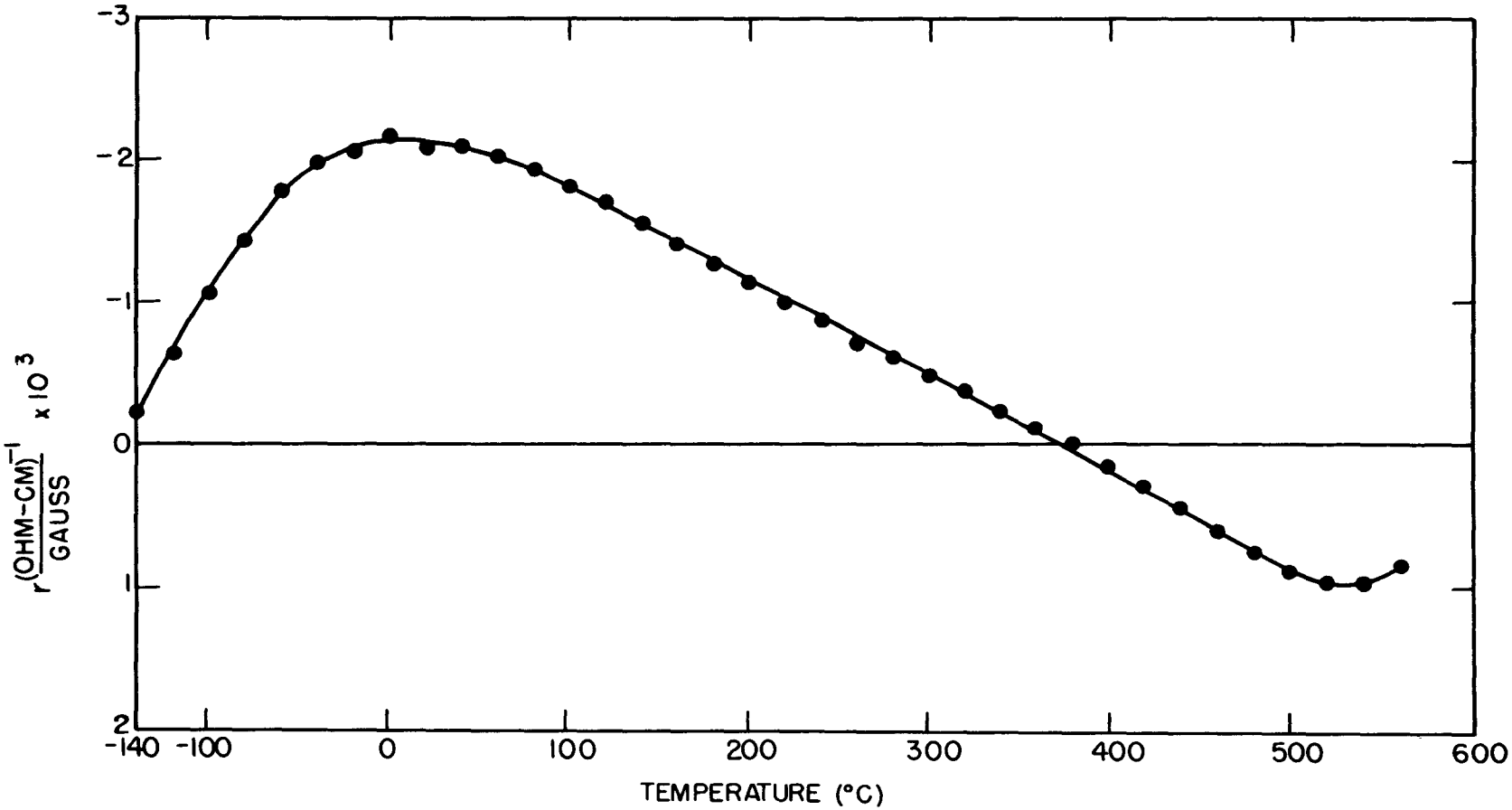

FIG. 6—14 PLOT OF r AS A FUNCTION OF TEMPERATURE FOR Fe_3O_4

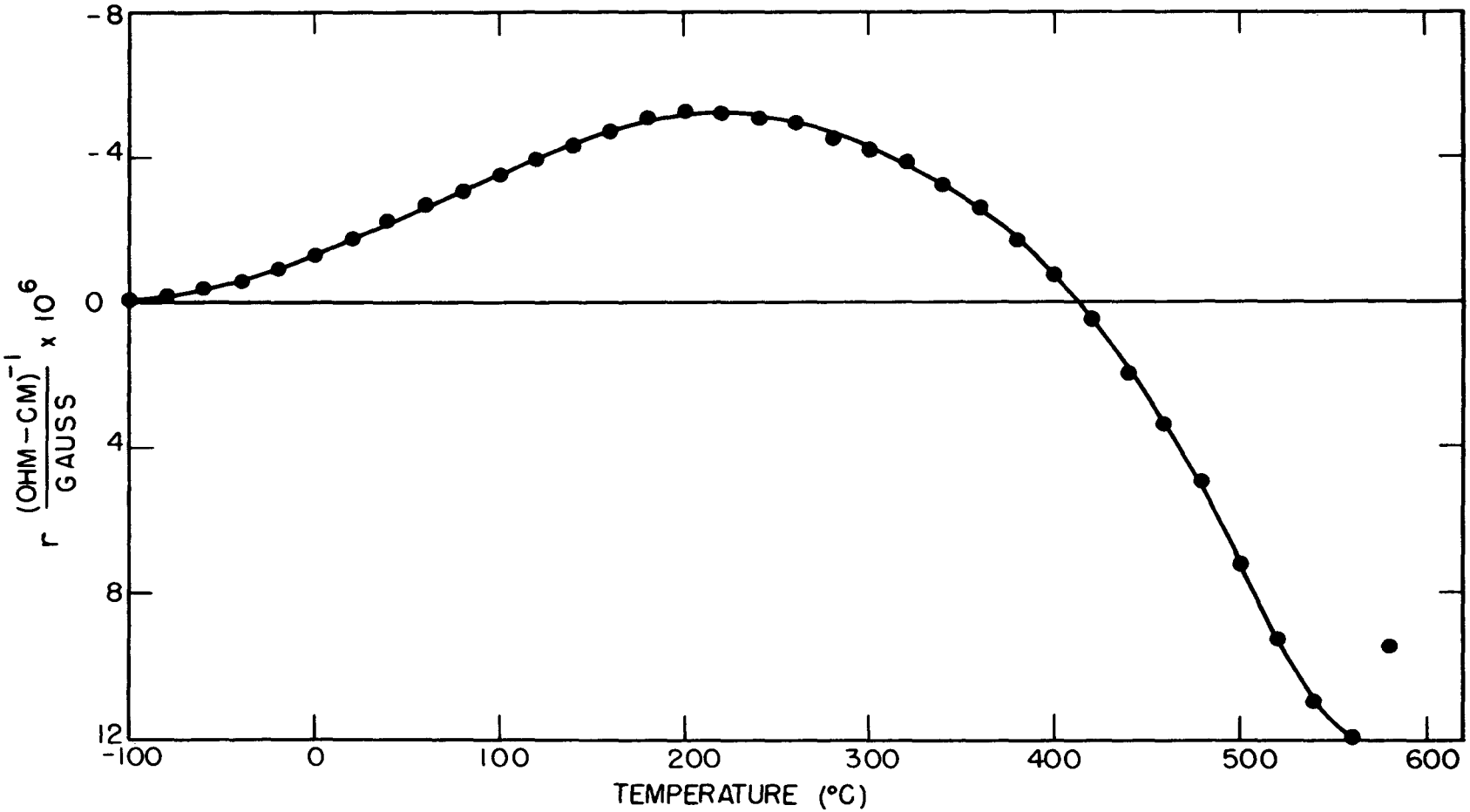

FIG. 6–15 PLOT OF r AS A FUNCTION OF TEMPERATURE FOR $(NiO)_{.75}(FeO)_{.25}(Fe_2O_3)$

materials as much as it points out our present lack of understanding of both r and the electrical properties of the ferrites.

The Karplus-Luttinger theory will probably stimulate new experimental effort toward this problem, because it has considerably simplified the experimental situation. For example, although the voltages measured in observing the extraordinary Hall effect are by no means large voltages, they are for the most part much larger than the voltages observed in the ordinary Hall measurement, and therefore measurements of R_1 may now be undertaken on ferromagnetic metals and semiconductors which were previously excluded because of the difficulties in measuring R_o and the requirement of the effective field formulation that both R_1 and R_o be measured. It would be of interest to investigate the extraordinary effect as a function of temperature in Co, and in the Ni-Co alloy series, especially in the region around 70 Ni - 30 Co, where the data of Foner [82] and Smit and Volger [81] indicate that both signs of R_1 are observed. Measurements made on the binary alloys of Fe, Co, and Ni may help in our understanding the nature of the 3d electrons. In this respect the measurements reported in this chapter do not present a very comprehensive picture because they were not made on binary alloys nor were they spaced throughout an alloy series. It would also be of interest to explore the behavior of R_1 in Ni of even greater purity than 499 Alloy and to extend the measurements to alloy concentrations greater than 5 per cent around both Ni and Fe. At the present, there seems to be no obvious suggestion for future work on the ferrites.

Acknowledgment

The author gratefully acknowledges the assistance of Professor Harvey Brooks and other members of the Gordon McKay Laboratory of Applied Science.

APPENDIX A

Discussion of Errors

It is the purpose of this appendix to supplement the discussion of error of Chapter III and to point out some of the inherent difficulties in the measurement of R_o in both Fe_3O_4 and Ni. However, for a complete and detailed analysis of the errors involved, the reader is referred to the original thesis [84].

A. 1 Errors in the Measurement of R_o

In the measurement of the ordinary Hall coefficient, errors arise because of the temperature and magnetic field dependence of the relatively large voltages that are subtracted in order to deduce the value of R_o. In Chapter II we have detailed the field-reversal technique of making the ordinary Hall measurement. We first discuss the errors that arise due to the uncertainty in setting the magnetic field.

If we apply a magnetic field, H_1 down, to the sample [Fig. 2-4] we obtain a voltage across the Hall probes

$$V(H_1) = IR + I\Delta R(H_1) + R_1 M(H_1) I/t + R_o H_1 I/t, \tag{A. 1}$$

where IR is the voltage due to the misalignment of the Hall probes; $I\Delta R(H_1)$ is the magnetoresistance voltage associated with the resistance between the probes; $R_1 M(H_1) I/t$ is the extraordinary Hall voltage; and $R_o H_1 I/t$ is the ordinary Hall voltage. The field-reversal technique requires that we reverse the field exactly to H_1 up. If we reverse the field to the value $H_1 + \Delta H_1$ up, we obtain

$$V(H_1 + \Delta H_1) = IR + I\Delta R(H_1 + \Delta H_1) - R_1 M(H_1 + \Delta H_1) I/t - R_o (H_1 + \Delta H_1) I/t \tag{A. 2}$$

The error voltage, denoted by $\Delta V(H_1)$, is obtained from the difference in absolute value of each term in Eqs. (A.1) and (A.2).

$$\Delta V(H_1) = \left| \frac{\partial}{\partial H} [I \Delta R(H_1)] \Delta H_1 \right| + \left| R_1 \frac{\partial M}{\partial H} (H_1) \Delta H_1 \right| + \left| R_o \Delta H_1 \frac{I}{t} \right|, \tag{A. 3}$$

where

$$\frac{\partial}{\partial H}\left[I\Delta R(H_1)\right]\Delta H_1 = I\,\Delta R(H_1 + \Delta H_1) - I\,\Delta R(H_1) \qquad (A.4)$$

and

$$\frac{\partial M}{\partial H}(H_1) = M(H_1 + \Delta H_1) - M(H_1) \qquad (A.5)$$

In the case of Ni at room temperature, the largest contribution to the error voltage arises from the third term with a relatively large contribution from the first term of Eq. (A.3), the magnetoresistance term. In order to keep the uncertainty in the measurement of R_o to about 1.0 per cent, the uncertainty in the magnetic field must be less than 0.6 per cent.

In the case of Fe_3O_4 at room temperature, the largest contribution to the error voltage arises from the magnetoresistance term, and requires that the uncertainty in the magnetic field be less than 0.25 per cent at H_1, in order that the uncertainty in R_o be less than 1.0 per cent. At H_2, [Chap. II] the requirement on the field is relaxed to about 0.6 per cent because the magnetoresistance saturates.

The sources of error contributing to the uncertainty, ΔH_1, were the resolution of the ammeter used to read the magnet current, the drift of the magnet current due to the long time constant of the magnet and power supply filter, and the failure of the magnet to effect a complete reversal of magnetic field with reversal of current. At H_1, these errors, treated as random errors plus an error of about 0.5 per cent due to calibration of the magnet, total about 0.92 per cent and at H_2 they total about 1.08 per cent. In the case of the R_o measurement of Ni this error results in about 2.3 per cent error in R_o. It is pointed out, however, that repeated observation plus resolution of the V_H, H curve of Ni reduces this error considerably. In the case of Fe_3O_4, these uncertainties in H result in about 4.1 per cent error in R_o. In the case of $(NiO)_{.75}(FeO)_{.25}(Fe_2O_3)$, the error is somewhat less than 4.0 per cent since the ratio of magnetoresistance voltage to Hall voltage is smaller.

In the case of the R_o measurements of Ni above room temperature, the error is somewhat less than at room temperature since the magnetoresistance decreases with increasing temperature except in the vicinity of the Curie temperature.

In the case of the 70 Ni-30 Cu measurement at -195°C, the error is about the same as in Ni at room temperature, since the magnetoresistance is about the same.

Above the Curie temperature, the uncertainty in H will introduce error only in the $R_o H$ term which we estimate to be of the order of 1.0 per cent in both Ni and 70 Ni-30 Cu.

In calculating the errors due to temperature variation, we treat the temperature dependence of each of the contributions to the voltage observed across the Hall probes.

$$V(T_1) = IR(T_1) + I\,\Delta R(T_1) + R_1(T_1)M_s(T_1)I/t + R_o(T_1)H\,I/t \qquad (A.6)$$

If, during the time of measurement, the temperature shifts to the value $T_1 + \Delta T_1$, the resultant error voltage is given by

$$\Delta V(T_1) = \left|\frac{\partial}{\partial T} IR(T_1)\ \Delta T_1\right| + \left|\frac{\partial}{\partial T}\left[I\,\Delta R(T_1)\right]\Delta T_1\right| + \left|\frac{\partial}{\partial T}\left[R_1(T_1)M_s(T_1)\right]I/t\ \Delta T_1\right| + \left|\frac{\partial R_o(T_1)}{\partial T} H\,I/t\ \Delta T_1\right| \qquad (A.7)$$

In section 2-2E we have implied that the major contribution to the thermal error arises from the IR drop, the first term in Eq. (A.7). In the case of Ni at room temperature, the IR contribution is about double the contribution from the third term of Eq. (A.7) and the other two terms contribute negligibly. The temperature requirement for the Ni room temperature measurement is about 4×10^{-2}°C for 1.0 per cent uncertainty in R_o.

In the case of Fe_3O_4, the contribution from the IR term is much larger than the contribution from all other terms and requires a temperature stability of the order of 2×10^{-3}°C in order to limit the uncertainty in R_o to 1.0 per cent.

In the case of the Ni room temperature measurement, temperature stability of the order of 0.01°C was maintained and this error was negligible. In the case of Fe_3O_4, thermal instability caused appreciable difficulty. As indicated in Section 2-2E, the current through the sample was limited to a value which provided good stability and reasonable signal. Care was taken to place the sample jacket in good thermal contact with the water-cooled magnet. Both sample current and magnet water supply were run for periods

of four to eight hours before measurements were made. Since the allowed temperature variation was so small, even the energy provided the sample by cycling the magnetic field through a sample hysteresis loop was sufficient to perturb the equilibrium condition. Therefore, the magnet was cycled at a rate conforming to the speed employed in the measurement for a period in excess of five minutes. During this period, the stability of the system was observed at the output meter. No measurement was made until the sample evidenced stability within the noise level of the system. In spite of these precautions, thermal instability probably provides the largest contribution to the spread of values observed in the R_o measurement of Fe_3O_4. However, since a temperature variation can add uncertainty to $2V_{H_2}$, [Sect. 2.5] the error is random and we are justified in averaging.

In the case of the R_o measurements on Ni above room temperature, all of the contributing effects increase with increase of temperature. Since the field dependence of M_s makes the measurement uncertain above 200°C, we are concerned only with the temperature requirement between room temperature and 200°C. In this region, the third term of Eq. (A.7) involving $\frac{\partial}{\partial T}(R_1 M_s)$ provides the largest contribution to the error and requires that the temperature to be held to 0.02°C. Temperature stabilities of this order of magnitude were achieved. It is noted that the chromel-alumel thermocouple could easily detect temperature changes of 0.008°C.

In the case of the R_o measurement on the 70 Ni-30 Cu alloy at liquid-air temperature, temperature stability requirements were no worse than in Ni at room temperature. Therefore, error due to temperature instability is small, since temperature can be held to better than 0.05°C at liquid-air temperature.

We point out one other large source of error in the determination of R_o. In Section 2-2D we have indicated that error will occur in the measurement of R_o because M is not constant at high fields. In the case of polycrystalline samples, in the region of fields used in the R_o measurements, we write Eq. (2.32)

$$M = M_s\left(1 - \frac{a}{H} - \frac{8K^2}{105 M_s^2 \left(H + \frac{4\pi M_s}{3}\right)^2} \cdots + K_o H \right) \quad \text{(A. 8)}$$

since the work of Holstein and Primakoff [31] and Néel [28] indicates that H

should be replaced by $H + \frac{4\pi M_s}{3}$ in the second-order term. As previously indicated, $\underline{a}$ is due to nonmagnetic cavities and inclusions in the sample, and K is the first-order anisotropy constant. In calculating the change of M with H in Ni we have used a value of $\underline{a} = 1/3$ suggested by Bozorth [12, p. 487] . Since $\underline{a}$ was not measured, and since it can vary from sample to sample, the choice of this value requires some justification. The V_H, H curve of Fig. 4-1 shows the approach to saturation, since the Hall voltage is proportional to M at low fields. The approach to saturation in this curve can be reasonably fitted by the second-order term in H with a value of $K = -59000$ ergs/cm^3. It can also be fitted with the first-order term and a value of $\underline{a} = 20$. Such a value of $\underline{a}$ is unlikely in the Ni sample used in this measurement, and it is probably reasonable to assume that the curvature in the vicinity of 7000 oersteds [Fig. 4-1] is due to anisotropy and perhaps to some strain, unrelieved by annealing. If $\underline{a} = 20$, then this effect would result in an additional 8 per cent error at room temperature. If $\underline{a} = 1/3$, then the important contribution to error comes from the K_o term and is estimated to be about 3 per cent. In the case of Fe_3O_4, this error may be significantly large and is treated in Appendix B.

In the case of the R_o measurements on Ni above room temperature, the K_o term increases with increase of temperature and renders the measurement indeterminate in the vicinity of the Curie temperature. This effect is seen in the data of Fig. 4-2. At 140°C, the K_o term may introduce an error as large as 5 per cent. An estimated value of K_o at 200°C indicates that an error as large as 10 per cent may be introduced at this temperature.

In the case of the other measurements, these effects are estimated to cause reasonably small error.

A. 2 Errors in the Measurement of R_1

The analysis of error of Section A. 1, above, is used to determine the error in the measurement of R_1. The error voltage introduced by mis-setting the magnetic field during the field reversal, in the R_1 measurement, is compared with the voltage $2R_1M_sI/t$, rather than with the voltage $2R_oI/t(H_2-H_1)$, from which R_o is deduced. However, at room temperature, the extraordinary Hall voltage is 25 times larger than the ordinary Hall voltage in the case of Ni, and 150 times larger in the case of Fe_3O_4;

negligible error in the determination of R_1 therefore arises from missetting the magnetic field. Even though the contribution from the magnetoresistance term to the error voltage increases with decrease of temperature, in the case of Ni, while the extraordinary Hall voltage decreases, the error in the determination of R_1 is much less than 1.0 per cent between liquid-air temperature and room temperature. Above room temperature, the contribution from the second term of Eq. (A. 3) increases, but in the region between room temperature and 50°C below the Curie temperature, the total uncertainty in R_1 from these sources is less than 1.0 per cent.

In the case of the ferrites, the error in R_1 at room temperature and above, from this source, is also very small except in the vicinity of $R_1 = 0$. However, the uncertainties in R_1 at these temperatures are averaged out by the values measured at temperatures above and below. At temperatures below room temperature, the magnetoresistance effect may contribute as much as 3.0 per cent error in R_1 of Fe_3O_4 at -143°C, and probably about the same error in $(NiO)_{.75}(FeO)_{.25}(Fe_2O_3)$ at -100°C.

With respect to thermal contributions to error in the measurement of R_1, we estimate negligibly small error in both the metals and the ferrites. The error voltages deduced from Eq. (A. 7) are compared with the much larger extraordinary Hall voltage and hence the thermal stability requirement in the measurement of R_1 is much less than in the case of the R_o measurements. Furthermore, measurements of R_1 required only a single field reversal which was made in a time very short compared to the time elapsed in the measurement of R_o. Therefore, not only at room temperature, but also over the temperature range observed, temperature variation is estimated to have caused negligible error in all of the metal measurements. For example, in the measurement of 499 Alloy which had the lowest value of R_1 observed at liquid-air temperature, the requirement for this temperature was 0.3°C stability for a 1.0 per cent error in R_1. At the highest temperature at which R_1 was observed in this material, the temperature requirement was 2.0°C at 250°C. We also estimate the error in the R_1 measurements of the ferrites to be small at all temperatures except in the vicinity of $R_1 = 0$. For example, at the lowest temperature at which measurements were made

on Fe_3O_4, the stability requirement was 0.05°C at -143°C. At the highest temperature, the stability requirement was 1.0°C at 500°C. Such temperature stabilities were achieved by the techniques outlined in Chapter III.

One significant source of error in the determination of R_1 occurs from the failure to measure M_s, in the samples used. In the case of Ni, M_o, the saturation magnetization at 0°K is accurately known and therefore the value estimated for both the Grade A Ni and 499 Alloy is in error by less than 1.0 per cent. The value of M_s at other temperatures was deduced from a universal curve of M_s/M_o vs T/T_c which was obtained from Jan's [11] data. A very conservative estimate of error over the range of temperature below $T = 0.9\ T_c$, including the error in absolute value of M_o, is 1.0 per cent. Above $T = 0.9\ T_c$, the determination of M_s is most difficult because of its strong field dependence.

In the case of the values used for the R-63 Alloy (95 Ni, 4 Mn, 1 Si) the uncertainty is somewhat larger. A value of $4\pi M_s$ at room temperature was deduced from the saturation value of applied field in the plot of V_H as a function of applied field for this material. Using the universal curve of M_s/M_o vs T/T_c for Ni, a value of $M_o = 552$ gauss was deduced, or a value about 10 per cent higher than M_o for Ni. Bozorth [see 12, p. 317] indicates that M_o increases linearly for small concentration of Mn in Ni, and at 4 per cent Mn a value about 10 per cent higher than the value for Ni is indicated. Therefore, the value deduced above is probably within 2 per cent of the correct value over the temperature range.

In the case of the 80 per cent Ni - Fe alloys, the value of M_s at room temperature was obtained from the source of the material, probably no better than 5 per cent. Since the curve of M_s/M_o vs T/T_c for Fe lies within 1 per cent of the curve for Ni, over the range of temperature employed, values deduced from the Ni curve probably add no more than 1 per cent to the error in the absolute value of M_s. However, we are primarily concerned with the temperature dependence of R_1, and error in this determination occurs only

through the error in the temperature dependence of M_s which we estimate to be about 1 per cent.

In the case of Fe_3O_4, the value of M_o was obtained from the Bohr magneton number given by Pauthenet [77] and the density of the sample. The variation with temperature was obtained from Pauthenet's data, and M_s is estimated to have no more than 2 per cent error over the temperature range.

In the case of $(NiO)_{.75}(FeO)_{.25}(Fe_2O_3)$, the value of M_o was calculated from 1/4 of the known value of M_o in Fe_3O_4 and from 3/4 of a calculated value of M_o in $NiOFe_2O_3$. This value agreed within 1.5 per cent of a calculation assuming a composite value of Bohr magneton number and the measured density of $(NiO)_{.75}(FeO)_{.25}(Fe_2O_3)$. The values used were $M_o(Fe_3O_4) = 510$ gauss and $M_o(NiOFe_2O_3) = 281$ gauss, resulting in a value for $(NiO)_{.75}(FeO)_{.25}(Fe_2O_3)$ of $M_o = 338$ gauss. The temperature dependence of M_s was similarly obtained by calculating a value of M_s at each temperature from Pauthenet's data for Fe_3O_4 and $NiOFe_2O_3$. Since $NiOFe_2O_3$ and Fe_3O_4 do not have the same temperature dependence, the value of M_s at temperatures different from 0^oK may have a large but unestimatable error.

Another source of error in the determination of R_1 arises from the correction that must be taken into account to subtract out the effect of the internal field acting on the conduction electrons which is probably $H + 2\pi M$ instead of H. Some error also occurs due to the fact that the extraordinary Hall voltage is measured somewhat above the saturation bend of the V_H, H curve and hence a small contribution from the ordinary Hall effect is present in the observed voltage. As pointed out in Eq. (1.7) we may write the expression for the Hall voltage as

$$V_H = \left\{R_o[H + 2\pi(1+p)M] + R_1'M\right\} I/t \qquad (A.9)$$

where R_1' has been calculated by Karplus and Luttinger [13], and p has been estimated by Wannier to be very nearly equal to zero for most conduction electrons. Therefore, if we measure the Hall voltage where M is saturated, and if we assume that saturation is achieved with $H \ll 2\pi M_s$, where H is the field inside the material, then

$$V_H = [\ R_o 2\pi M_s + R_1' M_s]\ I/t = R_1 M_s\ I/t \qquad (A.10)$$

and the error in considering $R_1' \simeq R_1$ is $2\pi R_o/R_1$. Since this can be a reasonably large error in most of the samples measured, corrections have been applied. Also, as mentioned above, the extraordinary Hall voltage was measured at fields for which H was not very much less than $2\pi M_s$. Therefore, corrections were also made to take this into account. Because of the uncertainty in R_o in those cases where R_o was not measured, because p may be different from zero, and because of the uncertainty in the value of H to be associated with the correction term, error occurs in these corrections. In the case of the 499 Alloy, for which the smallest value of R_1 at liquid air temperature was observed, we estimate about 3 per cent error in these corrections. In the case of those samples for which R_o was not measured, estimated values of R_o probably cause less than 3 per cent error.

APPENDIX B

The Change of Magnetization Above Technical Saturation in Fe_3O_4 And $(NiO)_{.75}(FeO)_{.25}(Fe_2O_3)$

In this appendix, we show that the value of R_o deduced from the ordinary Hall measurement of Fe_3O_4 may be incorrect. At least three sources can contribute to the change of magnetization above saturation and hence produce a voltage proportional to R_1, which is added to the ordinary Hall voltage.

In Eq. (2.32), we have given the expression for the approach to saturation.

$$M = M_s\left(1 - \frac{a}{H} - \frac{b}{H^2} \cdots\right) + K_o H \qquad \text{(B. 1)}$$

It can be shown that the K_o term is sufficiently small to cause small change of M for fields of the order of 5000 oersteds. We can show that the $\frac{a}{H}$ term contributes a voltage which is probably much less than the observed voltage. However, because the $\frac{b}{H^2}$ term is dependent upon the orientation of external field with respect to the crystal axes, and because the sample used was not a single crystal, but was composed of several large grains, very little can be said about this term except that it may be large. In the following sections we examine the effects of each of the terms of Eq. (B. 1) in the region where the ordinary Hall voltage was measured.

B.1 The K_o Term

The room temperature value of K_o in Ni has been observed by Polley [85] to be 1.5×10^{-4} gauss/oersted. A value of K_o of this order of magnitude in Fe_3O_4 would result in a 25 per cent error in R_o.

The usual method of determining M_s, at the temperature T, is to extrapolate the value of M, measured with a magnetometer, and plotted as a function of $\frac{1}{H}$, to infinite fields. Such determinations assume that the first two terms of Eq. (B. 1) describe the material. If the term in K_o is not insignificant, then at high fields we expect a departure from

linearity. In Fig. B-1, the room temperature data of Weiss and Forrer [86] show this departure in the case of Ni, and indicate a value of K_o in agreement with the value given above. On the other hand, the only high field data for Fe_3O_4 reported by Pauthenet [77], has been plotted on a scale which does not clearly show the behavior of σ' in the region of high fields. These data are shown in Fig. B-2. However, if the total change of σ' over the observed range were due to the K_o term only, then K_o for Fe_3O_4 would be about the same order of magnitude as K_o for Ni. However, the term in $\underline{a}$ probably accounts for much of the change in σ' and therefore the magnitude of the effect is probably smaller in Fe_3O_4. Therefore, we estimate no more than 10 per cent uncertainty in R_o due to this effect.

B.2 The $\frac{a}{H}$ Term

The term in $\underline{a}$ is sample-dependent, and has been related to the number of cavities and nonmagnetic inclusions in the sample. In spite of this dependence, both Pauthenet [77] and Weiss and Forrer [86] have observed values of $\underline{a} = 17$ for different natural crystals of Fe_3O_4. Since the sample used in this research was of much better grade than natural crystals, we expect a smaller value of $\underline{a}$. To support this argument, we note that if $\underline{a} = 17$, then the change of M between 1000 and 6000 oersteds, would result in $\Delta M = 7$ gauss and a voltage due to $R_1 \Delta M$ roughly 2.4 times larger than the observed voltage. Hence we may conclude that $\underline{a} \leq \frac{17}{2.4}$ in this sample. In order to keep the uncertainty in R_o less than 10 per cent, we require that $\underline{a}$ be less than 0.6.

Since measurements of M involve rather complicated apparatus which was not available, we have resorted to an indirect measurement to establish a rough value of $\underline{a}$. A transformer was wound on the cylindrical Fe_3O_4 sample and an alternating voltage e_1 was applied to the primary. The secondary voltage is given by,

$$e_2 = \frac{e_1 \, j\omega M' Z_2}{(Z_1 + j\omega L_1)(Z_2 + j\omega L_2) + \omega^2 M'^2} \qquad \text{(B. 2)}$$

where Z_1 is the impedance of the generator plus the resistance of the transformer primary, Z_2 is the impedance of the load plus the resistance

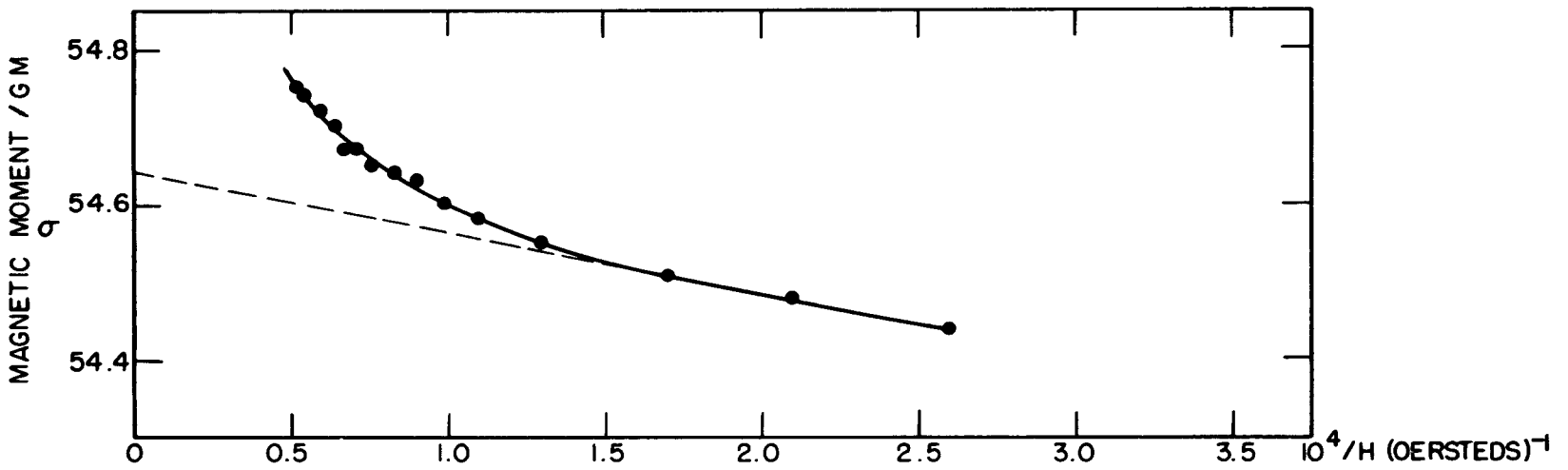

FIG. B-1 σ AS A FUNCTION OF H^{-1} FOR Ni . DATA OF P. WEISS AND R. FORRER

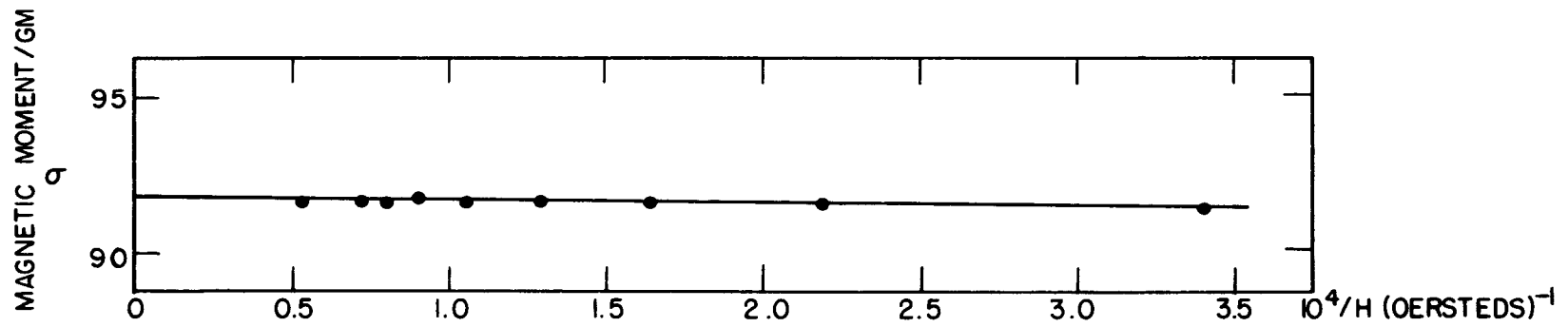

FIG. B-2 σ AS A FUNCTION OF H^{-1} FOR Fe_3O_4 . DATA OF R. PAUTHENET

of the transformer secondary, L_1, L_2 are primary and secondary inductances, and M' is the mutual inductance. L_1, L_2, and M' are related to the permeability, μ, by geometric factors. We are interested in the permeability above technical saturation where μ is very nearly unity. Therefore, if we insert the transformer in a magnetic field applied along the direction of the magnetic field due to the primary current, then a change of applied field, ΔH, produces a change of secondary voltage Δe_2 due to the change of μ. Since Z_1 and Z_2 have been chosen so that

$$Z_1 \gg \omega L_1$$

$$Z_2 \gg \omega L_2$$

$$\text{and} \qquad Z_1 Z_2 \gg \omega^2 M'^2 \tag{B.3}$$

the logarithmic derivative of Eq. (B.2) becomes

$$\frac{1}{e_2}\frac{\Delta e_2}{\Delta H} = \frac{1}{M'}\frac{\Delta M'}{\Delta H} = \frac{1}{\mu}\frac{\Delta \mu}{\Delta H} = \frac{\Delta \mu}{\Delta H} \tag{B.4}$$

The permeability, μ, is given by

$$\mu = 1 + 4\pi \frac{\partial M}{\partial H} \tag{B.5}$$

and

$$\frac{\partial \mu}{\partial H} = 4\pi \frac{\partial^2 M}{\partial H^2} \simeq \frac{\Delta \mu}{\Delta H} \tag{B.6}$$

If we insert the second derivative of Eq. (B.1) into this expression, we obtain

$$\frac{\Delta \mu}{\Delta H} \simeq -8\pi M_s \left(\frac{a}{H^3} + \frac{3b}{H^4}\right) \tag{B.7}$$

Figure B-3 shows the observed values of $\frac{\Delta \mu}{\Delta H}$ as a function of applied magnetic field. The asymptotic increase of $\frac{\Delta \mu}{\Delta H}$ at 750 oersteds indicates that the field inside the material is approximately zero at this value of applied field. The measurements were made at 1 kc and 3 kc in order to show that the skin depth did not influence the results. While an estimate of a may be obtained from these data, we cannot determine the value of a exactly. First, we have not measured a true derivative, and in fact, above 5000 oersteds, the increment of H was increased by a factor of 4 in order to observe an output voltage. Also, any departure from exact

alignment of sample axis with the applied field results in a larger value of $\frac{\Delta\mu}{\Delta H}$ because the permeability transverse to the magnetic field is larger than the permeability parallel to the magnetic field. The perpendicular component of the permeability falls off less rapidly than the parallel compents and its presence is seen in the data above 2000 oersteds. Thus the value of $\underline{a}$ may be deduced only between 750 and 1500 oersteds. These data indicate a value of $\underline{a} \simeq 0.2$. Thus the term in $\underline{a}$ probably introduces less than 10 per cent uncertainty in R_o.

B.3 The $\frac{b}{H^2}$ Term

The term in $\underline{b}$ has been measured for both single crystals and polycrystalline samples and found to be related to the anisotropy constant, K. In the case of single crystals,

$$b = \frac{f(\theta,\phi)K^2}{M_s^2} \qquad (B.8)$$

where $f(\theta,\phi)$ is a function of the polar angles θ, ϕ, describing the direction of the magnetization vector, M_s. In the case of polycrystalline samples, the value of $\underline{b}$ is obtained by averaging $f(\theta,\phi)$ over all possible orientations.

In order to develop the expression for $\underline{b}$, we consider the anisotropy energy of a cubic crystal defined by a single anisotropy constant and the energy of the system due to the applied field. We exclude the effects of strain which may alter the energy of the system. The anisotropy energy, within an additive constant, is given by

$$E_k = K(\alpha_1^2\alpha_2^2 + \alpha_1^2\alpha_3^2 + \alpha_2^2\alpha_3^2) \qquad (B.9)$$

where α_1, α_2, α_3, are the direction cosines of the magnetization vector M_s referred to the cube edges. The energy of the magnetization vector M_s in the applied field H is given by

$$E_H = -M_s H\cos\beta \qquad (B.10)$$

where β is the angle between M_s and H. Thus, the total energy is given by

$$E_t = E_k - M_s H\cos\beta \qquad (B.11)$$

The equilibrium position of the magnetization vector in the field H is that position which minimizes the total energy. Differentiating Eq. (B.11)

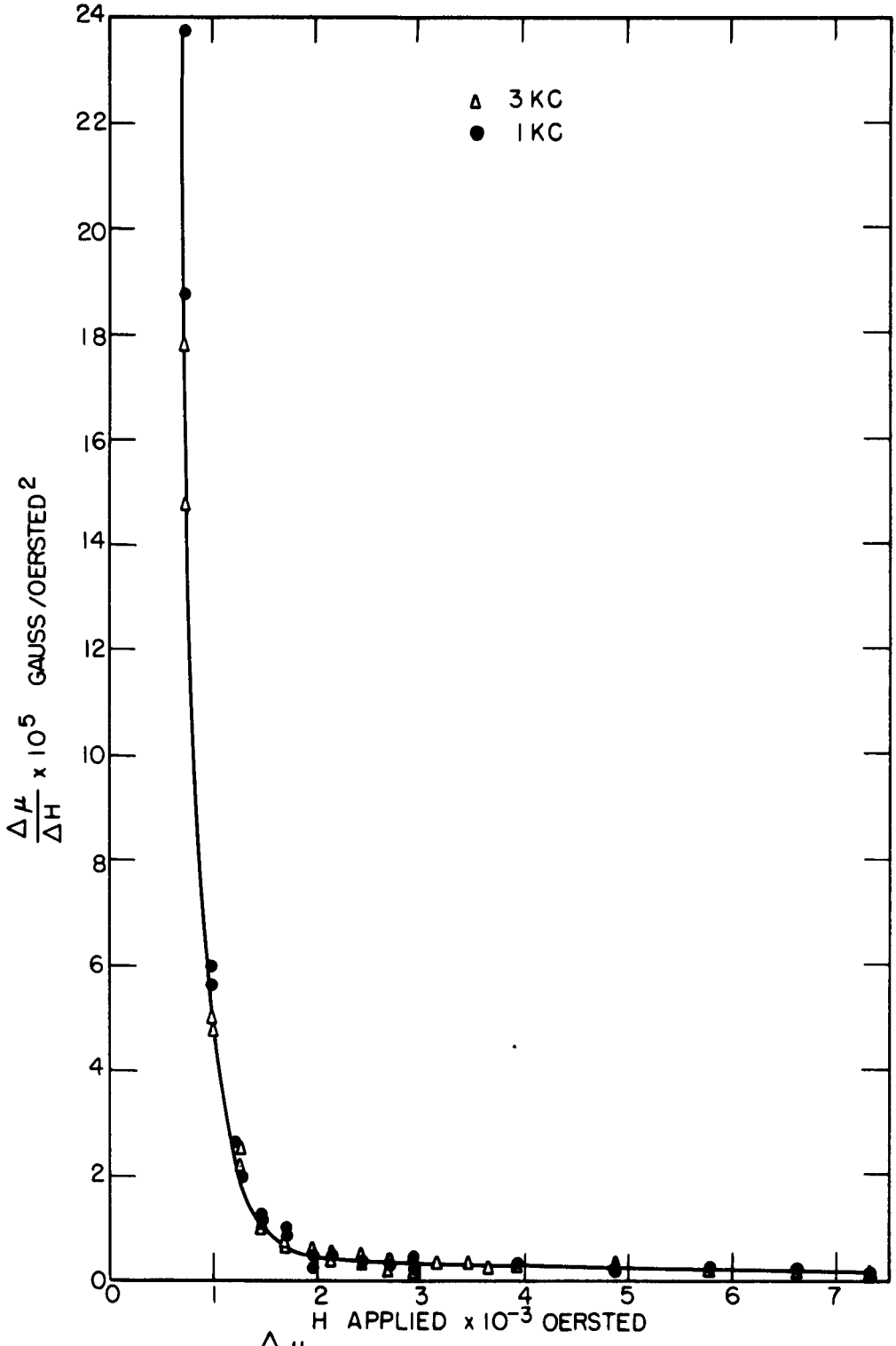

FIG. B-3 $\frac{\Delta\mu}{\Delta H}$ AS A FUNCTION OF APPLIED MAGNETIC FIELD FOR Fe_3O_4

with respect to β we obtain

$$\frac{\partial E_t}{\partial \beta} = \frac{\partial E_k}{\partial \beta} + M_s H \sin \beta = 0 \qquad \text{(B. 12)}$$

The component of magnetization along the direction of applied field is given by

$$M = M_s \cos \beta \qquad \text{(B. 13)}$$

These expressions apply only for fields which are sufficiently large to insure that the magnetization vector lies initially along the direction of easy magnetization. As the field is increased, the magnetization vector is pulled away from the direction of easy magnetization toward the direction of the applied field. We consider the case where the field is sufficiently large so that the angle β between M_s and H is small and we approximate,

$$\cos \beta \simeq 1 - \frac{\beta^2}{2} \qquad \text{(B. 14)}$$

$$\sin \beta \simeq \beta$$

For this condition

$$M = M_s\left(1 - \frac{\beta^2}{2}\right) \qquad \text{(B. 15)}$$

and

$$\sin \beta \simeq \beta = \frac{-\frac{\partial E_k}{\partial \beta}}{M_s H} \qquad \text{(B. 16)}$$

Therefore,

$$M = M_s \left(1 - \frac{1}{2}\left[\frac{\frac{\partial E_k}{\partial \beta}}{M_s H}\right]^2\right) \qquad \text{(B. 17)}$$

We thus observe, that in the general case where $\frac{\partial E_k}{\partial \beta} \neq 0$ we require an infinite field to completely saturate or to exactly align the magnetization vector parallel to the applied field. There are, however, certain crystal directions for which $\frac{\partial E_k}{\partial \beta} = 0$, and along these directions, fields of the order of $\frac{2K}{M_s}$ are sufficient to saturate. This situation may be alternatively described in the following manner. The field energy, E_H, is altered only to the second order (β^2) by having the magnetization vector slightly divergent from the direction of H. On the other hand, for many crystal directions, the anisotropy energy is altered to the first order (β) by having the magnetization vector lie away from the field direction. Hence, the system can lower its energy by having the magnetization lie along a direction slightly different from

the field direction.

The expression for E_k may be cast into polar coordinates as well as the $\cos\beta$ term. This has been done by Akulov [29] and Gans [30], who have then averaged the resulting expression for $\frac{\partial E_k}{\partial \beta}$ and obtained in the case of polycrystalline material

$$M = M_s \left(1 - \frac{8 K^2}{105 M_s^2 H^2}\right) \qquad \text{(B. 18)}$$

If the Fe_3O_4 sample had been polycrystalline, then the change of M would have been of the order 1 gauss over the region of H used in the measurement, and the resultant voltage would have been about 40 per cent of the total voltage observed. However, the sample cannot be considered polycrystalline because it was composed of several large crystals. This may be seen in Fig. 5-1, which shows a photograph of the sample after etching in HCℓ .

There are certain directions in the crystal along which the change of M, for the fields used, may be of the order of 10 gauss. However, the probability that all of the individual crystals are oriented along such directions is small, and there is undoubtedly some reduction in ΔM because of interaction between crystals. However, strains in the lattice might tend to worsen the situation. Therefore, there is no a priori reason for excluding a large voltage due to this effect. However, during each series of measurements of the ordinary Hall voltage, measurments were made between 4000 and 6500 oersteds and between 6500 and 9000 oersteds of applied field. These were made as a precaution against voltages due to vibration and voltages due to failure to saturate. However, because the signal-to-noise ratio was reduced by a factor of 2 and because of the spread of values, nothing very precise could be inferred from these observations. However, these observations do exclude the possibility that the voltage dropped to 1/10 of the value observed between 4000 and 9000 oersteds, and thus, effectively exclude the possibility that the $\frac{a}{H}$ and/or the $\frac{b}{H^2}$ term provides the entire voltage observed. This may be seen by calculating the reduction in ΔM. Since the demagnetizing factor was roughly 2π, the internal field is given by the external field minus $2\pi M_s$, or

3000 gauss. Between 4000 and 9000 oersteds applied, the internal field ranges between 1000 and 6000 oersteds, thus

$$\Delta M = a\left(\frac{1}{H_1} - \frac{1}{H_2}\right) + b\left(\frac{1}{H_1^2} - \frac{1}{H_2^2}\right) \qquad \text{(B. 19)}$$

$$\Delta M = .83\ a \times 10^{-3} + .97\ b \times 10^{-6} \qquad \text{(B. 20)}$$

Between 3500 and 6000 oersteds,

$$\Delta M = .012\ a \times 10^{-3} + .055\ b \times 10^{-6} \qquad \text{(B. 21)}$$

Therefore, if the total observed voltage were due to R_1 ΔM, a reduction by about 10 would have been observed when the field was reduced by a factor of 2. Since this was not observed, the value of R_o deduced from the measurement is at least the right order of magnitude, but nothing more precise may be stated.

In the case of $(NiO)_{.75}(FeO)_{.25}(Fe_2O_3)$ it was possible to resolve the V_H, H curve above saturation and thus obtain a fairly good test of the presence of nonlinear terms in H. If the points lying above the curve [Fig. 5-3] at about 9000 oersteds are due to these effects, then the maximum error in R_o is less than 20 per cent. However, it is also probable that some of this scatter at 9000 oersteds is due to thermal instability. In this respect we note that the temperature requirement for the $(NiO)_{.75}(FeO)_{.25}(Fe_2O_3)$ measurement was roughly the same as that for the Fe_3O_4 measurement. Therefore, because of the good linearity of the average values both above and below these points, the error in these data due to the $\frac{a}{H}$ and $\frac{b}{H^2}$ terms is probably small. However, we cannot estimate the uncertainty in R_o due to the K_o term. Pauthenet's data suggest that K_o for both $NiOFe_2O_3$ and Fe_3O_4 is probably smaller than K_o for Ni. If K_o for $(NiO)_{.75}(FeO)_{.25}(Fe_2O_3)$ is the same as K_o for Ni, then there is about 16 per cent error in R_o. However, if we may infer that K_o for $(NiO)_{.75}(FeO)_{.25}(Fe_2O_3)$ is about the same order of magnitude as K_o for $NiOFe_2O_3$ and Fe_3O_4, then the error is less then 10 per cent.

References

1. E. H. Hall, Phil. Mag. 12, 157 (1881).
2. E. H. Hall, Am J. Sci. 29, 117 (1885).
3. E. H. Hall, Phil. Mag. 19, 419 (1885).
4. A. L. Clough and E. H. Hall, Proc. Am. Acad. Arts Sci. 28, 189 (1892).
5. A. Kundt, Wied. Ann. 49, 257 (1893).
6. A. W. Smith, Phys. Rev. 30, 1 (1910).
7. A. W. Smith and R. W. Sears, Phys Rev. 34, 166 (1929).
8. E. M. Pugh, Phys. Rev. 36, 1503 (1930).
9. E. M. Pugh and T. W. Lippert, Phys. Rev. 42, 709 (1932).
10. E. M. Pugh, N. Rostoker, and A. Schindler, Phys. Rev. 80, 688 (1950).
11. J. P. Jan, Helv. Phys. Acta 25, 677 (1952).
12. R. M. Bozorth, Ferromagnetism, (D. Van Nostrand Company, Inc., New York, 1951) Chapter 10.
13. R. Karplus and J. M. Luttinger, Phys. Rev. 95, 1154 (1954).
14. G. H. Wannier, Phys. Rev. 72, 304 (1947).
15. G. Hilpert, Verhandl. deut. physik. Ges. 11, 293 (1909).
16. L. Néel, Ann. Phys. 3, 137 (1948).
17. C. G. Shull, E. O. Wollan, and W. C. Koehler, Phys. Rev. 84, 912 (1951).
18. B. P. Calhoun, Phys. Rev. 94, 1577 (1954).
19. E. J. W. Verwey and P. W. Haayman, Physica 8, 979 (1941).
20. E. J. W. Verwey, P. W. Haayman, and F. C. Romeijn, J. Chem. Phys. 15, 181 (1947).
21. J. L. Snoek, New Developments in Ferromagnetic Materials (Elsevier, New York, 1947).
22. R. L. Harvey, I. J. Hegyi and H. W. Leverenz, R.C.A. Rev. 11, 321 (1950).

23. A. Fairweather, F. F. Roberts and A. J. E. Welch, Rep. Prog. Phys. 15, 142 (1952).

24. A. Sommerfeld and N. H. Frank, Revs. Modern Phys. 3, 1 (1931).

25. V. A. Johnson and F. M. Shipley, Phys. Rev. 90, 523 (1953).

26. F. Seitz, Modern Theory of Solids, (McGraw-Hill Book Company, Inc., New York, 1940) p. 179.

27. H. Masumoto and Y. Shirakawa, Phys. Rev. 60, 835 (1941).

28. L. Néel, J. phys. et radium [8] 9, 184 (1948).

29. N. Akulov, Z. Physik 69, 78 (1931).

30. R. Gans, Ann. Physik [5] 15, 28 (1932).

31. T. Holstein and N. Primakoff, Phys. Rev. 58, 1098 (1940).

32. Metals Handbook (The American Society for Metals, Cleveland, Ohio, 1948), p. 1047.

33. G. E. Valley, Jr. and H. Wollman, Vacuum Tube Amplifiers, (McGraw-Hill Book Company, Inc., New York, 1948).

34. A. van der Ziel, Noise (Prentice-Hall, Inc., New York, 1954).

35. B. V. Rollin and I. M. Templeton, Proc. Phys. Soc. (London) B66, 259 (1953).

36. B. V. Rollin and I. M. Templeton, Proc. Phys Soc. (London) B67, 271 (1954).

37. P. H. Miller, Proc.I.R.E. 35, 252 (1947).

38. K. M. Van Vliet, C. J. Van Leeuwen, J. Blok and C. Ris, Physica 20, 481 (1954).

39. T. Des Coudres, Arch. Néel [2] 5, 622 (1900).

40. B. R. Russell and C. Wahlig, Rev. Sci. Instr. 21, 1028 (1950).

41. E. M. Pell and R. L. Sproull, Rev. Sci. Instr. 23, 548 (1952).

42. J. A. Pierce, The Diurnal Carrier-Phase Variation of a 16-Kilocycle Transatlantic Signal (Technical Report No. 209, Cruft Laboratory, Harvard University, October 10, 1954).

43. C. G. Montgomery, Technique of Microwave Measurements (McGraw-Hill Book Company, Inc., New York, 1947) p. 501.

44. D. W. Healey, Jr., Ferromagnetic Resonance in Some Ferrites as a Function of Temperature (Technical Report No. 135, Cruft Laboratory, Harvard University, August 15, 1951), p. 31.

45. G. J. Kevane, S. Levgold, and F. H. Spedding, Phys. Rev. 91, 1372 (1953).

46. J. Smiltens, J. Chem. Phys. 20, 990 (1952).

47. A. I. Schindler and E. M. Pugh, Phys. Rev. 89, 295 (1953).

48. P. Weiss and R. Forrer, Ann. phys. [10] 5, 153 (1926).

49. W. Schockley, Bell System Tech. J. 18, 645 (1939).

50. E. C. Stoner, Phil. Mag. 15, 1018 (1933).

51. N. F. Mott, Proc. Phys. Soc. (London) 47, 571 (1935).

52. J. C. Slater, Phys. Rev. 49, 537 (1936).

53. N. F. Mott, Proc. Roy. Soc. (London) A153, 699 (1935).

54. E. M. Pugh, Research on the Electronic Configuration in the Ferromagnetic Materials (Final Report, Carnegie Institute of Technology, July 1954).

55. E. M. Pugh, Phys. Rev. 97, 647 (1955).

56. P. Cohen (Ph.D. Thesis, Carnegie Institute of Technology, June 1954) unpublished.

57. E. C. Stoner, Proc. Roy. Soc. (London) A165. 372 (1938).

58. E. C. Stoner, Proc. Roy. Soc. (London) A169, 339 (1939).

59. E. C. Stoner, J. Phys. et radium 12, 372 (1951).

60. E. P. Wohlfarth, Proc. Roy. Soc. (London) A195, 434 (1949).

61. E. P. Wohlfarth, Proc. Phys. Soc. (London) 60, 360 (1948).

62. A. H. Wilson, The Theory of Metals, (The University Press, Cambridge, 1953) 2nd edition, p. 271.

63. Prof. H. Brooks, Harvard University, private communication.

64. I. Isenberg, B. R. Russell and R. F. Greene, Rev. Sci. Instr. 19, 685 (1948).

65. J. H. DeBoer and E. J. W. Verwey, Proc. Phys. Soc. (London) A49 (extra part), 59 (1937).

66. N. F. Mott, Proc. Phys. Soc. (London) A62, 416 (1949).

67. A. H. Wilson, Proc. Roy. Soc. (London) A134, 277 (1931).

68. A. H. Wilson, Proc. Roy. Soc. (London) A134, 458 (1931).

69. E. J. W. Verwey, Nature 144, 327 (1939).

70. F. J. Morin, Phys. Rev. 93, 1195 (1954).

71. F. J. Morin, Phys. Rev. 93, 1199 (1954).

72. G. H. Jonker and J. H. Van Santen, Physica 16, 337 (1950).

73. J. H. Van Santen and G. H. Jonker, Physica 16, 599 (1950).

74. C. Zener, Phys. Rev. 82, 403 (1951).

75. D. O. Smith (Laboratory for Insulation Research, Massachusetts Institute of Technology) unpublished data.

76. E. J. W. Verwey, "Oxidic Semiconductors," Semi-Conducting Materials (Butterworths, London, 1951), p. 151.

77. R. Pauthenet, Ann. phys. 7, 710 (1952).

78. E. W. Gorter, Phillips Research Reports 9, 295 (1954).

79. S. Foner, Phys. Rev. 99, 1079 (1955).

80. C. Kooi, Phys. Rev. 95, 843 (1954).

81. J. Smit and J. Volger, Phys. Rev. 92, 1576 (1953).

82. S. Foner, Phys. Rev. 91, 20 (1953).

83. L. Bickford, Phys. Rev. 78, 449 (1950).

84. J. M. Lavine, (Ph. D. Thesis, Harvard University, May 1955).

85. H. Polley, Ann. Physik [5] 36, 625 (1939).

86. P. Weiss and R. Forrer, Ann. phys. [10] 12, 279 (1929).

DISTRIBUTION LIST

Technical Reports

Chief of Naval Research
Department of the Navy
Washington 25, C. C.

2	427
1	460
1	421

6 Director (Code 5250)
Naval Research Laboratory
Washington 25, D. C.

2 Commanding Officer
Office of Naval Research Branch Office
150 Causeway Street
Boston, Massachusetts

1 Commanding Officer
Officer of Naval Research Branch Office
1000 Geary Street
San Francisco 9, California

1 Commanding Officer
Office of Naval Research Branch Office
1030 E. Green Street
Pasadena, California

1 Commanding Officer
Office of Naval Research Branch Office
The John Crerar Library Building
86 East Randolph Street
Chicago 1, Illinois

1 Commanding Officer
Office of Naval Research Branch Office
346 Broadway
New York 13, New York

3 Officer-in-Charge
Office of Naval Research
Navy No. 100
Fleet Post Office
New York, New York

Chief, Bureau of Ordnance
Navy Department
Washington 25, D. C.

1	Re4-1
1	AD-3

Technical Reports

Chief, Bureau of Aeronautics
Navy Department
Washington 25, D. C.

1 EL-1
1 EL-4

2 Chief, Bureau of Ships (810)
Navy Department
Washington 25, D. C.

1 Chief of Naval Operations
Navy Department
Washington 25, D. C.

1 Op-413
1 Op-20
1 Op-32

1 Director
Naval Ordnance Laboratory
White Oak, Maryland

2 Commander
U. S. Naval Electronics Laboratory
San Diego, California

1 Commander(AAEL)
Naval Air Development Center
Johnsville, Pennsylvania

1 Librarian
U. S. Naval Post Graduate School
Monterey, California

50 Transportation Officer
Building 151
Squier Signal Laboratory
Fort Monmouth, New Jersey
Attn: Director of Research

Commanding General
Air Research and Development Command
Post Office Box 1395
Baltimore 3, Maryland

3 RDTRRP
2 RDDDE

1 Commanding General(WCRR)
Wright Air Development Center
Wright-Patterson Air Force Base, Ohio

Technical Reports

Commanding General
Wright Air Development Center
Wright-Patterson Air Force Base, Ohio

1 WCRRH
2 WCLR
1 WCLRR
2 Technical Library

2 Commander
Wright Air Development Center
Attn: WCREO
Wright-Patterson Air Force Base, Ohio

Commanding General
Rome Air Development Center
Griffiss Air Force Base
Rome, New York

1 RCREC-4C
1 RCR-1
2 RCRW

Commanding General
Air Force Cambridge Research Center
230 Albany Street
Cambridge 39, Massachusetts

6 CRR
1 Technical Library

2 Director
Air University Library
Maxwell Air Force Base, Alabama

1 Commander
Patrick Air Force Base
Cocoa, Florida

1 Chief, European Office
Air Research and Development Command
Shell Building
60 Rue Ravenstein
Brussels, Belgium

1 U. S. Coast Guard (EEE)
1300 E Street, N. W.
Washington, D. C.

1 Assistant Secretary of Defense
(Research and Development
Research and Development Board
Department of Defense
Washington 25, D. C.

Technical Reports

5	Armed Services Technical Information Agency Document Service Center Knott Building Dayton 2, Ohio
1	Office of Technical Services Department of Commerce Washington 25, D. C.
1	Commanding Officer and Director U. S. Underwater Sound Laboratory New London, Connecticut
1	Federal Telecommunications Laboratories, Inc. Technical Library 500 Washington Avenue Nutley, New Jersey
1	Librarian Radio Corporation of America RCA Laboratories Princeton, New Jersey
1	Sperry Gyroscope Company Engineering Librarian Great Neck, L. I., New York
1	Watson Laboratories Library Red Bank, New Jersey
1	Professor E. Weber Polytechnic Institute of Brooklyn 99 Livingston Street Brooklyn 2, New York
1	University of California Department of Electrical Engineering Berkeley, California
1	Dr. E. T. Booth Hudson Laboratories 145 Palisade Street Dobbs Ferry, New York
1	Cornell University Department of Electrical Engineering Ithaca, New York
1	University of Illinois Department of Electrical Engineering Urbana, Illinois

Technical Reports

1	Johns Hopkins University Applied Physics Laboratory Silver Spring, Maryland
1	Professor A. von Hippel Massachusetts Institute of Technology Research Laboratory for Insulation Research Cambridge, Massachusetts
1	Director Lincoln Laboratory Massachusetts Institute of Technology Cambridge 39, Massachusetts
1	Mr. A. D. Bedrosian Room 22A-209 Signal Corps Liaison Office Massachusetts Institute of Technology Cambridge, Massachusetts
1	Mr. Hewitt Massachusetts Institute of Technology Document Room Research Laboratory of Electronics Cambridge, Massachusetts
1	Stanford University Electronics Research Laboratory Stanford, California
1	Professor A. W. Straiton University of Texas Department of Electrical Engineering Austin 12, Texas
1	Yale University Department of Electrical Engineering New Haven, Connecticut
1	Mr. James F. Trosch, Administrative Aide Columbia Radiation Laboratory Columbia University 538 West 120th Street New York 27, New York
1	Dr. J.V.N. Granger Stanford Research Institute Stanford, California
1	Library Central Radio Propagation Laboratory National Bureau of Standards Boulder, Colorado

Technical Reports

1	Library of the College of Engineering New York University University Heights Library University Heights 33, New York
1	Documents and Research Information Section Raytheon Manufacturing Company Engineering Equipment Division 148 California Street Newton 58, Massachusetts
1	Professor Henry G. Booker School of Electrical Engineering Cornell University Ithaca, New York
1	M. A. Krivanich, Technical Advisor to Deputy Chief Ballistics Research Laboratory White Sands Annex White Sands P.G., New Mexico
1	Doris P. Baster Head, Document Section Technical Information Division Naval Research Laboratory Washington 25, D. C.
1	Dr. C. H. Papas Department of Electrical Engineering California Institute of Technology Pasadena, California
1	Airborne Instrument Laboratory Mineola New York
1	Radiation Laboratory Johns Hopkins University 1315 St. Paul Street Baltimore 2, Maryland
1	Mr. Robert Turner General Electric Company Advanced Electronics Center Cornell University Ithaca, New York

Technical Reports

1	Acquisitions Officer ASTIA Reference Center The Library of Congress Washington 25, D. C.
1	Librarian National Bureau of Standards Library Connecticut Avenue and Van Ness Street, N.E. Washington 25, D. C.
1	Secretary Working Group on Semiconductor Devices, AGET 346 Broadway, 8th Floor New York 13, N. Y.
1	Professor R. E. Norberg Washington University St. Louis, Missouri